

On the Development of a Universal Automated Fixturing System through Encapsulation Techniques

by

Elmer C. Lee

B.S., Mechanical Engineering
Massachusetts Institute of Technology(1996)
M.S., Mechanical Engineering
Massachusetts Institute of Technology(1999)

Submitted to the Department of Mechanical Engineering in
partial fulfillment of the requirements for the degree of

Doctor of Philosophy in MECHANICAL ENGINEERING

at the

MASSACHUSETTS INSTITUTE OF TECHNOLOGY

September 2001

© Copyright, 2001, Massachusetts Institute of Technology. All rights reserved.

Author

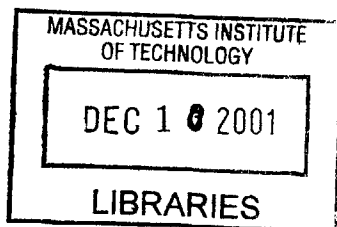
.....
Department of Mechanical Engineering
August 23, 2001

Certified by

.....
Sanjay E. Sarma
Associate Professor of Mechanical Engineering
Thesis Supervisor

Accepted by

.....
Ain A. Sonin
Chairman, Department Committee on Graduate Student



BARKER



Room 14-0551
77 Massachusetts Avenue
Cambridge, MA 02139
Ph: 617.253.2800
Email: docs@mit.edu
<http://libraries.mit.edu/docs>

DISCLAIMER OF QUALITY

Due to the condition of the original material, there are unavoidable flaws in this reproduction. We have made every effort possible to provide you with the best copy available. If you are dissatisfied with this product and find it unusable, please contact Document Services as soon as possible.

Thank you.

Page 10 is missing from the Archives copy. This is the most complete version available.

On the Development of a Universal Automated Fixturing System through Encapsulation Techniques

by

Elmer C. Lee

Submitted to the Department of Mechanical Engineering on August 23th 2001 in partial fulfillment of the requirements for the degree of

Doctor of Philosophy in MECHANICAL ENGINEERING

Abstract

Universal automated fixturing can transform a machine tool into a rapid prototyping machine with many advantages over current rapid prototyping methods. Using this modified machine tool, prototype parts can be manufactured using the intended engineered materials, allowing for not only visual inspection of the prototype but also functional testing. The entire design process can be sped up, allowing companies to be more responsive to market changes. This research is aimed at showing that the techniques known as Reference Free Part Encapsulation (RFPE) can be used to develop such a fixturing system.

Within this dissertation, the machines and systems that are needed to develop an automated fixturing system are discussed. We describe work done to experimentally investigate the effects of various parameters such as encapsulation pressures and temperatures on encapsulation quality. The goal of this research is to build upon the conventional understanding of molding in general and to bring the cumulative understanding of the encapsulation process to a point where universal automated fixturing through Reference Free Part Encapsulation is demonstrably feasible.

This thesis will elaborate on the current machines and systems developed as testbeds for performing RFPE. We examine the effectiveness of these testbeds to carry out the encapsulation procedures. We shall also discuss design innovations developed and process refinements. Recommendations shall be made to further refine these machines.

A set of simulations will be presented that have been used to model and optimize the encapsulation procedure. These simulations are used to explore, analytically, the various temperature parameters that effect encapsulation quality. The results shall be presented and an optimal process window described. These simulations will be further supported by closed-form analysis.

Lastly, we present a case study to show the effectiveness of Reference Free Part Encapsulation fixturing. Production cost and time data shall be presented to display the fixturing effectiveness of RFPE fixturing in juxtaposition to conventional fixturing methods. This case study shall lead to recommendation of industrial applications for RFPE that can be readily applied and result in immediate cost and time savings.

Thesis Supervisor: Sanjay Sarma

Title: Associate Professor of Mechanical Engineering

Acknowledgements

I would like to thank my advisor and friend, Professor Sanjay Sarma, for giving me the opportunity to work within his research group. Thank you for letting me pursue the research in methods and ways I saw best, letting me make my own mistakes and learn from them as well. But also, thank you for always being close enough to the research and my work to be able to light a fire underneath my ass and drive me forward when the going was rough. I have learn a tremendous amount from you about being a scholar, a teacher, and a student. My success in the future will be largely because of your example.

I would also like to thank my thesis committee for contributing their support and advise. Thank you Professor Bora Mikic. Thanks for letting me take your advanced heat transfer class three times. Every time I stepped into class I learned something new. Yours was by far one of the most challenging classes I have taken at MIT. It was also one of the most rewarding. Thank you Professor David Wallace. Your practical advise and your supportive nature has been truly comforting. Your classes and your teaching have given me insights to myself that will stay with me for the rest of my life.

To the guys in the machine shop, Fred Cote, Gerry Wentworth, Mark Belanger, Dave Dow and Bob Kane, thanks for your support and advise on everything practical. I learned much from you all about the real world and how to get thing done. I hope that I have made an impact on your daily lives as you have made on mine. I hope that I will not be soon forgotten.

Thank you so much Sally Stiffler. Sally, you have always made me feel welcomed. Your caring and support made the ugliest parts of MIT seem bearable. I will cherish yours and Jack's friendship for the rest of my life. And yes, the invitation will be mail to you as soon as Audrey and I figure out when we're actually getting married. All the best to you.

To David Rodriguera, thanks for fixing all the messes I created. I might just let you beat me in "mech-death 5." Nah!!!

To Maureen Lynch, thank you for fixing all my other messes. Thank you for caring and always making me feel special among thousands of MIT students.

To the three masters students who work with me, Paula Valdavia y Alvarado, Winston Fan and Ceani Guevara, thanks for your help and company.

To my UROP's, Edmund Golaski, Stallion Yang, Crystal Hsu, Miriam Betnum, Seppo Helava, and Jeff Hayashida, thanks for making my life just that much more challenging. I hope I was a good teach to you and not simply an easy paycheck.

Lastly, thanks to MIT. Never have I understood the phrase, "what doesn't kill you makes you stronger," better than when I was here. IHTFP²

This Work and My Life
I Dedicate Them To:

My Father, who always stood above me giving me something to reach for,
pulling me upward to become a better person

My Mother, who always stood beneath me ready to catch me if I fell,
ready to comfort me if I failed

My Loving Wife to Be, who always stood with me through all the good and bad times,
making the journey worthwhile

My Brother and Sister, who always stood on the side and cheered, and
give me perspective when I was too close to see the truth myself

Table of Contents

Chapter 1: Acknowledgements	3
Chapter 2: Introduction	12
2.1 Motivation	12
2.2 Technology Review	14
2.3 Basic Process Steps	18
2.4 Encapsulation in Industry	20
2.5 Material Selection	21
2.5.1 Selection Criteria	22
2.5.2 Fusible Alloys	25
2.5.3 Fixturing Polymers	26
2.5.4 Engineering Plastics	27
2.6 Advantages Other Fixturing Methods	27
2.6.1 Ease of Automation	28
2.6.2 Machining Thin Members and Odd Shapes	28
2.6.3 Developing Manufacturing Processes Without Hard Tooling	30
2.6.4 Machining Parts in Small Batch Sizes	30
2.7 Summary	32
Chapter 3: Development of the Encapsulation Techniques	33
3.1 Process Classification	33
3.1.1 3-D milling	33
3.1.2 2 1/2-D milling	34
3.1.3 2-D milling	34
3.2 The Importance of Orientation	36
3.3 Molds	37
3.3.1 3-D molds	38
3.3.2 2-D Molds	40
3.3.3 2 1/2-D Molds	41
3.4 Summary	43
Chapter 4: Encapsulation Testbeds	44
4.1 Large Encapsulation Machine	45
4.1.1 Injection System	47
4.1.2 Clamping System	50
4.2 Portable Encapsulation Machine	58
4.3 Summary	61

Chapter 5: Analysis of the Encapsulation Process	63
5.1 General Defects	63
5.2 Unique Defects Found Only in the Encapsulation Process	65
5.3 The Rewelding Defect and its relationship to the Remelting Effect	67
5.4 Development of a Computational Model	68
5.5 The Simulation Models and Results	70
5.5.1 <i>Rewelding</i>	70
5.5.2 <i>Remelting</i>	75
5.5.3 <i>The Process Window for BiSn Eutectic</i>	79
5.6 Simulation on the Rigidax™ Material	80
5.6.1 <i>Rewelding and Remelting Results</i>	82
5.6.2 <i>Development of a New Process Window for Rigidax™</i>	85
5.7 Summary: The Process Window of RFPE	87
Chapter 6: Verification of the Runge Kutta Simulation	88
6.1 Analytical Model of the Slab	88
6.2 Analytical Model Which Includes Phase Change	91
6.3 Stability of the Runge Kutta Simulation	98
6.4 Summary	100
Chapter 7: Industrial Application Experiment	102
7.1 Three Fixturing Strategies and Their Machining Procedures	103
7.1.1 <i>Soft Tooling</i>	104
7.1.2 <i>Make-Shift Tooling</i>	106
7.1.3 <i>RFPE Fixturing</i>	107
7.2 Results	111
7.3 Conclusion	116
Chapter 8: Research Conclusions	117
8.1 Machine Design	117
8.1.1 <i>Machine Components and Sample Encapsulations</i>	117
8.1.2 <i>Failure Modes</i>	122
8.2 Immediate Applications for RFPE Fixturing	124
8.3 Future Work	125
8.4 The Future of RFPE	129
Appendix A:	130
Appendix B:	133
BIBLIOGRAPHY	137

List of Figures

Chapter 1:	12
Figure 1.1: Illustration of the General Model of the Envisioned Rapid Prototyping Center Using Machining Cells	13
Figure 1.2: Illustration of the different techniques for implementing a universal fixturing system	17
Figure 1.3: Illustration of the Encapsulation Process Steps	19
Figure 1.4: Illustration of a Turbine Blade Encapsulation Process	21
Figure 1.5: Illustration Showing Toolpaths for Machining Special Elements with the Aid of Encapsulation Fixturing	28
Figure 1.6: Photograph of sample parts machined using encapsulation fixturing	29
Figure 1.7 Illustration of Encapsulation Fixture's Ability to Transform Two Different Parts into One Generic Norm	31
Chapter 2:	33
Figure 2.1: Illustration of the Three Fundamental Machining Strategies	35
Figure 2.2: Illustrations of the importance of machine orientation	36
Figure 2.3: Illustration of the 3-D mold pieces- (top) gate plate, (middle) L pieces for the main cavity, (bottom) bottom plate	39
Figure 2.4: Side view illustration of the 3-D mold side clamping mechanism	40
Figure 2.5: Illustration of the 2-D pieces and the fixturing plate that will allow the 2-D fixture to be mounted into a machine tool	41
Figure 2.6: Illustration of the 2 1/2D mold pieces	42
Chapter 3:	44
Figure 3.1: CAD Models of Encapsulation Testbeds	44
Figure 3.2: Illustration of All Three Components of the Encapsulation System-Clamping Systems, Injection piston, and Melting/Storage Tank	46
Figure 3.3: Process Window for Pressure and Surface Roughness	47
Figure 3.4: Cutout Illustration of the Injection Piston	49
Figure 3.5: Illustration of the Primary and Secondary Clamping Stage	51
Figure 3.6: Illustration of the Gate Valve and Elastomer Cutoff Diaphragm	53
Figure 3.7: Illustration of the Head Base and the Wedge Clamping Mechanism	54
Figure 3.8: Illustration of the Cooling/Heating Plate placed on the Primary Clamping Stage, Beneath the Mold	55
Figure 3.9: Illustration of the ProMechanica FEM model.....	57
Figure 3.10: Illustration of the Portable Encapsulation System	58
Figure 3.11: Illustration of the Primary Components of the Portable Encapsulation System	59
Figure 3.12: Cutout Illustration of Clamping Head, Wedge Clamp Mechanism, and Mold Placement	60
Figure 3.13: Illustration of the Flow Pattern inside the Portable Encapsulation Machine	61

Chapter 4:63

Figure 4.1: Examples of Common Encapsulation Defects Also Found in Other Industrial Molding Applications64

Figure 4.2: Picture of Rewelding Defect Unique to Encapsulation Molding66

Figure 4.3: Graphical Representation of the Breaking Down of the Oxide Layer by Super-Heating the Injected Metal68

Figure 4.4: Illustration of the Rewelding and Remelting Problems68

Figure 4.5: Diagram of the Algorithm to Solve the Heat Transfer Problem using Runge Kutta and the Proper Governing Equations69

Figure 4.6: Depiction of the Model for the Heat Transfer of Rewelding70

Figure 4.7: Graph of How the Maximum Penetration Depth Changes with for a Given Cooling Rates71

Figure 4.8: Graph of the Temporary Retreat of the Solidification Front as Predicted by the Simulation73

Figure 4.9: Comparison of Rewelding Line Derived from Simulation with Experimental Tensile Test Results Superimposed75

Figure 4.10: Pictures of Failed Sections of Tensile Test Specimens showing increasing ductility75

Figure 4.11: Depiction of the Model for the Heat Transfer of Remelting76

Figure 4.12: Graph of the Temperature at the Workpiece/Alloy Interface for Various Preheat Temperatures as Injection Temperature is Fixed at 450K77

Figure 4.13: Graph of the Temperature at the Workpiece/Alloy Interface for various Preheat Temperatures as Injection Temperature is Fixed at 475K78

Figure 4.14: Graph of the Temperature at the Workpiece/Alloy Interface for Various Preheat Temperatures as Injection Temperature is Fixed at 500K78

Figure 4.15: Graph of the Process Window for Preheat and Injection Temperatures for the BiSn Alloy80

Figure 4.16: Graph of the Temporary Retreat of the Solidification Front as Predicted by the Simulation for the Rigidax™ Material at an Injection Temperature of 385K .82

Figure 4.17: Graph of the Temporary Retreat of the Solidification Front as Predicted by the Simulation for the Rigidax™ Material at an Injection Temperature of 400K .83

Figure 4.18: Graph of the Temperature at the Workpiece/Rigidax™ Interface for Various Preheat Temperatures as Injection Temperature is Fixed at 385K84

Figure 4.19: Graph of the Temperature at the Workpiece/Rigidax™ Interface for Various Preheat Temperatures as Injection Temperature is Fixed at 400K84

Figure 4.20: Graph of the Temperature at the Workpiece/Rigidax™ Interface for Various Preheat Temperatures as Injection Temperature is Fixed at 425K85

Figure 4.21: Graph of the Process Window for Preheat and Injection Temperatures for the Rigidax™ Material86

Figure 4.22: Graphical comparison of process window for preheat and injection temperatures for the BiSn alloy and the Rigidax™ material87

Chapter 5: 88

Figure 5.1: Illustration of the One Dimensional, Unsteady Slab Heat Transfer Model88
Figure 5.2: Verification of 4th Order Runge Kutta Simulation to Closed Form Solutions of a Unsteady Slab Conduction Model90
Figure 5.3: Illustration of the Modified One Dimensional, Unsteady Heat Conduction Model with Phase Change91
Figure 5.4: Comparison of Results of Melt Front Location as Plotted with Time Derived by an Infinite Series Solution (solid lines) and by the 4th Order Runge Kutta Simulation (points)96
Figure 5.5: Graphical Comparison of the Maximum Melt Depth as Predicted by Both the Simulation and the Analytical Model97
Figure 5.6: Graphical Illustration of the Stability Criterion for the Runge Kutta Simulation 99

Chapter 6: 102

Figure 6.1: Mechanical Drawing of the Body Mount Test Part Courtesy of the FORD Motor Company 102
Figure 6.2: Pictorial Depiction of the Machining Steps Using Soft Tooling 105
Figure 6.3: Pictorial Depiction of the Machining Steps Using Make-Shift Tooling 107
Figure 6.4: Wireframe Drawing of a 2-D Frame used to Encapsulate and Fixture the FORD Test Part 108
Figure 6.5: Pictorial Depiction of the Machining Steps for RFPE Fixturing 110
Figure 6.6: Graphical Comparison of the Times for Different Production Components using Various Tooling Options 115
Figure 6.7: Graphical Comparison of the Percentage of the Times of Each Production Component Using Various Tooling Options 115
Figure 6.8: Graph of the Per Piece Cost to Manufacture the Test Part Using Various Tooling Options 116

Chapter 7: 117

Figure 7.1: Picture of the 2 1/2-D Mold, Gateplate and Sample 119
Figure 7.2: Picture of the 2 1/2-D Fixturing Assembly 120
Figure 7.3: Picture of 2 1/2-D Encapsulation Assembly Installed in a Machine Tool 120
Figure 7.4: Picture of the 2-D Mold Components 121
Figure 7.5: Picture of the 2-D Encapsulation Assembly 121
Figure 7.6: Picture of the Melted Encapsulation Assembly with the Finished Parts and Excess Stock Shown 122
Figure 7.7: Picture of the Piston Cup and O-ring 123
Figure 7.8: Photograph of the Aluminum Piston Cylinder with Surface Erosion and Pitting due to BiSn reaction 124
Figure 7.9: Illustration of the G-code parser module: 126
Figure 7.10: Illustration of software control scheme 127



Room 14-0551
77 Massachusetts Avenue
Cambridge, MA 02139
Ph: 617.253.2800
Email: docs@mit.edu
<http://libraries.mit.edu/docs>

DISCLAIMER

MISSING PAGE(S)

Page 10

List of Tables

Chapter 1	12
Chapter 2	33
Chapter 3	44
Chapter 4	63
Table 4.1: Material Properties of BiSn and Rigidax TM	81
Chapter 5	88
Chapter 6	102
Table 6.1: Machining and Setup Time for Soft Tooling	112
Table 6.2: Machining and Setup Time for Make-Shift Tooling	113
Table 6.3: Machining and Setup Times for RFPE Fixturing	114
Chapter 7	117

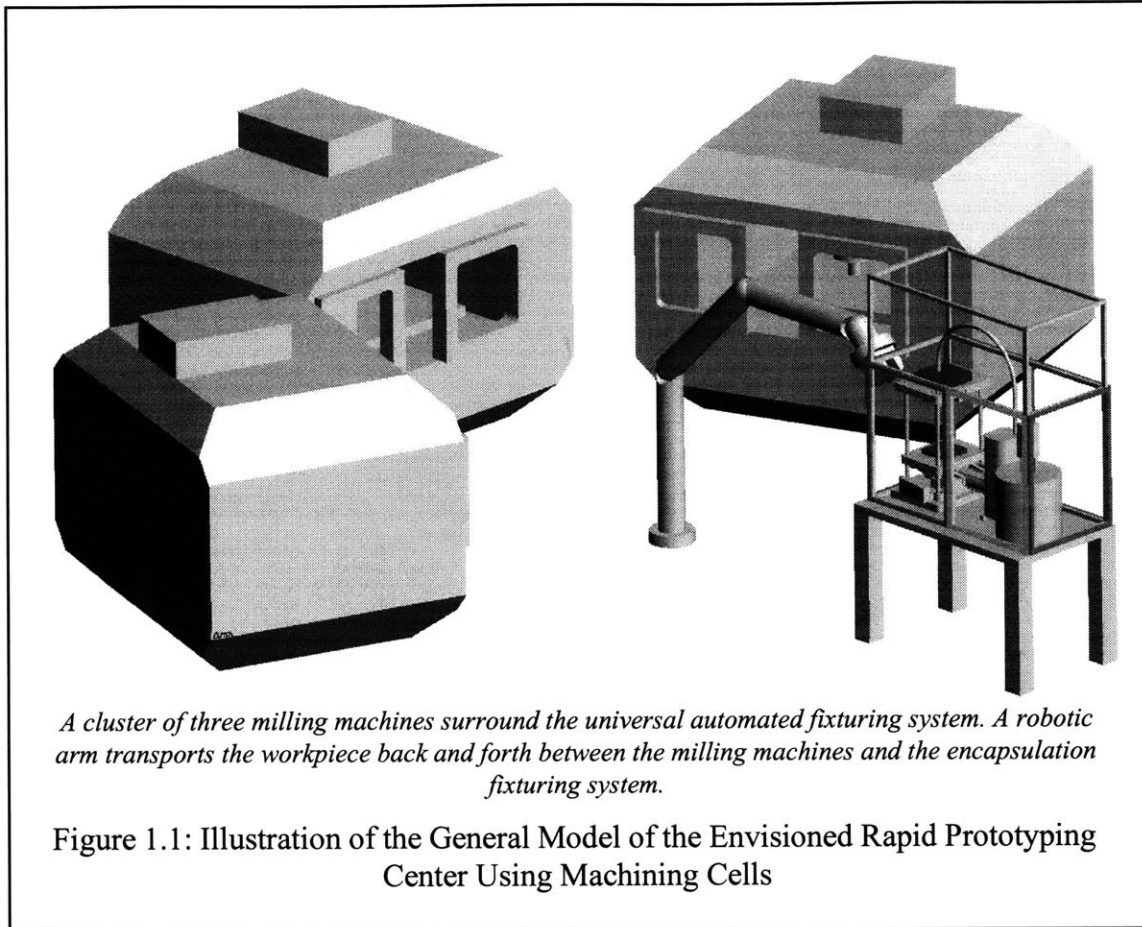
Chapter 1

Introduction

1.1 Motivation

Imagine if one were able to transform a milling machine into a manufacturing vending machine. One would simply have to provide a CAD file of the desired part, upload it into the manufacturing environment and could then simply walk away. A few hours later, the milling machine will have successfully generated the correct toolpaths, checked for errors and gouges, designed the fixturing system, selected the correct stock size, and machined the part completely. As simple as putting a few quarters into a drink machine and waiting for a bottle of soda to come out, this machine would be able to deliver prototype parts quickly and economically. Rapid prototyping could then be performed using the intended engineered material. Immediately, engineers and designers would not only “get a feeling” for the appearance of their designs, but they would also be able to test their functionality and performance. Development of new products could be reduced to weeks, instead of months or years.

A key part of this manufacturing vending machine is the fixturing system that will allow the automatic location, immobilization and support of any part regardless of its shape or material. Unfortunately, current industrial practices only provide automation of conventional fixturing on a part by part basis. Usually, special “hard” tooling is designed and manufactured to automate part handling, positioning and workholding for a single part or a single class of similar parts. Consequently, for short runs, normally associated with prototyping and one of a kind products, the development of specialized fixturing accounts



for a large percentage of the engineering time and manufacturing costs. This of course results in long lead times and high fixed cost.

Creating an automated universal fixturing system is one of the steps in creating a better rapid prototyping system. Alone, this fixturing system could allow an operator to manually create complex one-off parts. Alone, this system could save the operator time and effort, and reduce operator errors. Combined with sophisticated CAM software being developed at the Rapid Autonomous Machining Laboratory at MIT, and with robotic material handling systems, one can turn a milling machine into a rapid prototyping vending machine.

The automated universal fixturing system, discussed in the coming chapters, will allow one to fixture and machine two completely different parts in the same setup, using the same machine tool and fixtures. These two parts are essentially treated as if they were exactly identical. In essence, with this fixturing system, one will be able to apply mass production techniques and optimization to prototyping situations. A fixturing system which transforms unique, arbitrary parts into one generic geometry allows those parts to be machined as if they were the same. A cluster of machine tools, meant to run one-off parts, can now be used as a rapid prototyping machining cell.

Such a system, shown in Figure 1.1, would revolutionize the way engineers and designers think about product development and manufacturing. Just as the concepts of mass production—assembly lines, interchangeable parts—have revolutionized manufacturing, so will rapid prototyping through machine tools. The ability to create one part as quickly, efficiently, and as economically as creating a thousand of those parts, that is one of new frontiers in manufacturing and product development.

1.2 Technology Review

Many researchers have attempted to build universal fixturing systems. The approaches to developing such a system, though they vary quite extensively in their detailed designs and physical implementation, can be generally categorized into three different methods. They are described below. It is interesting to note that a majority of these devices and technologies have been patented. However, few have been implemented in industry. Those which have have found limited use. Because of intrinsic flaws, none have had any widespread success in the marketplace.

The first method is the use of a finite number of fingers or pins to conform and support the arbitrary part geometry. A variety of patents have been issued to deal with the fixturing of turbine blades through this conformal finger technique. The earliest device of

this type was patented in 1951 by Lombard, US Patent # 2,565,925. The latest patent to be issued for a device of this type was in October of 2000, to Dwyer, US Patent # 6,139,412. Fifteen or more patents have been issued between these two. All of these deal with the fixturing of turbine blades. While each device is design to accommodate slight changes in geometry, none can be expect to fixture parts that vary radically. A variety of other technology and devices have been developed to fixture other classes of parts in this manner. However, again, none have the capability to become universal.

The second method in developing a universal fixturing device is through the use of a fluidized bed, where the workpiece is submerged in a bath of a finite number of microspheres, conforming as a liquid would to any geometry placed within. By applying pressure to the top surface of the bath or a magnetic or electric field, a holding force will be applied to the workpiece through contacting microspheres. The earliest documentation of such a device is by Coes [Coes 72]. He describes a fluidized bed in which ferromagnetic particles are used to provide a holding force, activated by introducing a magnetic field. The United States patent office issued a patent, #3,660,949, to Coes for the concept. A number of later patents site this as prior art. The most recent was issued in July of 2001, to Zhang, US Patent # 6,267,364.

The last method is the use of phase changing materials which, in their liquid state, will conform to the arbitrary geometry and when solidified, will encapsulated the part and maintain holding forces on it. While there has been academic interest in using this technique, thus far no technology has been patented that enables this type of fixturing system. Boyes provides descriptions of industrial uses of phase change fixturing. This has primarily been limited to rudimentary fixturing and make-shift, on-the-fly fixturing. For the most part, none of these practices have been automated and thus still require a fair amount of human interaction with the fixturing setup [Boyes 85].

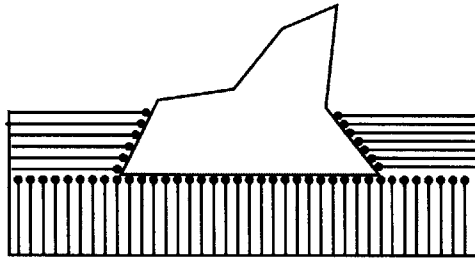
Each of these three methods, depicted in Figure 1.2, have their disadvantages. The finger approach is fairly difficult to implement. The long slender fingers can be prone to buckling which make the stability of the entire fixturing system questionable. The resulting point contacts with the workpiece produce very little damping, another reason why this method has had little success. The fluidized bed also has stability issues which are highly dependent on the size of the microspheres. Perfect packing is impossible to achieve. Thus, voids and inclusions inside the bed can allow the part to shift slightly. The maximum holding force of fluidized beds is relatively small. Thus, most applications of fluidized bed fixturing has been in assembly, where fixturing is generally less demanding. In addition, both of these methods create access problems for the cutting tool. The toolpath cannot intersect the fixturing system without damaging itself or the fixturing system. On the other hand, the use of phase change material to encapsulate a workpiece allows one to escape the problems faced by the other two. The stability of the fixturing system depends on the yield strength and Young's modulus of the encapsulation material, the encapsulant. Cutting into the encapsulant will not likely damage the work tool or the fixturing system because the encapsulant is usually much softer than the workpiece or the cutting tool. In addition, because phase change fixturing results in greater surface area contact between the part and the fixturing elements, one can be sure that it will offer superior damping. However, the need for heating systems, a delivery system for the liquid encapsulant, and a variety of other supporting devices, will tend to increase costs and complicate the design of such a fixturing system.

All three methods still face the challenge of locating the part or positioning the part accurately if features already exist within the workpiece. Without modification, none of these three different methods provide a means to creating a reliable universal automatable fixturing system.

Categories of Universal Work holding Techniques

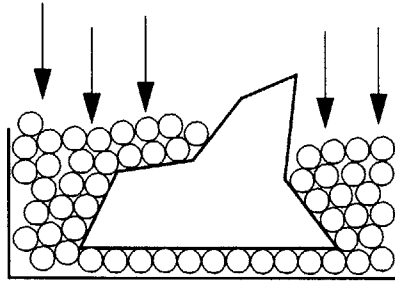
Disadvantages

Bed of Fingers



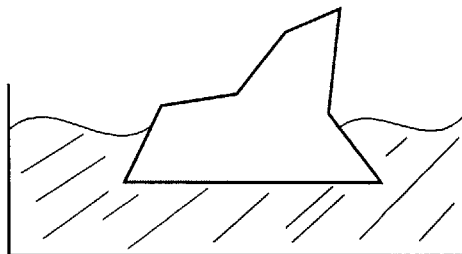
*Fingers are unstable
Provides little damping
Interferes with toolpaths
Mechanically complicated*

Fluidized Bed



*Instability due to voids
Can not interfere with toolpaths
Requires additional external forces*

Phase Change Encapsulation



*Hardware intensive
Complex Process*

Figure 1.2: Illustration of the different techniques for implementing a universal fixturing system

1.3 Basic Process Steps

In designing the universal fixturing system, it has been decided to develop the system using phase change fixturing techniques. Although extremely design intensive, phase change fixturing, otherwise known as encapsulation fixturing, demonstrates the most plausible techniques for the successful creation of an automatable universal fixturing system.

One of the fundamental challenges in using phase change encapsulation is that of locating and aligning a workpiece with pre-existing features. The common practice has been to use locating dies for which the features of the part are aligned to matching features specially machined into custom dies. Unfortunately, the use of the locating die essentially compromises the ability of the system to be automated and universal. For each new part, a unique die must be designed and manufactured. Thus, our approach will steer way from the use of locating dies and to, instead, develop a process plan which will not require pre-encapsulation location. This technique was first discussed by Sarma as part of his doctoral work at Berkeley in 1995, with Wright [Sarma 95].

The process, in its most abstract form, can be described as follows. A piece of stock, free of any existing features, rough cut to the approximate dimensions of the finished product, is encapsulated in a lower melting temperature material, molded into a perfect rectangular block. This block is then placed inside the machining environment so that a machining procedure or part of one can be performed on the block. Being a block form, the fixturing within the machine tool is a simple task and completely automatable. The machining procedure is usually, but not always, limited to one side of the block. The block is removed once the first machining procedure is finished. The workpiece is placed back into the encapsulation machine and the features that have been machined into the block are covered with the lower melting material in order to restore the block to its original

rectangular shape. Once remolding is complete, the block is placed into the machining center again so that additional features can be placed on the present or another side of the block. These steps, the machining and refilling, are repeated until all features have been machined into the block. After such time, the block is taken out of the machine tool and its temperature raised above the melting point of the encapsulant but lower than that of the original stock. After the entire volume of the encapsulant has been liquefied and has drained away, the finished piece can be easily extracted.

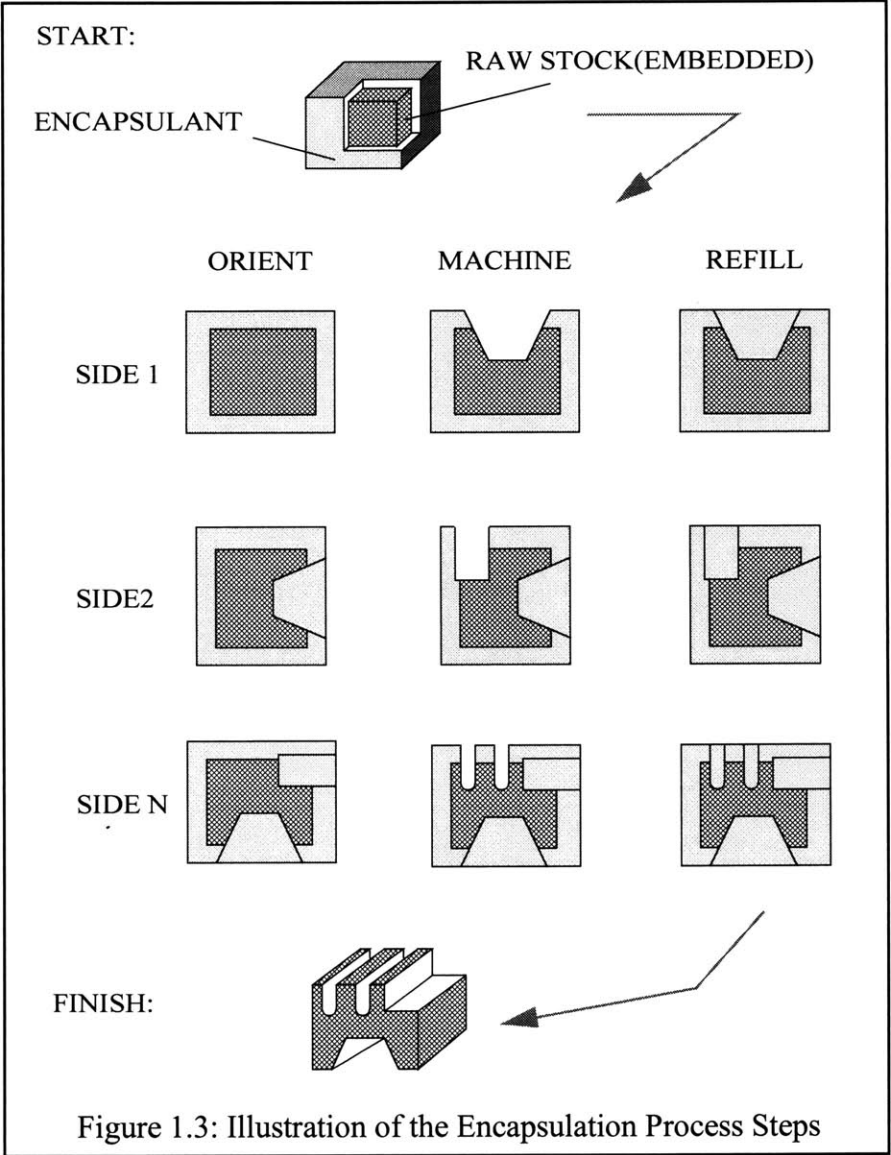


Figure 1.3: Illustration of the Encapsulation Process Steps

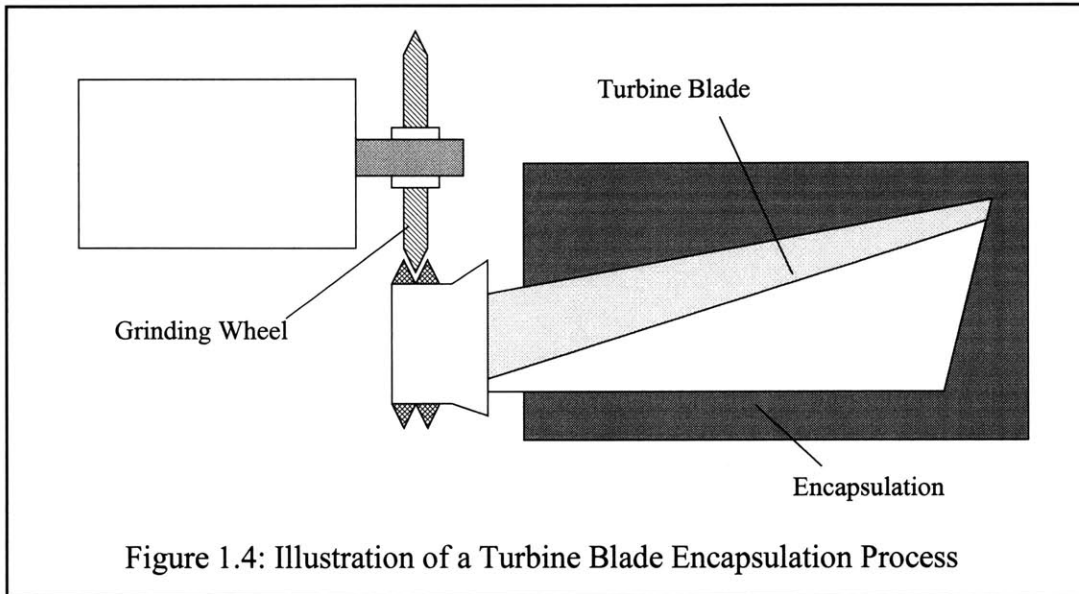
This process plan is a modification of the classical encapsulation technique described in research literature in the 1980's. The usage of locating dies is avoided by prohibiting features to exist in the workpiece before encapsulation. The locational datums are taken from the precision molded walls of the encapsulation cube. All features machined into the block after the encapsulation is referenced from those walls. While this constraint prevents RFPE fixturing from being used for every fixturing scenario, the following chapters will show that a variety of applications exist for RFPE fixturing and that it will provide a tremendous amount of utility to manufacturing in general.

1.4 Encapsulation in Industry

Phase change encapsulation fixturing, by itself, is hardly a new idea in the machining and manufacturing industry. One of the most prevalent uses of phase changing fixturing is in the aerospace industry. Manufacturing turbine blades is a particularly challenging task. Fixturing these oddly shaped turbine blades for machining has received a large amount of attention. Many of the industry's technology leaders have turned to encapsulation to fulfill their fixturing needs.

Pratt & Whitney's North Haven, Connecticut facilities use a modified encapsulation process to fixture post-cast turbine blade in order to grind tail features into the blades which allow the blades to be inserted into the main turbine hub. The plant itself was built in 1953 but only started to use encapsulation fixturing in the early 1970's. The entire factory floor is setup to handle every facet of encapsulation. Special workholding devices have been designed to locate and hold the turbine blades while it is being encapsulated. Each encapsulation cell is manned by one operator, inserting new blades into the workholding/molding device and removing an encapsulated one roughly every 5 seconds. These encapsulated blades are then moved to a different cell where they are automatically

located and fixtured within a grinding machine. Once machined, they are then transported to the encapsulation removal stations. Loaded into a high pressure steam chamber, the encapsulation surrounding the turbine blades are melted off and the finished blades are inspected for residue [Sprinkle 96].



1.5 Material Selection

One of the key factors to the success of designing an autonomous fixturing system using encapsulation is the selection of the encapsulating material, the encapsulant. Thus far, the materials that have been investigated are fixturing polymers such as RigidaxTM and Freeman'sTM machinable wax, fusible alloys such as alloys of tin and bismuth, and various types of higher melting temperature engineering plastics such as acetels, acrylics, nylons, and polycarbonates, which have found success in other molding processes such as injection molding. In choosing the encapsulant, one has to take into account the hardness and stiffness of the material, its machinability, thermal conductivity and moldability, the intensity of its adhesion to the workpiece, its melting temperature, its coefficient of

thermal expansion, its ease of reclaim, the stability of these properties after numerous reclaims, and, of course, its price and its safeness. Many of these selection criteria result in conflicting functional requirements. The following section describe the trade-offs in choosing certain materials and provide justification for those decisions.

1.5.1 Selection Criteria

The primary objective in selecting an encapsulant is to minimize the molding cycle times while also maximizing the quality of the moldings. The quality of the molding can be defined by many parameters such as the accuracy and the level of surface finish attainable through molding and through machining once encapsulated. Furthermore, these two objectives are balanced by a third, that of minimizing the cost of support equipment such as the injection machine that must handle and deliver the encapsulant. And of course, all these considerations are blanketed with the need to produce a safe and healthy working environment.

The material properties that been have identified to be important are the following:

- **Yield Strength/Young's Modulus:** For precision machining, the encapsulant should have a high Young's modulus, but have a fairly low yield strength. This allows the encapsulant to be more machinable while also minimizing the errors in deflection caused by the cutting forces in the machining process.
- **Thermal Conductivity:** A high thermal conductivity aids in cooling the encapsulant quickly once molded, allowing the encapsulation cycle time to be reduced. However, high conductivity will result in a high rate of heat loss and a likelihood of premature freezing during the molding process if the encapsulation stream comes into contact with a cold surface. This can result in short shots or scarred surfaces. Maintaining a

warm mold will thus be a requirement of the molding system if a high conductivity encapsulant is used.

- **Viscosity:** A low viscosity allows for easier delivery of the encapsulant to the mold at lower temperatures. Less pressure is needed to deliver the encapsulant, thus reducing the cost of the injection piston system. However, low viscosity also encourages flashing during the encapsulation and a variety of sealing complications.
- **Melting Temperature:** A lower encapsulant melting temperature allows for less complex molding devices. Since the temperatures on the mold and delivery systems do not need to be set as high, there can be less insulation around the heaters, and the heaters themselves need not be as large or use as much power. In addition, since machining is performed on the encapsulation at room temperature, a lower melting temperature reduces the temperature change the encapsulation must endure between molding and machining. This reduces the effects of thermal strains caused by the mismatch in the coefficients of thermal expansion between the encapsulant and the stock within.
- **Eutectic/Non-Eutectic:** A eutectic encapsulant need not be super heated to ensure low viscosity during injection and subsequently would not soften the existing encapsulant that already surround the workpiece. However, there are drawbacks in using an eutectic alloy. Most notable is the sealing/dripping difficulties and the flash that arise around mold mating surfaces. Eutectics exhibit a sharp change in viscosity at its melting temperature, and therefore it is very difficult to control a eutectic's viscosity through temperature. Eutectics can, thus, only be used as either a hard solid which will not flow and a low viscosity liquid that will readily flow. On the other hand, a

non-eutectic, because it has a melting range, will gradually soften with the increase in its temperature. Thus the control of its viscosity can be done quite easily by controlling its temperature. The encapsulant could be injected at temperatures where it exists as a fairly viscous liquid, preventing any dripping or flashing. Encapsulation using a higher viscosity encapsulant would allow less stringent flatness specifications on mold mating surfaces. Also, when the mold is open, the surface tension of the high viscosity encapsulant would be enough to prevent dripping from the gates. There would be no need to design valving within the gates.

- **Coefficient of Thermal Expansion:** It is advantageous to minimize the coefficient of thermal expansion in order to reduce shrinkage after cooling. In fact, the encapsulants should be formulated with a slightly negative CTE so that blocks will expand to fit the molds more accurately and grasp the workpiece upon cooling.
- **Chemical Interaction:** It is important that the encapsulant can be fully melted away from the workpiece once all the milling operations have been performed. The encapsulant must not disturb the surface finish of the finished part, alter its molecular state, or become permanently bonded to the workpiece. Trace amounts of the encapsulant in the workpiece can render the part useless for its intended application.
- **Damping:** encapsulants that can add extra damping to the fixturing system will reduce chatter during machining and thus increase the overall accuracy of the machining process.

- **Surface Energy/Adhesive Properties:** A less obvious material property is that of the quality of adhesion of the encapsulant to the stock. Without fairly good contact between the encapsulant and the workpiece, gaps will form from trapped air bubbles and shrinkage. When machining is performed, capillary action will tend to pull suck machining coolant in between the block and the encapsulant. As a result, the block will float slightly and jitter as it is machined. Good adhesion between the block and the encapsulant will prevent this by firmly anchoring the workpiece to the encapsulant and ensuring good contact. However, this will also complicate the melting/removal process, requiring agents and solvents to aid in the debonding for the encapsulant from the workpiece. The introduction of encapsulation under pressure may reduce the need for good adhesion.
- **Safety and Health:** Besides obvious reasons, an encapsulant should be chosen such that it does not possess particular danger to those who interact with it. Hazardous materials will increase system and process costs and complexity. Dangerous materials require special equipment to handle and treat it. Cleaning apparatus needs to be installed to insure that waste from the process does not affect the environment. A variety of safeguards must be set in place to deal with potential accidents and mishaps.

1.5.2 Fusible Alloys

This research has primarily relied upon a Bismuth/Tin eutectic alloy for encapsulation. Widely available, this eutectic binary alloy is composed of 58% Bismuth and 42% Tin. The alloy has a low melting point of 411.5K. It has a reasonably high Young's Modulus of 7.5GPa and an adequate yield strength of 60MPa. Its thermal conductivity is 18.4W/mK. Its thermal expansion efficient is 15 e-6/K. It has good stability properties.

The main disadvantage is that it has a high surface energy and thus will not easily wet most metallic materials and other materials that will easily oxidize.

Tin/Bismuth alloys fall within a broad class of alloys called fusible alloys which are low melting temperature metallic alloys. In general, they are used as solders or braises. Most contain lead and many contain cadmium. Since both lead and cadmium are carcinogenic, developing an encapsulation process using an alloy composed of either will not only become extremely hazardous but also cumbersome to the process.

Taking these considerations into account, the alloy that has been used as the primary encapsulation material was chosen specifically because it contains no substantial amounts of lead or cadmium. The fact that it also happens to be a eutectic and thus compliments other criteria is fortuitous. There are other combinations of the bismuth/tin binary alloy that are potentially useful in our study. There is a 40/60 bismuth/tin alloy that possesses a melting range on 411.5K to 441K. It has many merits that the eutectic does not possess. For example, its thermal conductivity is twice a large, at about 29.6W/mK. The growth and shrinkage of the 40/60 alloy is also significantly reduced.

1.5.3 Fixturing Polymers

While fixturing waxes, such as FreemanTM machinable wax can be easily machined, melt at low temperatures and provide considerable damping to the fixturing system, they have low thermal conductivity, high shrinkage, and very poor mechanical strength. Maintaining a good surface quality on such a soft material is extremely difficult if not impossible. The low conductivity and high shrinkage often causes sinks and bows on the surface of the moldings. What is more, there is a severe thermal expansion mismatch between the machinable polymers and most metals that will cause the encapsulation to crack and disintegrate upon cooling around its workpiece. The RigidaxTM machinable polymers possess fairly good adhesive qualities, adhering to metals and other materials

reasonably well. However, visco-elastic and adhesive properties cause the material to gum up endmill flutes and result in poor machinability. For this application, fixturing polymers proves to be unattractive.

1.5.4 Engineering Plastics

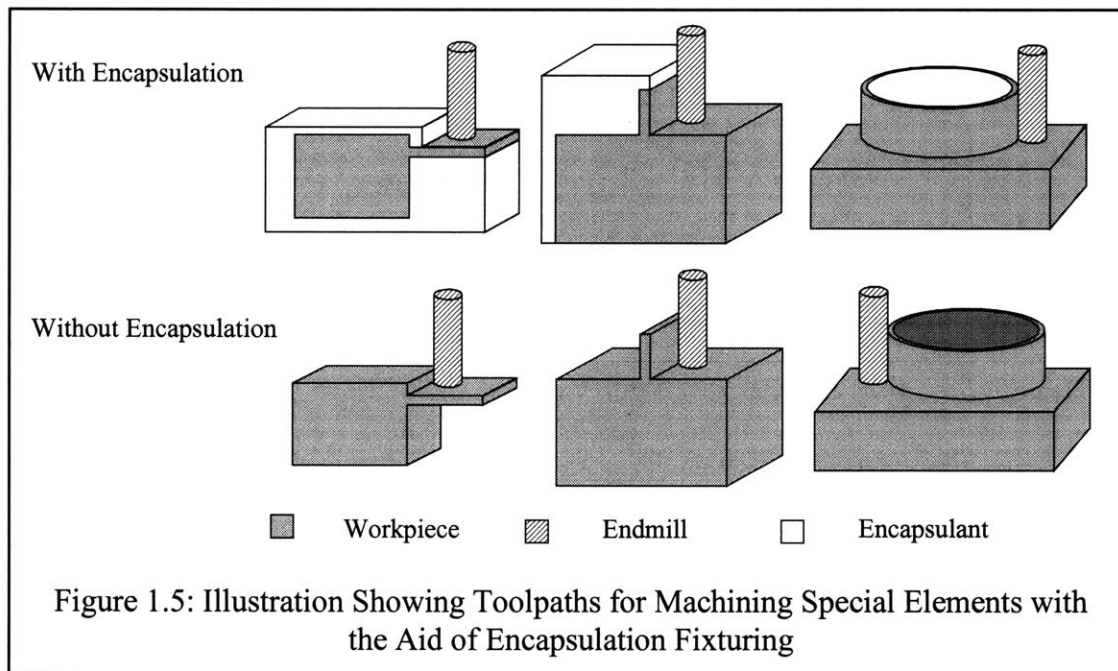
Engineering thermoplastics, which have been used in industry in many plastic molding applications, are not much better suited for encapsulation. Their high shrinkage is a major disadvantage. While shrinkage and sinks can be alleviated by using a packing routine during the encapsulation/injection process, sinks and bows are still visible when the thickness of plastic parts become substantial. While their mechanical properties are very appealing, they are non-eutectic and possess very high process temperatures. NylonsTM melt at 500K and Acetels (DelrinTM), 530K. Also, engineering plastics possess thermal conductivity an order of magnitude lower than fusible alloys, averaging about 2.3 W/m^oK. In general, they are difficult to machine compared to the other two material types. Because of their high strengths, milling will generate considerable heat which can not be dissipated due to the low thermal conductivity materials. As a result, endmill flutes often clog when the material removal rate is too high. Acetels are possibly the only exception.

1.6 Advantages Other Fixturing Methods

Having familiarized ourselves with encapsulation as a fixturing process, it is appropriate to return to the beginning and develop the reasons for developing the universal fixturing system using phase change fixturing methods. Within this section, the focus is to discuss the advantages of fixturing through encapsulation and its ability to accomplish tasks that no other fixturing process can.

1.6.1 Ease of Automation

Encapsulating the raw stock constrains the part shape to a generic norm, in this case a rectangular block with perfectly perpendicular walls. This constraint allows for a more intelligent workholding design. It allows one to easily design an algorithm that will carry out accurate/repeatable workholding of any arbitrarily shaped part. References are continuously maintained during setup changes using the boundaries of the filler block, which are independent of part features. Workholding can thus be easily automated since the fixturing system need only interact with that one generic norm and not tens of thousands of different geometries.



1.6.2 Machining Thin Members and Odd Shapes

Encapsulation can be used to fixture almost any arbitrary shape. Delicate features, such as spring elements, ribs, and thin walls, can be machined. Encapsulation fixturing provides the ability to machine features onto those spring elements without worry of deflection or deformation of those features. As shown in Figure 1.5, the encapsulation can

be filled so that it directly supports the feature while it is being machined. The encapsulant can fully support thin elements regardless of their location within the workpiece. For these special features, the remolding pattern must be carefully planned. Only one side of the feature can be cut in one pass. The workpiece must be remolded and the feature refilled before machining can proceed to the next side. It should not be difficult to develop CAD/CAM programs capable of identifying these thin features, which have large length to width ratios, and automatically plan the proper tool paths and remolding sequences.

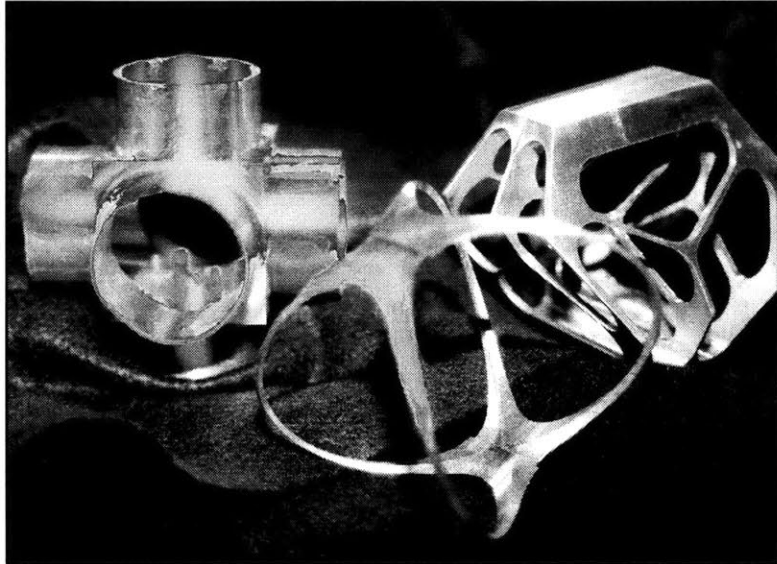


Figure 1.6: Photograph of sample parts machined using encapsulation fixturing

Parts that once needed to be machined separately, because of fixturing constraint, and then assembled later, can now be machined out of one piece, cutting assembly time and costs. Ordinarily, the three tube elements, shown in the back left in Figure 1.6, would be machined separately and then welded together. Here, encapsulation allows the machining of all three tube elements from the same piece of stock. The tube walls are all less than

0.01” thick and more than 1.00” high. The orb shaped part, shown in the front in Figure 1.6, and the intricate webbed part shown right back in Figure 1.6 were both manufactured on a 3 axis milling machine, out of a single piece of stock, despite their delicate spars. Without encapsulation, both parts would be extremely difficult to fixture and machine. Most likely, more expensive, time consuming manufacturing methods, such as wire electro-discharge machining, would have been used to manufacture these parts had encapsulation fixturing not been available.

1.6.3 Developing Manufacturing Processes Without Hard Tooling

While this encapsulation fixturing process was never designed to replace hard tooling in a mass production environment, it can be used during the preliminary stages when developing a mass production facility. During the preliminary testing of a manufacturing plant, machine tools and other equipment are constantly being changed and retrofitted in order to optimize the plant and increase the production rate and efficiency. Unfortunately, while machines can usually be sold or redistributed to others parts of the plant, changes in the plant layout usually result in changing to new types of tooling and fixturing system, leaving the old hard tooling, useless.

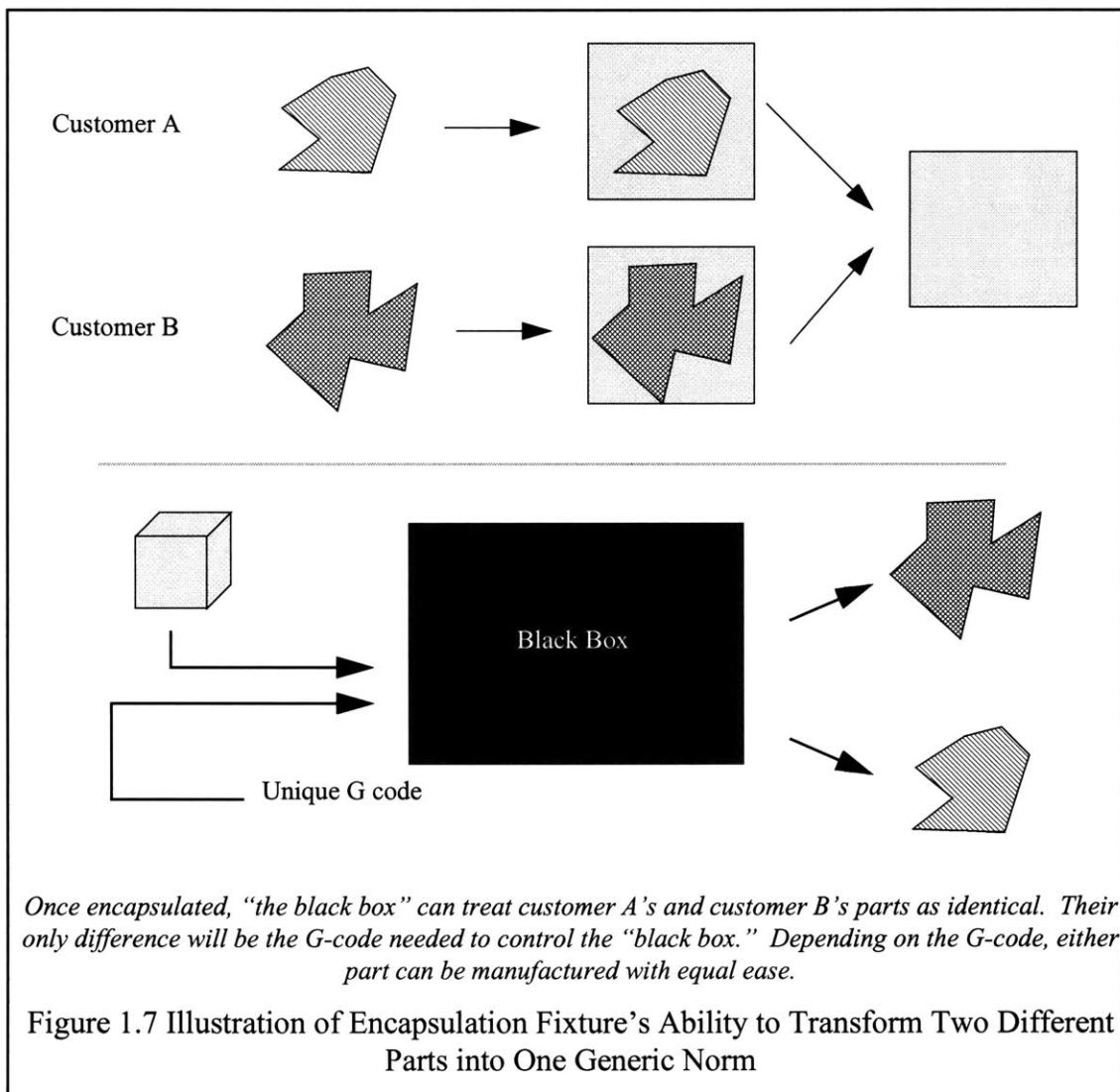
Instead, manufacturing engineering can develop their processes using the same universal fixturing we are developing. Once the machines and support equipment have been debugged, the encapsulation fixturing can be replace with permanent hard tooling. Such a practice removes the possibility of scrapping a piece of hard tooling because of equipment changes.

1.6.4 Machining Parts in Small Batch Sizes

The next frontier in manufacturing is likely to be in single part production, that of producing goods customized to the individual, on demand. It will be the ability to

manufacture one part as inexpensively and as efficiently as one thousand parts that will revolutionize the industry. An automated universal fixturing system will play an important role in achieve these goals.

Developing our fixturing system through encapsulation brings us one step closer to those goals. Once encapsulated, different parts are treated by the workholding device as the same. Thus, multiple parts can be machined in the same fixturing setup. There is no need to change setups and there will be no down time for the machine. With encapsulation, we can turn a mass production machine into a rapid prototyping machine.



1.7 Summary

The decision to develop the universal fixturing system through a modified phase change fixturing technique is justified by the fact that this technique possesses characteristic that none of the other candidates have. A host of features can be developed that will allow RFPE fixturing to be used in applications such as thin-wall sheet metal prototyping or one-off free form manufacturing. What remains to be discussed are the machines and systems needed to support the encapsulation process. The coming chapters will illustrate the state of the art in Reference Free Part Encapsulation fixturing techniques. Chapter 2 and chapter 3 shall describe the progress made in developing machine testbeds. The detailed machine designs shall be illustrated and key components of the machines will be elaborated upon. Within Chapter 4 and chapter 5, simulations which model the RFPE process are presented. These simulations give a better description of the effects of certain process parameters, such as injection temperature and mold preheat temperature, on encapsulation quality. Chapter 6 documents a case study in which the RFPE fixturing process is compared to conventional fixturing procedures. A picture of the effectiveness, both in terms of time and in cost, of RFPE fixturing is developed. Lastly, chapter 7 concludes with results of the testing done on the testbeds as well as recommended future works. From this research, it is possible to extrapolate industrial applications for which RFPE fixturing can be immediately applied with great benefits.

Chapter 2

Development of the Encapsulation Techniques

2.1 Process Classification

The encapsulation system is the key to making fixturing universal and automatable. The encapsulation system allows for the automatic fulfillment of the three basic functions of fixturing—the location, support, and immobilization of a workpiece during a machining process regardless of environment. To accommodate the different sizes of workpiece that might be used, different sized encapsulated blanks are produced. Therefore, one simply has to choose the best suited size to use to machine the part. Just as the paper industry does not create an infinite number of different sizes of paper for their users, the strategy of this method will also be only to allow users to machine parts using standard encapsulation sizes. Sizes of 1, 2, 4 and 6 inch are suggested as a baseline.

In addition, not only is it necessary to create discrete sizes of encapsulations, it is also beneficial to produce different types of molds for three distinct machining strategies. By splitting the machining into these strategies, one can increase the efficiency of the encapsulation fixturing system without increasing the complexity of the encapsulation process by too much. The three strategies are described below.

2.1.1 3-D milling

This is the broadest machining strategy. With this encapsulation, one can machine features in any orientation of the part. In any of the six orthogonal sides, a feature can be placed without any obstruction from the fixturing device. In this situation, the locational datum constantly change from setup to setup. Thus, it is necessary to keep track of them and insure that they remain true. This strategy is the most difficult to implement—the molding and the re-molding must be done

with great precision. The resulting molds are especially complex. A two-piece mold must be used in order to correctly form the main cavity and to facilitate part removal. This strategy does offer the most freedom and functionality. However, depending on the application, the other two strategies are equally vital and useful to the successful and cost-effective implementation of a fully automated universal encapsulation fixturing system.

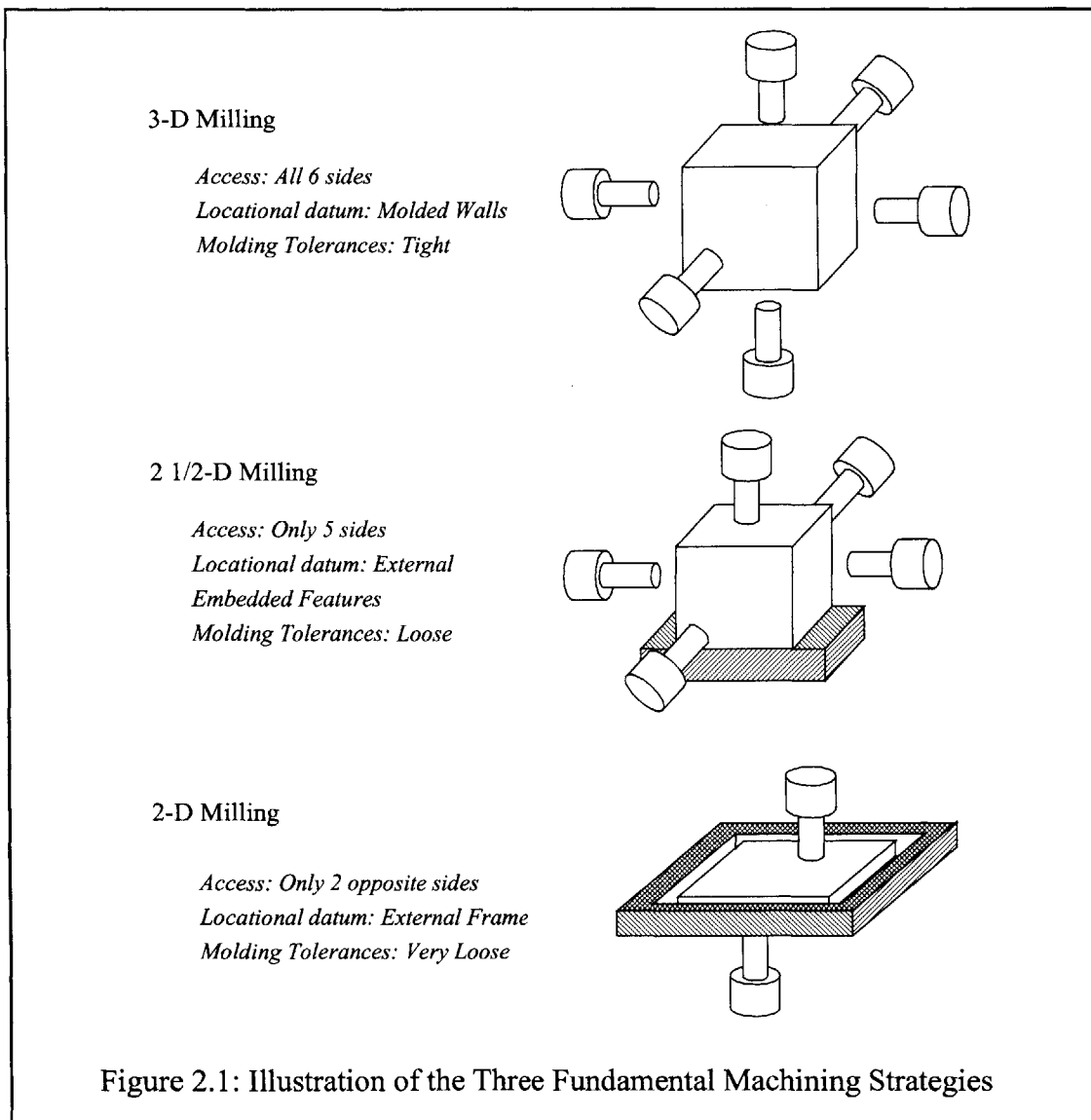
2.1.2 2 1/2-D milling

Slightly less complex, 2 1/2-D milling involves machining only five out of the six sides of a workpiece. Many times only 4 sides of the encapsulation will need to be machined. In these situations, multiple setup are still needed but only one set of locational datums is use to locate the part for all setups. Usually, a fixturing element is embedded into the sixth unused side during the encapsulation process and it serves to locate the part and anchor it to the fixturing device. The encapsulation material still serves to immobilize and support the workpiece. In this situation, it is not necessary that the molded walls be formed or reformed with such tight tolerances. Thus, the molding devices need not be so complex or machined to such tight tolerances. In addition, because the molded walls are not being used to locate the workpiece, draft angles can be used in each of these molds to facilitate part removal. This allows us to remove the perpendicular parting line within the mold and build a single piece mold. Despite its many advantages, this strategy does obscure and prevent one direction from being accessed and thus limits its use to only a certain class of parts.

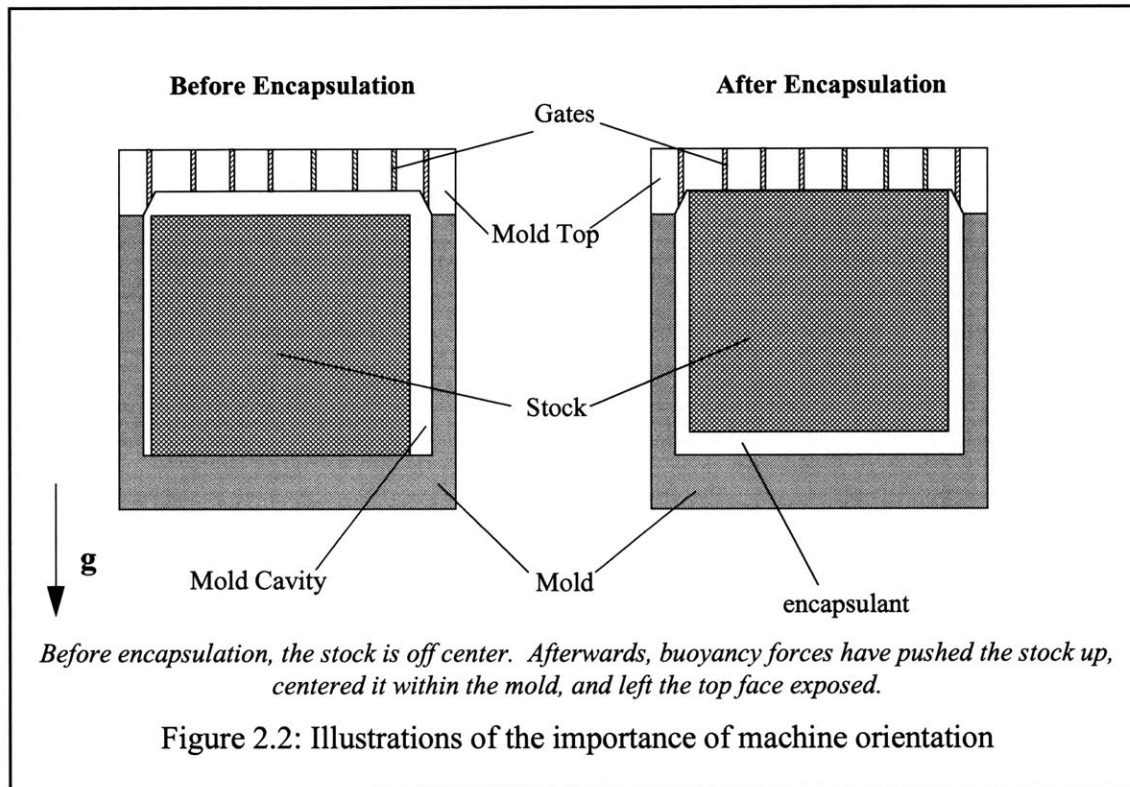
2.1.3 2-D milling

The most simple of the three machining strategies, 2-D milling involves placing features on only two opposite side of a piece of stock. Similar to the 2 1/2-D setup, its locational datums never change, always obtained through some external feature embedded into the encapsulation. The stocks that will be machined are dominantly plate form. This allows the simplification of the

mold design, even further. In this case, the embedded external features, used to locate the workpiece, is actually used to form the mold itself. The entire structure is transported between the encapsulation machine and the machine tool. The internal pocket of the mold/fixture do not need to be particularly accurate since the workpiece is never removed from the mold itself. Parting lines for the mold lie in one plane. Sealing can easily be accomplished using rubber gaskets. This strategy is by far the most easily implemented strategy of the three. But, of course, it is only suitable for a special group of parts.



2.2 The Importance of Orientation



The orientation of the molding system is very significant. A secondary objective of the initial encapsulation process is to only form five of the six sides of a cube. The sixth side should be left exposed so that machining can be done to that side immediately without having to machine away the encapsulant. A molding system that would mold only five sides of a block would prove to be advantageous and optimal.

To facilitate this, the clamping system is positioned upright and vertical. Since the encapsulant, in our experiments we were using a Bismuth/Tin alloy, is usually denser than most machined materials, we can expect the block to float to the top of the mold and mate with the mold top. By positioning the clamping machine in this direction, we can automatically, and with great ease, mold around five of the six sides of the rough-cut stock. The top side, the side that floats up and mates with the ceiling of the gateplate, is left exposed and available to be machined immediately. In addition, a chamfered feature is placed on the top portion of the mold cavity to

center and locate the workpiece as it floats up. The chamber features align the workpiece correctly and ensures that a uniform thickness of encapsulant surrounds all sides of the block. No features protruding from the sides of the mold walls are needed to hold the stock in place during encapsulation. These features would have complicated the removal of the encapsulated block from the mold and create undesirable divots and holes in the molding.

Orientation also plays a role in encapsulation quality. For example, if instead, the gates were located at the bottom of the mold and the injection stream traveled upward, the stream would impinge upward upon the previously molded encapsulation alloy during the re-encapsulation stages. However, since the mold does not fill instantaneously, much of the stream would not remain on the impingement surface. Instead, because of gravity, the liquid injection stream would fall to the bottom of the mold and slowly meet the old encapsulation layer as the mold filled. The extra distance the injection stream must travel, first upward, then downward and slowly upward again as the mold fills, cools the injection stream to the point where it no longer carries enough heat to superheat the previously molded encapsulation layer and dissolve the oxide layer that inhibits welding. The result would be a weak weldline between new and old encapsulation layers. Weak rewelding, of course, destroys the functionality of RFPE fixturing. Chapter 4 will discuss weldline quality in greater detail.

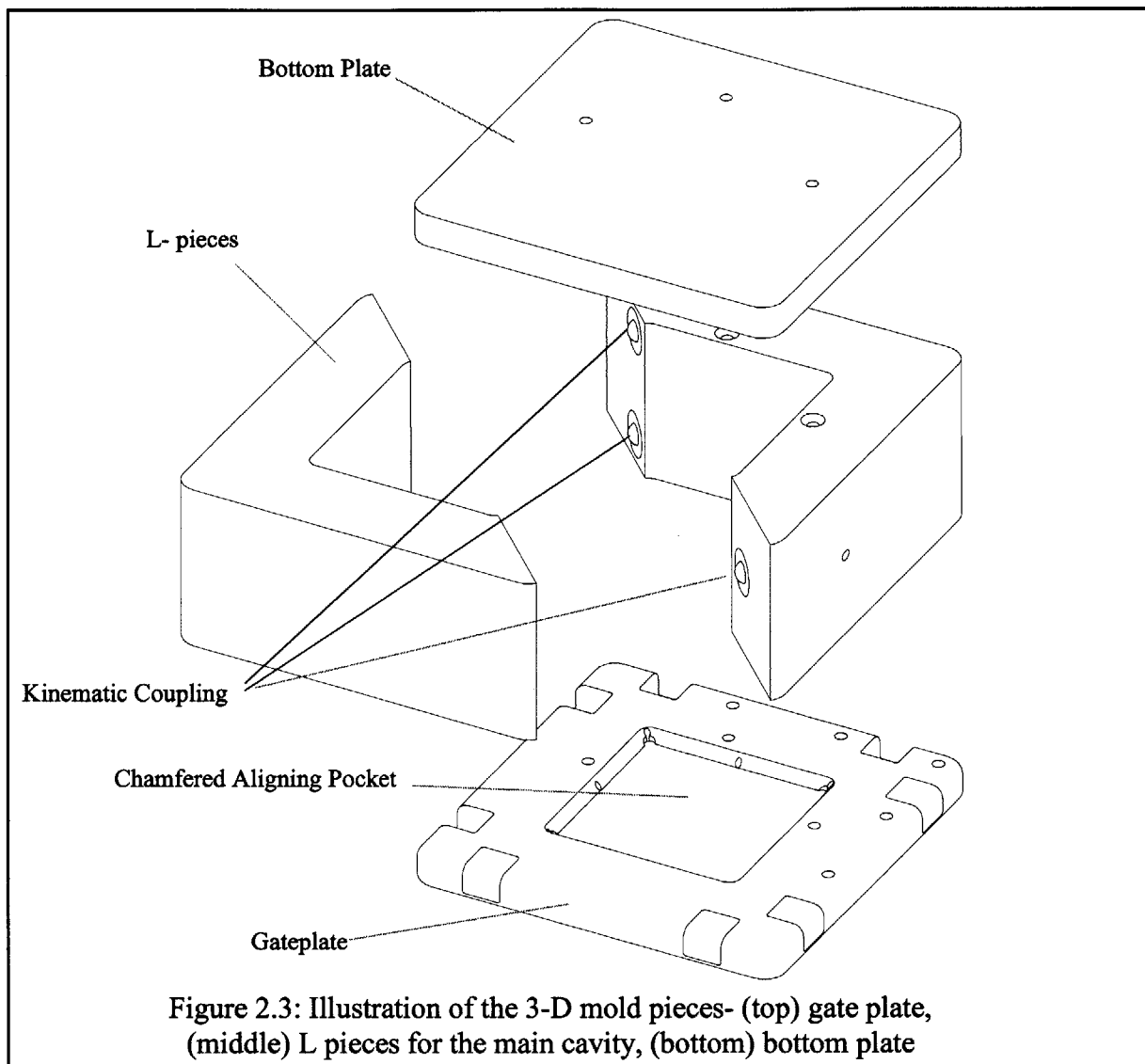
2.3 Molds

As was previously described, molds used for encapsulation are categorized in two ways, size and machining strategy. The more distinct classification refers to the machining strategy or "access" strategy and they have been named 2-D, 2 1/2-D and 3-D machining. Despite the differences in molding requirements, the embodiments of the molds can be generalized into three different types of components. They are the gateplate, through which the encapsulant enters the mold, the mold walls, which forms the molding chamber, and the bottom plate.

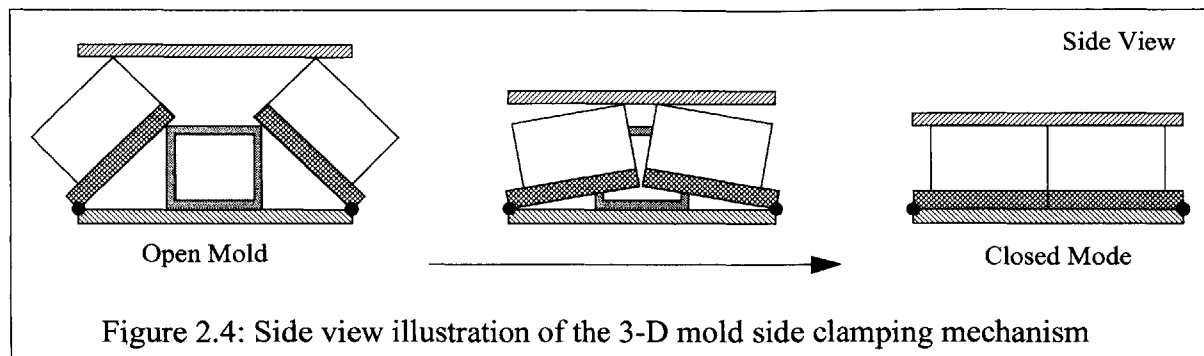
2.3.1 3-D molds

The 3-D mold is basically composed of 4 pieces. Assembled together, these four pieces create a perfectly cubic mold cavity in which the encapsulation of the rough-cut stock occurs. The pieces can be described as two plates, the top gateplate and the bottom plate, that sandwich two "L" shaped pieces. In the bottom plate a single square pocket is machined. Its dimensions are that of the finished cube and its depth is the thickness of the encapsulation layer that surrounds the stock. There is a 3-hole pin arrangement that allows the two "L" shaped pieces to locate and align to the bottom plate. To ensure that the two "L" pieces mate to each other repeatably, kinematic balls and V-grooves are manufactured onto the mating surfaces. In order to maintain a high tolerance in the mold cavity, the two "L"s are mated together machined as one piece using wire EDM to create the mold cavity. This assures that the mold walls are perfectly vertical and that the parting line exactly bisects the cube diagonally. If the parting line did not bisect the cavity diagonally, the encapsulation will become caught inside the cavity once the encapsulation material solidifies. The gate plate is located and mounted to the entire assembly using similar 3-hole pin arrangement. The top plate or gateplate also contains injection holes through which the encapsulant is delivered into the mold. A chamfer is machined into the gateplate so as to allow the stock to center itself during the encapsulation process. Furthermore, all mating surfaces need to be ground flat to ensure that they will be able to seal.

Because the 3-D mold cavity is composed of 2 pieces side, clamping action is needed to ensure the proper sealing along the diagonal clamping surfaces. The mold has been designed to use the vertical clamping force to transmit the needed side clamping action. The L-pieces are attached to mechanical pivots at their lower corners. It is very important that the location of the



pivots be place at the lower points of the L-pieces. Else, the L-pieces will interfere with each other as they pivot upwards. These pivots are spring loaded so that as the top gateplate is moved upwards, the side clamping device will automatically open the mold. As the top gateplate is lowered onto the mold, the pivots will shut the mold and allow it to remain shut for the duration of the encapsulation process. In this manner, only one clamping actuation source is needed thereby reducing cost and complexity of the clamping system.



2.3.2 2-D Molds

2-D molds are generally used to encapsulate plate stock or 2-D stock. In these cases, features need only be placed onto two opposite sides of the workpiece, instead of all six sides, as in the 3-D case. There are many advantages of using a 2-D when the situation allows it. The parting lines lie in one plane and are non-intersecting. Therefore, rubber O-rings can be used and sealing is fairly trivial. Also, since access is only needed in two directions, the other four can be obstructed. This allows us to develop a specialized fixture that can encompass the encapsulant and the stock. Thus, this fixture is used to locate and anchor the workpiece instead of using the molded encapsulant walls. Consequently, molding and injection requirements are not as stringent as before. No EDM work needs to be done to manufacture the molds, thus reducing the cost of these molds considerably.

Instead of being constructed from four pieces as the 3-D mold is, the 2-D mold can be constructed from 3 pieces, a bottom plate, a top plate, and a middle fixturing cage or frame. Again, injection holes are machined into the top plate to allow the encapsulant to enter the mold cavity. To locate the workpiece the, two precision ground dowel holes and pins are used to constrain the motion in the x- and y-planes. To constrain the z-plane, the frame is bolted down to a machine tool table via a fixture plate.

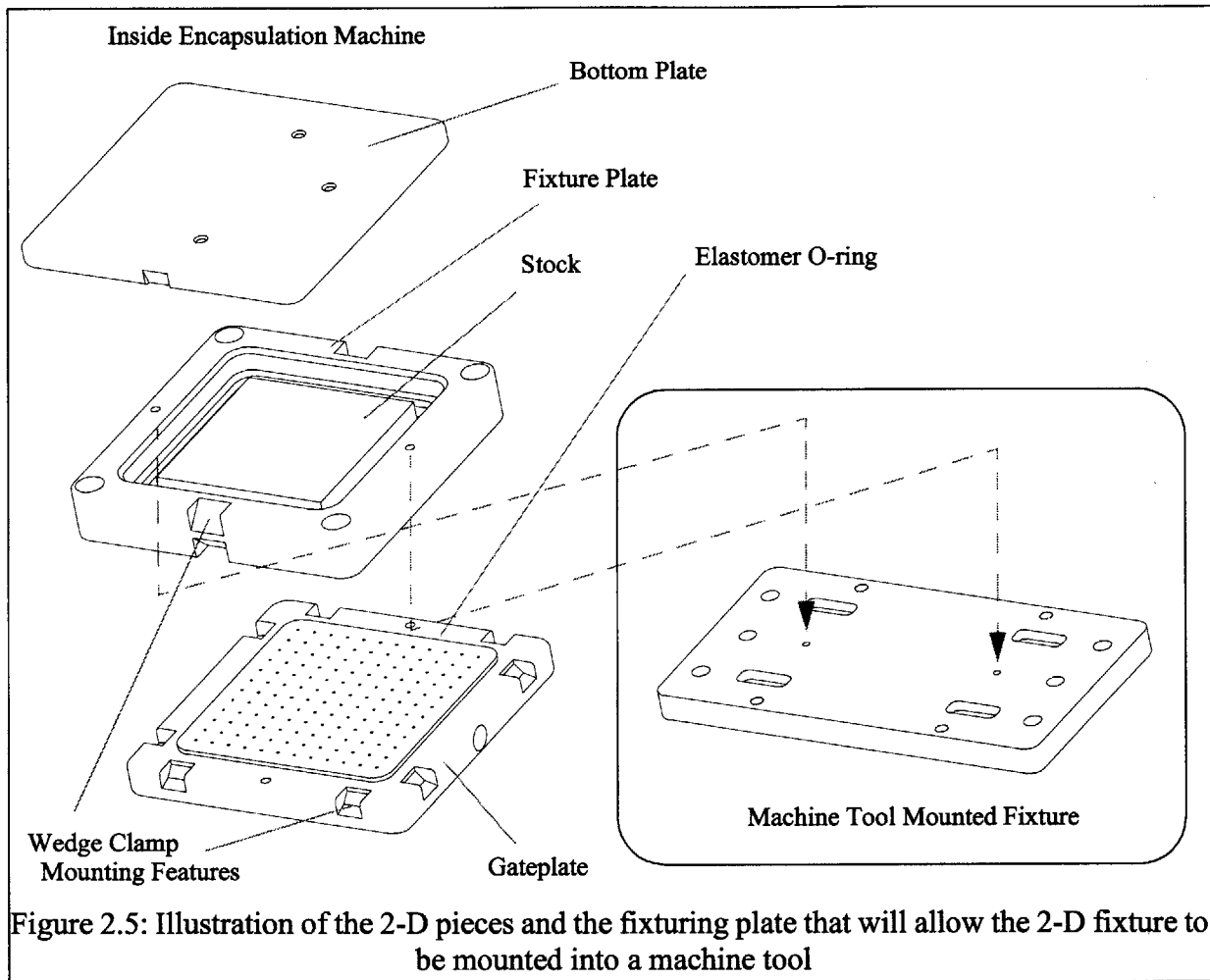


Figure 2.5: Illustration of the 2-D pieces and the fixturing plate that will allow the 2-D fixture to be mounted into a machine tool

2.3.3 2 1/2-D Molds

The 2 1/2-D class is designed to take advantage of the strong points of the two classes above. 3-D has far greater access capabilities and thus can machine more complex objects, while the 2-D has less stringent tolerances place on the manufacturing of the mold and thus will be easier and less costly to implement.

The 2 1/2-D molds allow access to only 5 of the 6 sides of a workpiece. The sixth side is obscured by mounting features, which mates securely to features of a vise, installed in a machine tool. Thus far, we have experimented with this technique using purchasable mounting systems

like those sold by the 3R Inc. The mount system that 3R offers can be index 90 degrees. Thus, four sides can be machined easily by rotating the workpiece and remounting the part.

Because the locational datums are not transferred through the molded surfaces of the encapsulation, but instead through the mounting features of the 3R device, the encapsulation accuracies can be relaxed.

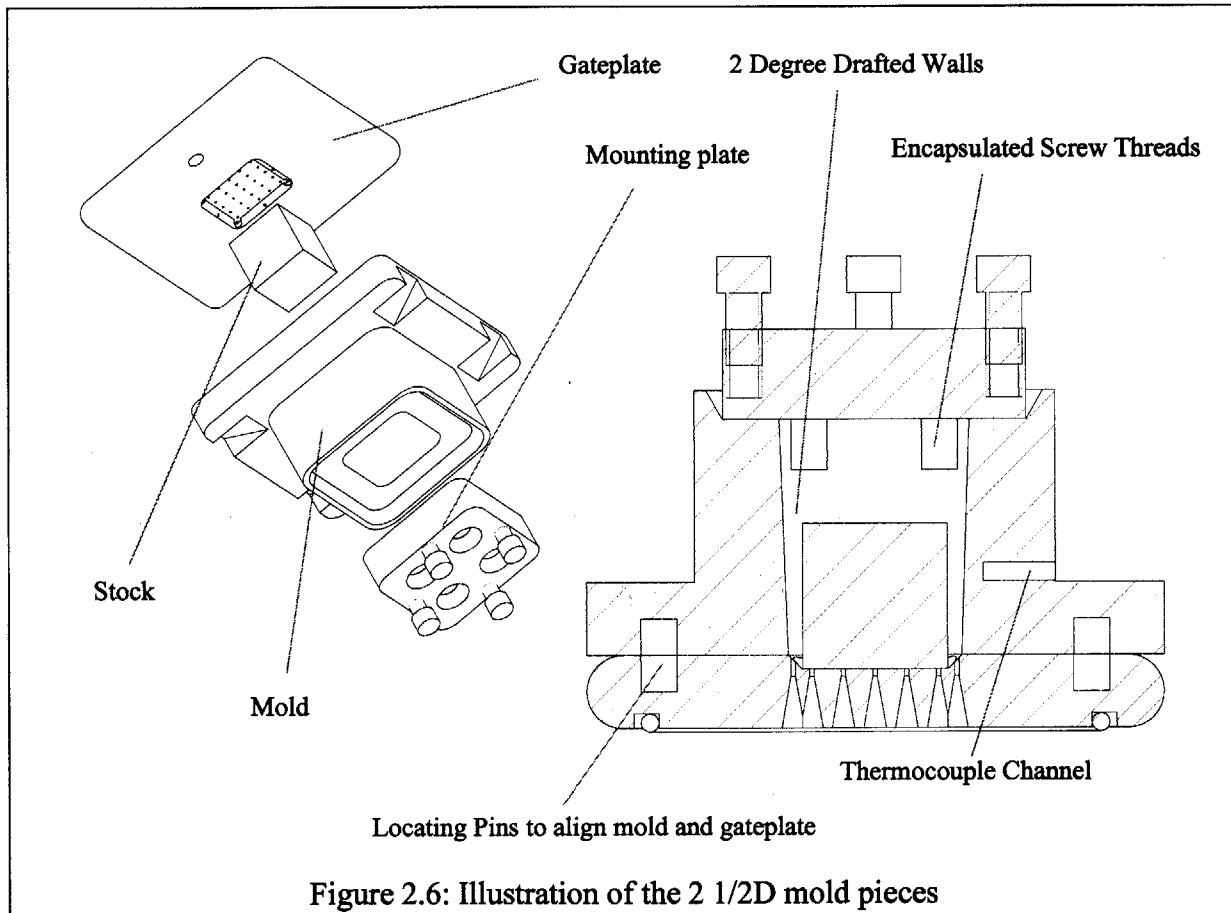


Figure 2.6: Illustration of the 2 1/2D mold pieces

Because the molded walls do not need to be perfectly perpendicular to one another, a single piece mold can be used to perform the encapsulation. Drafts can be placed into the mold cavity to facilitate the removal of the encapsulation. As in the 3-D mold, a chamfer is machined into the gateplate to allow the stock to float up and center itself. Instead of a normal bottom plate however, as in the 3-D case, a mounting plate is used. The mounting plate has protruding threads which become encapsulated and allow the plate to anchor itself onto the encapsulation assembly.

The other side of the plate contain features that allow it to be mounted onto the 3R device or any other commercially available fixturing system. This exterior fixturing device is then mounted onto the milling machine table through a mating device, which remains fixed inside the milling machine through out the duration of the operation.

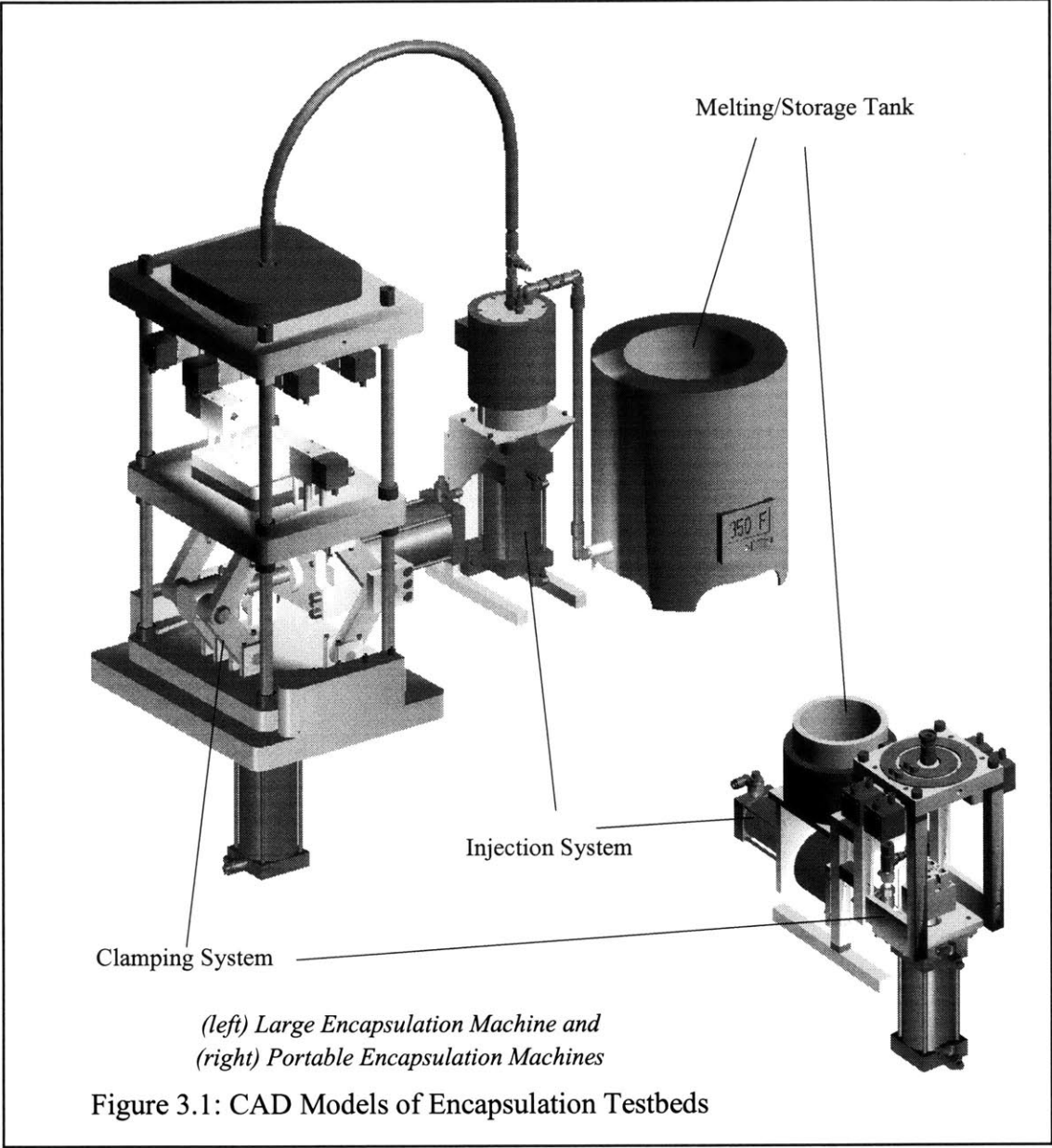
2.4 Summary

By classifying the encapsulation process into three types of machining strategies, it is now possible to develop specialized molds which meet the needs of each class. This not only allows for a more simplistic decoupling of the design requirements and constraints but it also allows the embodiments of the design to be more economical when the requirements and constraints of the fixturing are not as stringent.

The three machining strategies have been detailed in this chapter. Descriptions of each pay particular attention to how they are differentiated from each other. A set of hardware, the molds and fixuring devices, have been proposed which meet the needs of each class of encapsulation. It is now necessary to focus on the encapsulation process and to develop the machines and systems that will incorporate those manufacturing procedures.

Chapter 3

Encapsulation Testbeds



Two encapsulation systems have been developed in the course of this research. The first is a large machine, occupying roughly a footprint of 30" by 60". The second is a portable machine that can be easily transported by van. It measures roughly 10" by 25". Both machines perform roughly the same tasks. Their tasks are simply to melt the encapsulant, deliver it to the molding area under pressure, allow it to solidify and be removed. The major difference is their clamping capacity. The larger is capable of delivering more than 10,000lbs of clamping force, while the smaller can only deliver 1,000lbs. The larger machine was designed to encapsulate larger stock pieces, up to 6" by 6". The smaller was design to encapsulate stock no larger than 2" by 2".

3.1 Large Encapsulation Machine

The encapsulation machines can be broken down into three major sub-components—the clamping system, the injection system, and the melting/storage tank. Only two of these components are worth description in this thesis since the third, the melting tank, is readily available in industry.

The complete encapsulation system is illustrated in Figure 3.2. There is a hose that connects the melting tank to the injection piston and then to the clamping system. This hose allows the encapsulant to be transported between each of the different sub-components. The encapsulation process is as follows. The injection system generates a negative pressure inside its chamber and draws the encapsulant only from the tank. Check valves ensure that flow travels in the hose in only one direction. Once the injection piston is filled, the piston cup is driven forward, forcing the encapsulant into the clamping system. The injection stream enters a reservoir in the clamping unit and then into the molding chamber where it solidifies around a piece of stock and is subsequently removed.

The large encapsulation machine requires on 75psi of pneumatic pressure and requires 45A of 120VAC to power its heaters. There are 7 heating zones—the tank, the hose between the tank and

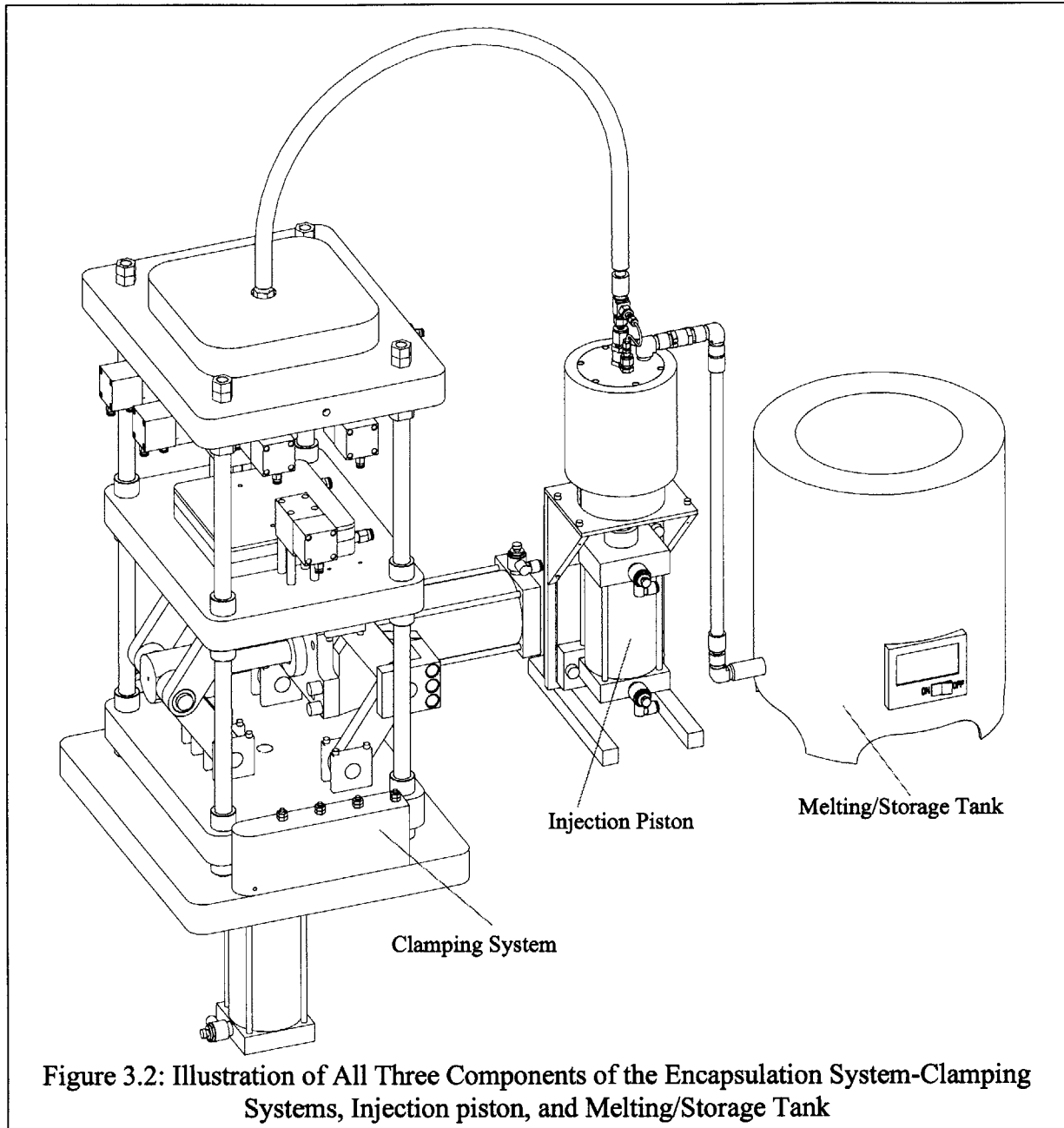


Figure 3.2: Illustration of All Three Components of the Encapsulation System-Clamping Systems, Injection piston, and Melting/Storage Tank

the injection system, the injection cylinder, the hose between the injection cylinder and the clamping system, the top of the reservoir on the clamping system, the reservoir cap, and lastly the mold heater below the mold. The heaters and pneumatics are controlled by a centralized computer based control system capable of switching 8 heaters zone and 8 pneumatics actuators, and reading up to 32 thermocouples.

3.1.1 Injection System

We recognized that the delivery of the encapsulant needs to be done under pressure to attain the sufficient molding accuracy and surface finish. This was experimentally shown by Fan in his masters research with Sarma in 2000 [Fan 00]. He showed that in order to attain a surface finish of “12 μ m”, which would provide acceptable fixturing accuracy and repeatability, one needed both a well finished mold and the addition of pressure to the encapsulation process. As shown in Figure 3.3, if the encapsulation is performed in a perfectly smooth mold, the minimum pressure required to attain the target encapsulation surface finish is 40 psi. As the roughness of the mold increases, greater pressure is needed. According to Fan, at about “2 μ m”, the surface finish attainable through conventional grinding operations, 65 psi is required to produce encapsulations at the targeted “12 μ m”. Thus low pressure encapsulation is considered fully justified and necessary.

To deliver the molten encapsulant at 65psi, a pneumatic injector system, comprised of a piston pump, valving and a pneumatic piston has been designed. It is able to inject the encapsulant in its liquid state at temperatures as high as 500K, at pressures as high as 250psi, delivering a volume up to 75in³. The seals around the piston and piston cup are maintained using commercially

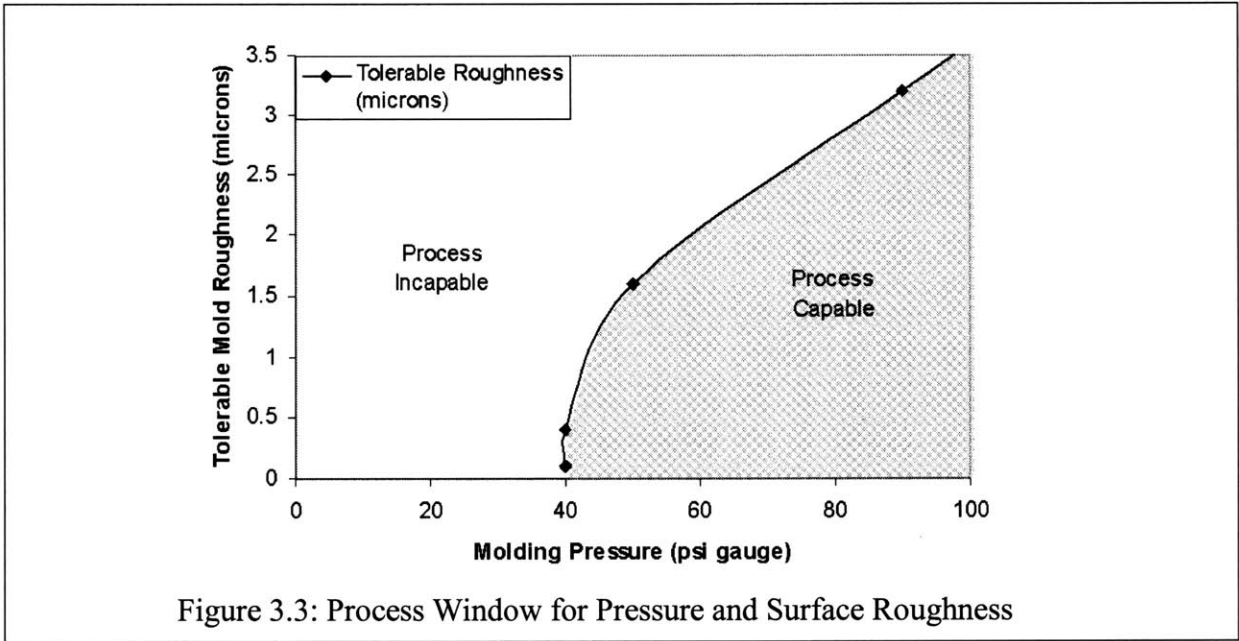


Figure 3.3: Process Window for Pressure and Surface Roughness

available Viton® fluoroelastomer O-rings. This injection machine differs greatly from conventional plastic injection machines in that it delivers the material at much lower pressures but in much greater volume. The injection cylinder is made of a stainless alloy to protect against corrosion and wear. The entire component, with the exception of the pneumatic actuator, is maintained at temperatures higher than the melting point of the encapsulant, using a ceramic band heater and some flexible heaters.

The injection flow piping/plumbing is also fairly novel. During the injection/filling cycle, it is necessary to hold the pressure and to pack the alloy into the mold as the encapsulant solidifies since the encapsulant will tend to shrink and leave voids and sinks. However, it is necessary to relieve that pressure after the injection cycle, in the mold and in the delivery system that connect the mold and the injection cylinder, so that when the mold is opened, excess encapsulant will not spill over.

To accomplish this task, there are two check valves that restrict the flow of the encapsulant to travel only in one direction, from the melting tank, to the injection piston and then to the clamping system and mold. There is also a third line that allows back flow from the mold to the injection cylinder. This allows the pressure within the mold to equalize to atmospheric conditions once the cylinder is contracted. Thus, when the mold is opened, the encapsulant, under no pressure, will not spill over the injection gates. The diameter of the third line is relatively small compared to the other lines. This restricts the flow to allow just enough of the encapsulant to flow back into the cylinder to equalize the pressure but not to create voids or a vacuum in the clamping system reservoir and injection lines.

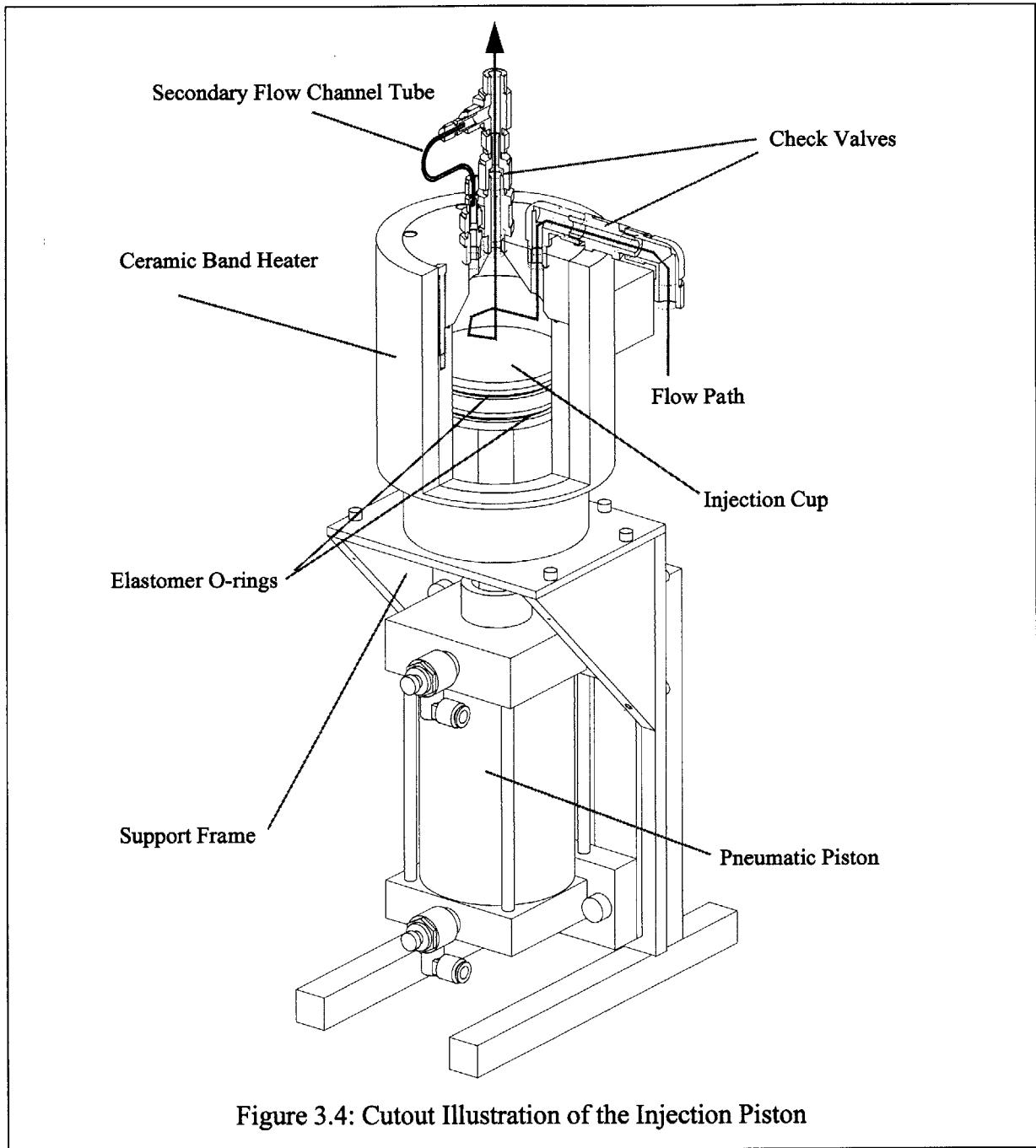


Figure 3.4: Cutout Illustration of the Injection Piston

3.1.2 Clamping System

The clamping device has a multifunctional role in the encapsulation process. Its primary purpose is to, of course, receive the molds and ensure that the molds remain sealed during the injection procedures. To be economical, the clamping system must be able to accept all the different types and sizes of molds that could and will be used. Therefore, the clamping unit is designed to be operated using two stages, both pneumatically actuated. The secondary stage adjusts the clamping height of the clamping walls, allowing the clamping system to receive molds of different sizes. Once moved to the correct height, locking blocks are placed underneath the stage to support the clamping load. A pneumatic piston directly actuates this secondary stage. The primary stage is coupled to the actuator through two four bar linkages. If directly driven, the pneumatic cylinders could only produce a clamping force of less than 1000lbs, given a supply pneumatic pressure of 75psi. With the mechanical linkage, the clamping force is increased 10 times. At the height of its travel, the primary stage can produce about 10,000lbs of force, given a 75psi pressure source. This would be sufficient to seal a 6" mold.

The alternative to the mechanical linkage design is to use of more powerful hydraulic actuators. Most hydraulic actuators are designed to exert greater force than pneumatics. Thus, in high pressure molding applications, such as conventional injection molding and diecasting, hydraulics are used to provide the clamping forces. However, using hydraulics increases the cost of the machine. Hydraulics require many auxiliary equipment that are not normally found in a machine shop environment, such as a hydraulic compressor and delivery lines. On the other hand, pneumatic pressure is readily available since all machine tools need a pneumatic source to operate tool changers or other subsystems of the machine.

The operation of the clamping unit is quite simple. The second stage pneumatic linear actuator drives the primary stage to the proper location, after which, locking blocks are placed underneath the stage to support the clamping loads. Since the sizes of molds are discrete, the

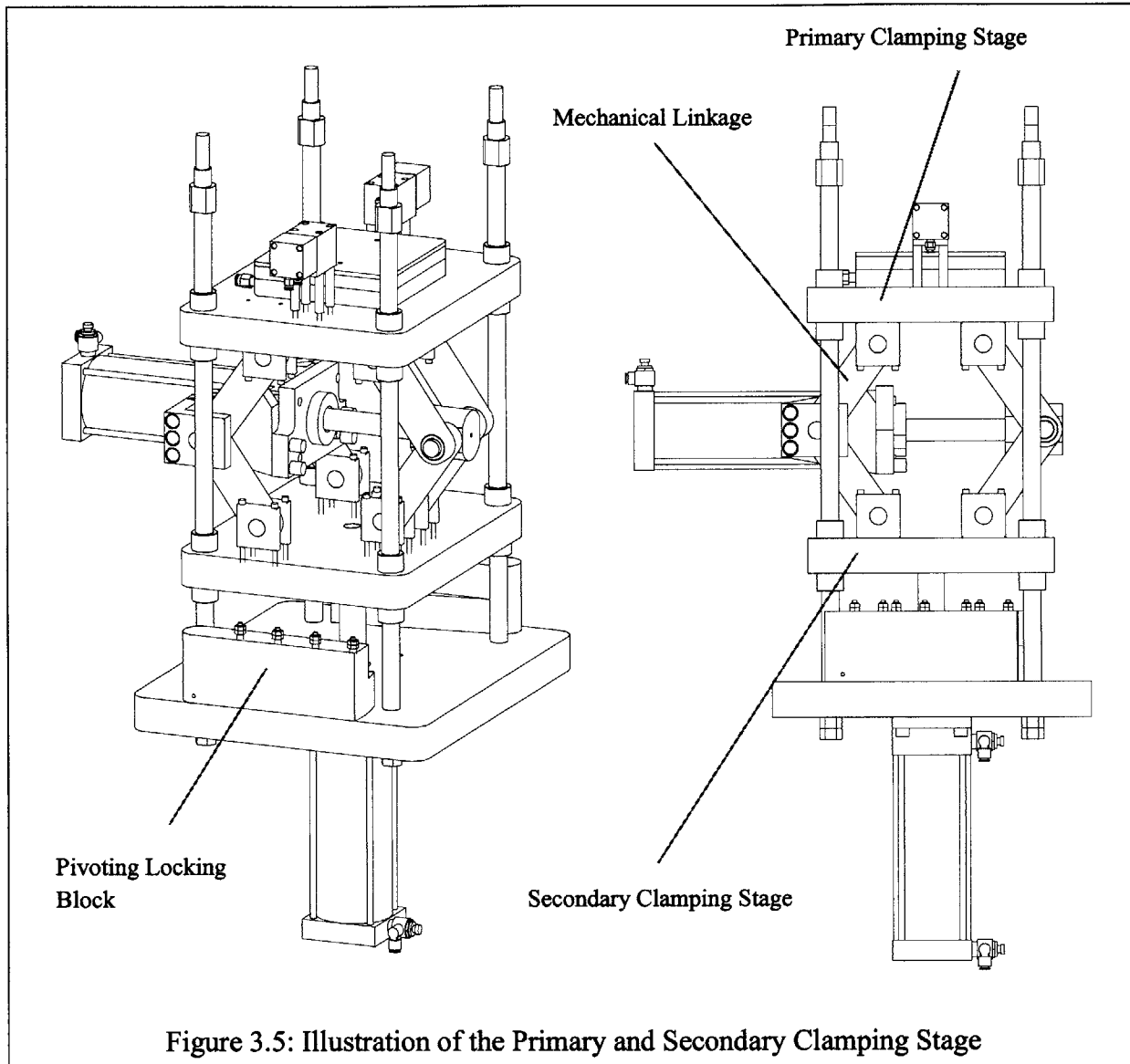


Figure 3.5: Illustration of the Primary and Secondary Clamping Stage

locking blocks have steps that are designed specifically suited for each mold size. Fine adjustment of the locking height is accomplished through sturdy bolts mounted on each step.

The second function of the clamping device is to aid in the delivery of the encapsulation material. Within the clamping device, located directly above the molds, there is a chamber we call the encapsulation reservoir. The reservoir holds the next shot of the encapsulant. Its temperature is monitored and controlled carefully through a computer based control system. Heaters are placed in specific location so as to achieve a uniform and efficient heating. One is

placed above the encapsulation reservoir and a second is placed inside the reservoir cap underneath the reservoir. Thermocouples are placed in each of these heating zones as well as on the mold and at the injection gates to determine the state of the encapsulation material and observe the overall progress of the injection cycle. A valve is placed underneath the encapsulant reservoir to cut off the flow of the encapsulant when the mold is in its open position and a workpiece is being removed or placed into the mold. The valve is operated by a pneumatic piston.

Unlike a polymer injection molding machine, it is not easy to separate the encapsulation piece and its sprue from the rest of the encapsulating material that waits in the injection chamber of the encapsulation machine, to be injected in the next shot. This is mainly because plastics are non-eutectic, meaning that they have a melting range instead of a melting point. They will tend to soften first before melting. Thus, it is easy to pull the molded piece from the rest of the injection shot because softened polymer exist between the mold, where the polymer has fully solidified and the encapsulation reservoir where the polymer is in a liquid state. The encapsulation alloy we use, being a eutectic, possesses no softened, mushy state. Thus removing the part requires that we physically yield and break the encapsulation sprue from the rest of the injection chamber. This would require a substantial amount of force which we would wish to avoid.

To physically disconnect the encapsulation material that has solidified within the mold and that which still resides inside the encapsulation machine, a rubber diaphragm is placed in the path of the flow right before it enters the mold. The diaphragm has a slit cut into them so as to allow the flow to pass though with a small addition of pressure. However, in a near static flow condition, as is the case when the mold has been completely filled, the diaphragm slit will close and separate the two bodies of liquid. The encapsulation that is molded can then be easily removed from the mold without having to break the sprue connections.

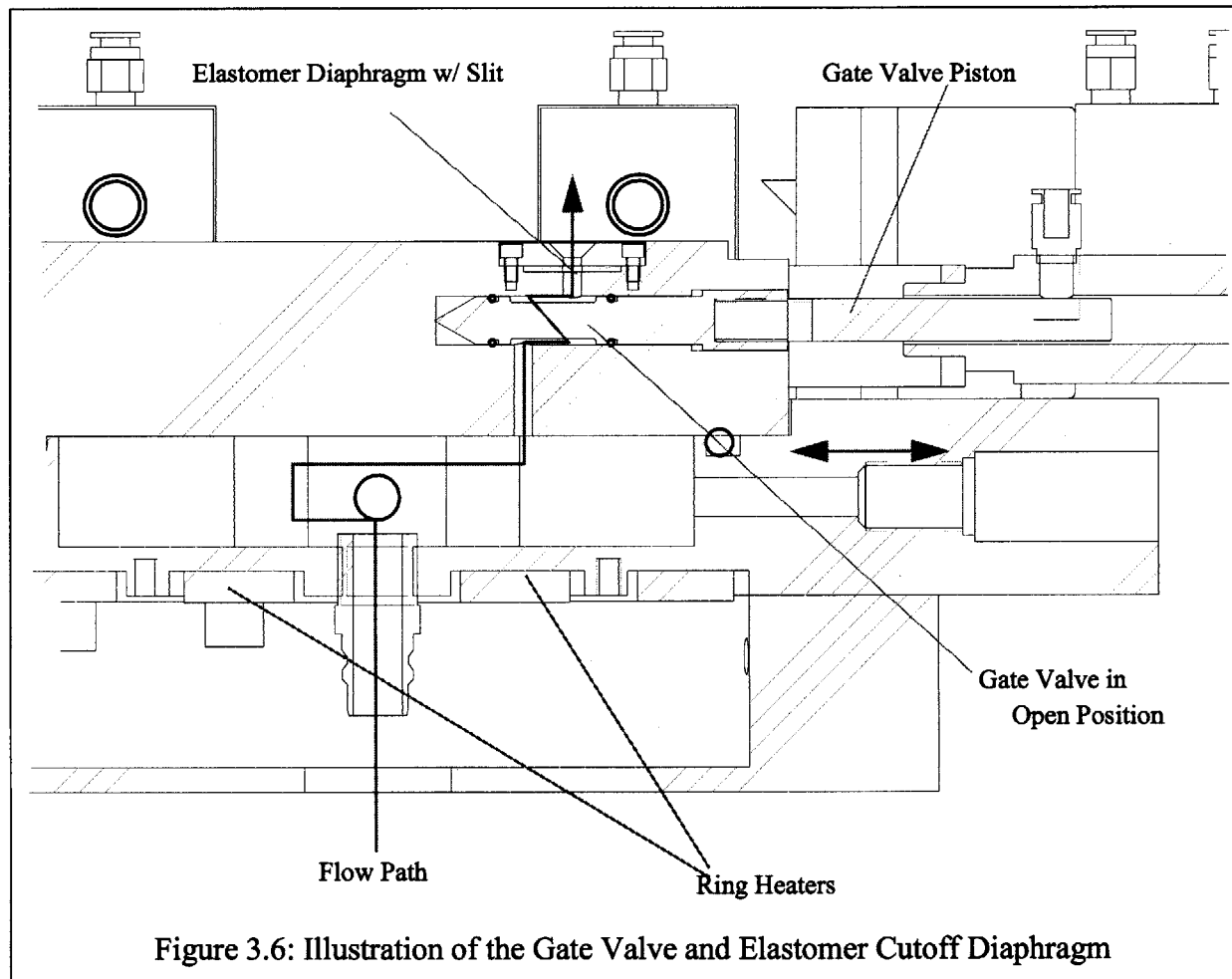
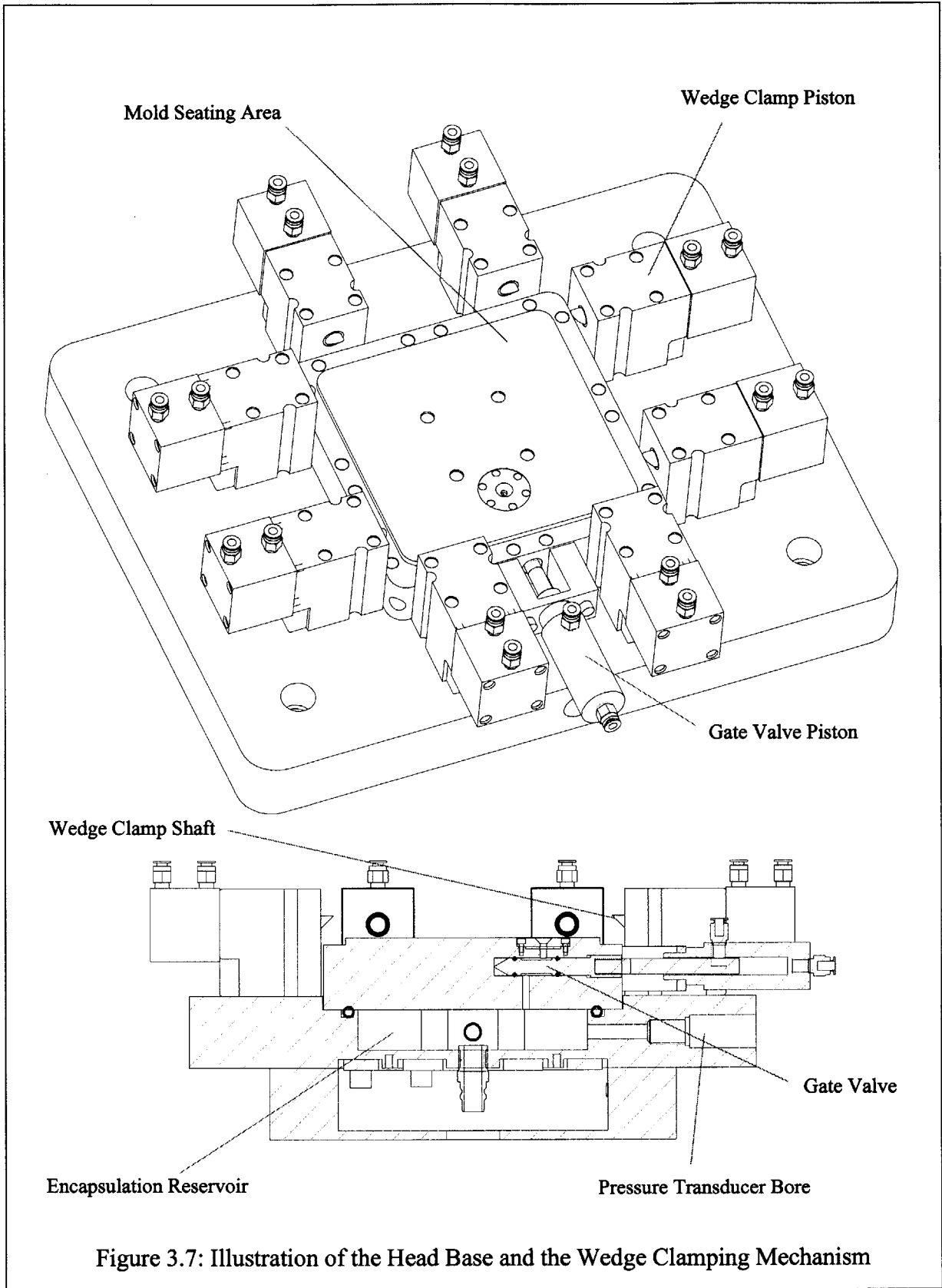
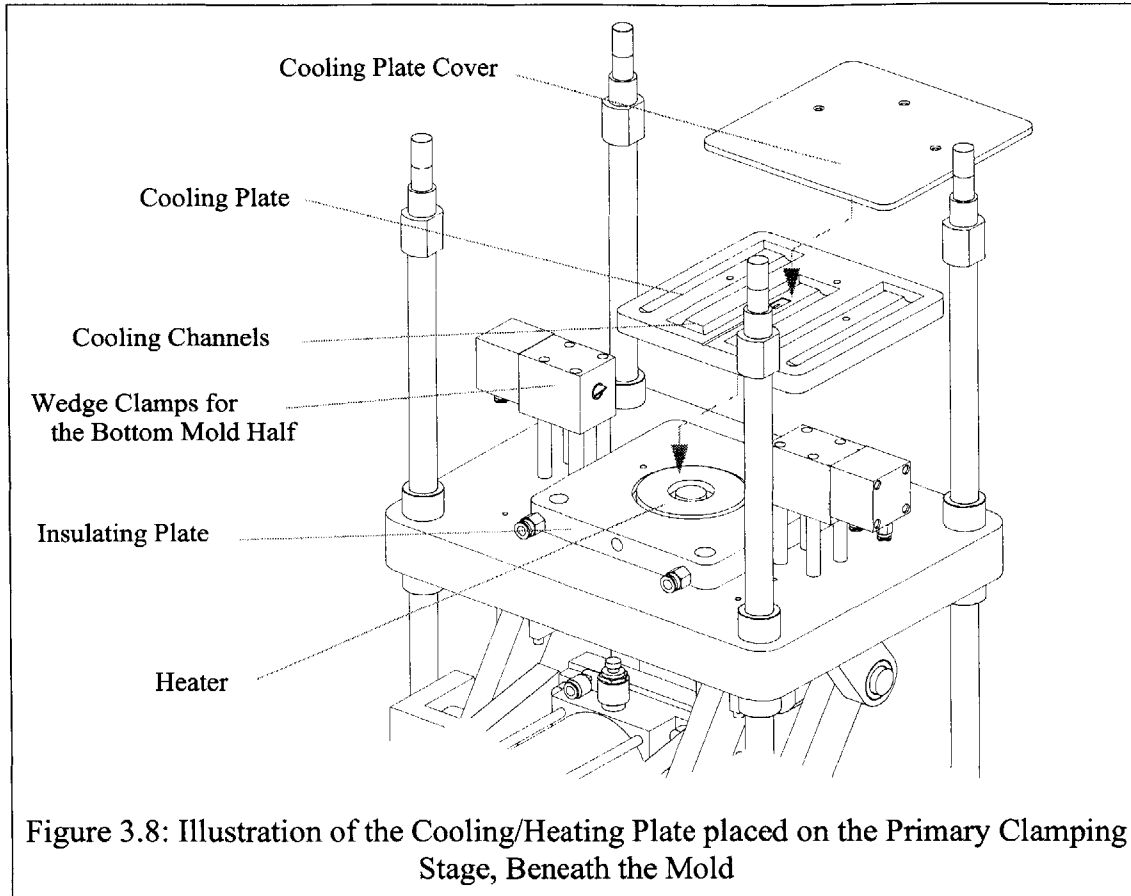


Figure 3.6: Illustration of the Gate Valve and Elastomer Cutoff Diaphragm

There are also auxiliary clamping features used to keep the top plate and bottom pieces of the molds in place when the molds are being opened. Actuated by linear pneumatic pistons, they simply drive a wedge-shaped shaft into a mating feature on the mold, producing a normal force that fights against the opening forces that are exerted on each piece when the molds are being opened. These clamps are not meant to serve the purpose of clamping. The primary clamping pistons is designed to solely performing that task. These wedge clamps simply secure the gateplate when the mold is opened and provide an simple quick release mechanism for changing out the mold components.





Because the molds have to be heated and cooled during each cycle, it is vital that the rest of the encapsulation machine not be disturbed by the temperature fluctuations of the mold. Furthermore, it is vital that we minimize the energy required to perform the heating; otherwise, the resulting long heating and cooling cycles of the molding process would detrimentally affect the performance of the encapsulation fixturing system as a whole.

In order to minimize molding cycle time, it is vital to isolate the mold from the rest of the heated zones of the clamp, specifically, the encapsulation reservoir, and minimize the energy required for its heating. We do this by placing pieces of an insulative material, above and below the mold and placing the heaters close to the molding area. To insulate the mold on the bottom, a cooling/heating plate is located beneath the mold, between the mold and the heating source. It circulates air at high velocity using the pneumatic air supply as a pressure source. Another layer

of insulation is placed beneath the mold heaters to isolate it from the rest of the clamping device. This is illustrated in Figure 3.8.

The mold gateplate is made of a stainless steel alloy and provides insulation on the top. Shown in Figure 3.9, a ProMechanica FEM model was developed to determine the effect of gateplate material on the heat transfer during the encapsulation cooling process. The model consists of a layer which represents the liquid encapsulation material within the mold, a layer which represents the liquid encapsulation material within the reservoir and a smaller layer representing the gateplate material sandwiched in between. The simulation computed the temperature of the front and back sides of gateplate as the mold material was cooled. Phase change was not included in the simulation. The graph shows the varying temperature lag between the front and back of the gateplate for three materials.

As expected, because of its high thermal conductivity, there are no thermal gradients within the aluminum gateplate. Cooling the plastic gateplate resulted in a large thermal gradient, while a mild one existed within the stainless steel gateplate model. From the simulation, an aluminum gateplate will obviously have detrimental impact on the heating and cooling cycles of the encapsulation machine. A plastic would be the best choice if one only considers the thermal constraints. However, since most plastics are incapable of maintaining structural integrity at the temperatures the gateplate will be subjected to, up to 500K, it is impractical to use such a material for this application. Stainless steel allows one to develop a gateplate that will meet both thermal and mechanical requirements.

Thus, the mold is sandwiched between the two layers of insulation so that it may be cooled to a temperature just below the melting point of the encapsulant without disrupting the thermal states of the rest of the machine. The stainless steel gateplate allows a 20 second lag between when the front of the gateplate will begin to freeze and when the back will. If cooling is removed within that time, the reservoir will not experience a phase change that would hinder the encapsulation cycle.

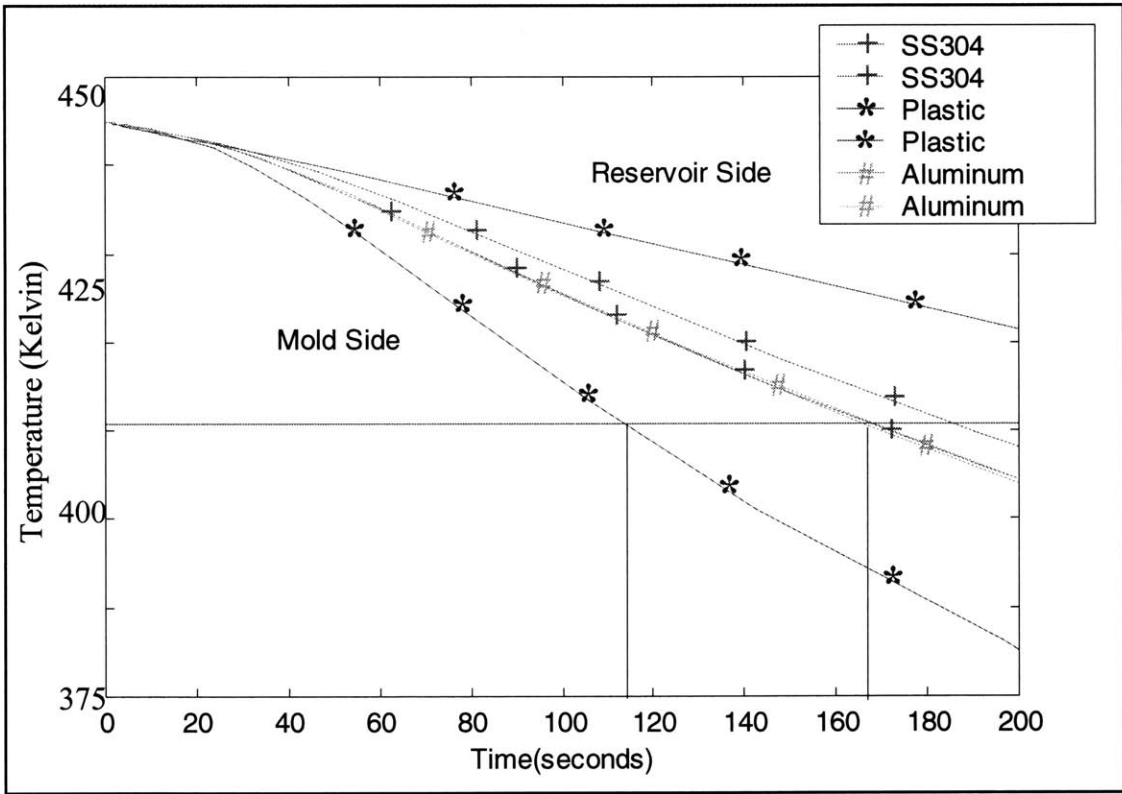
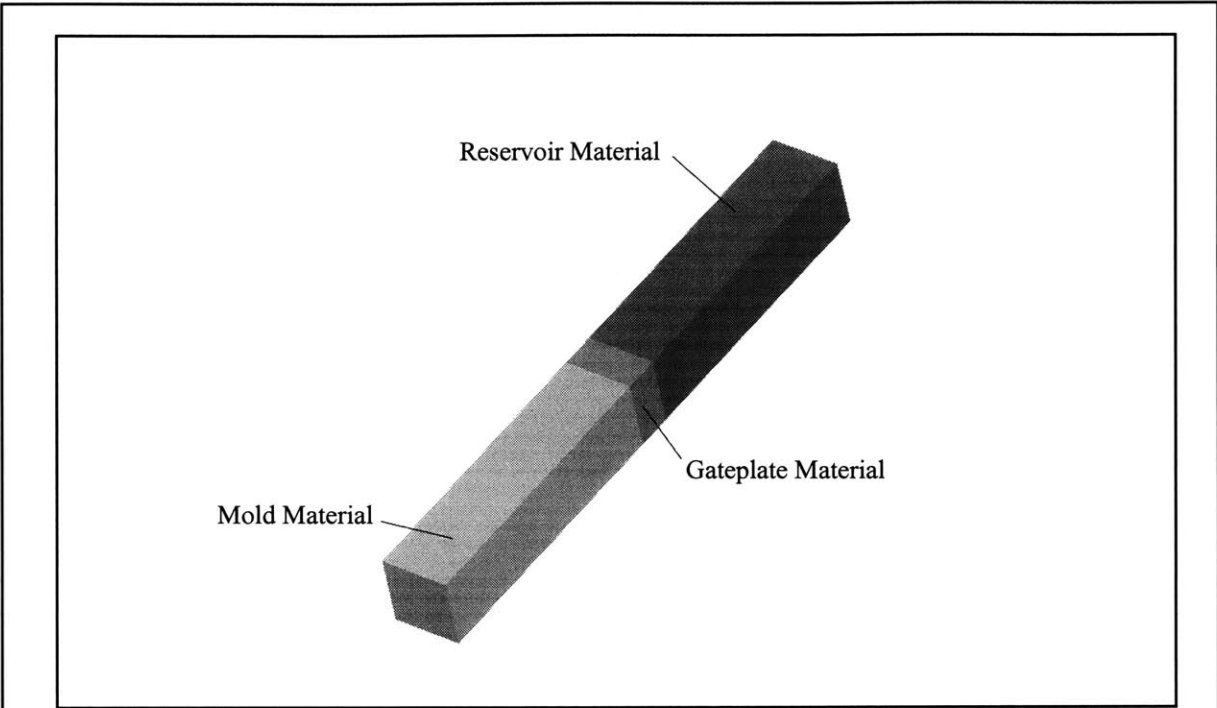
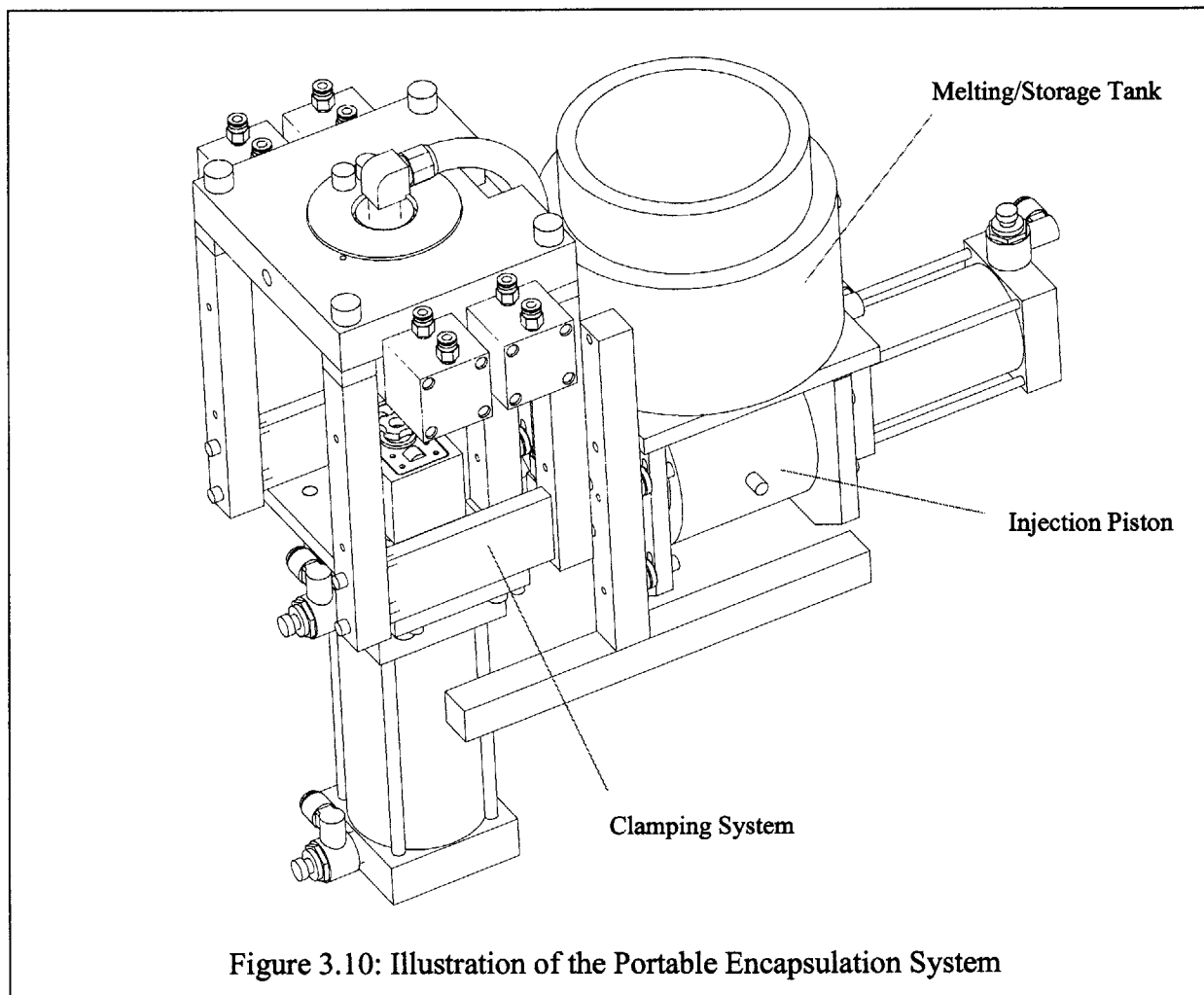


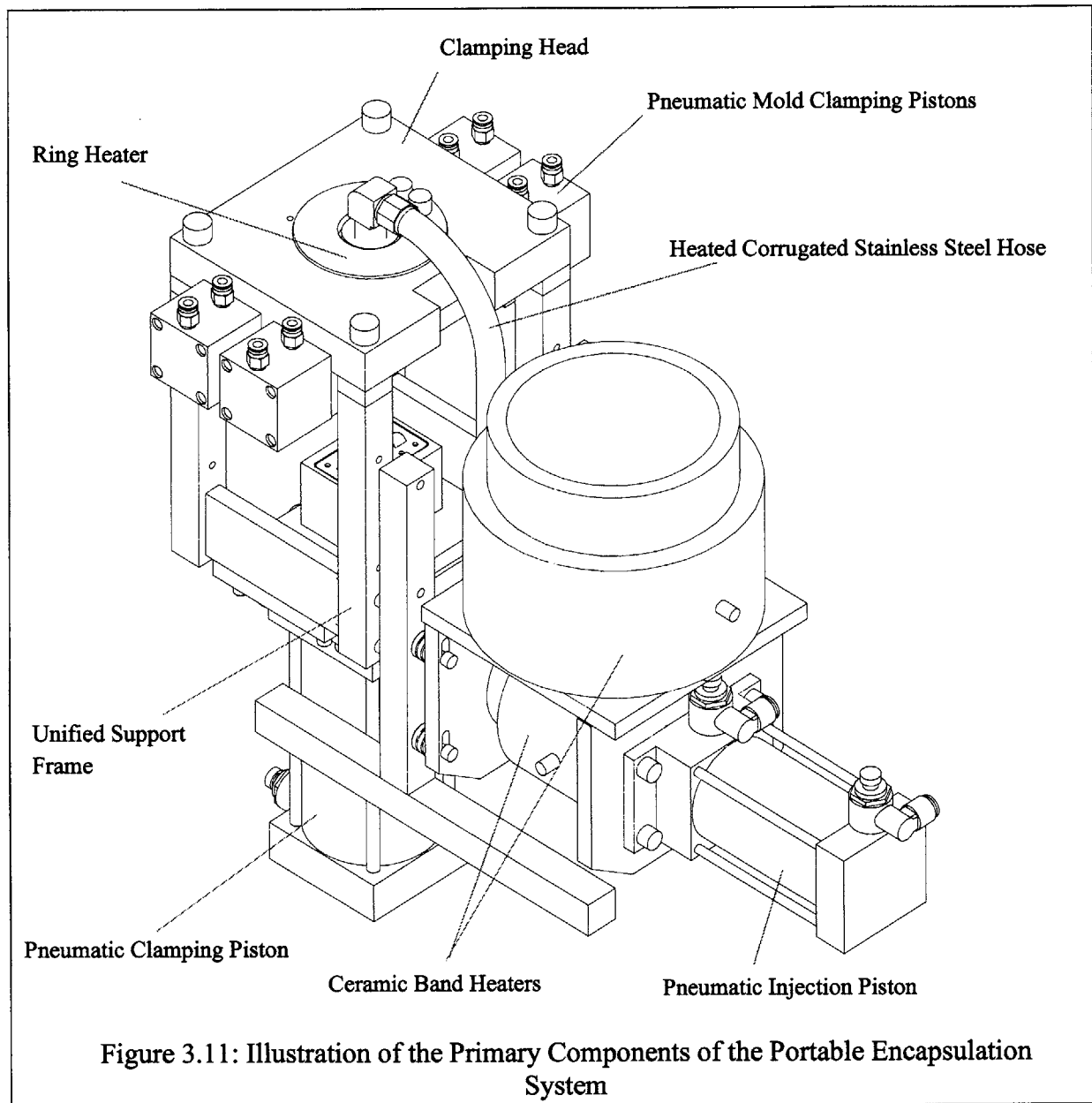
Figure 3.9: Illustration of the ProMechanica FEM model (top) and the Resulting Graph Depicting the Temperature Differential Between the Front and Back Side of the Gateplate for Three Materials (bottom)

3.2 Portable Encapsulation Machine

In Figure 3.10, it may be observed that the sub-components of the portable encapsulation machine are much less easily distinguished from one another. The connections between the three components have been shrunk and one overall structure has been used to mount and assemble the machine. This allows for a very compact and portable design.

The portable system runs on 60psi of pneumatic pressure and requires 15A of 120 VAC to power its heaters. There are four heating zones—the tank, the injection cylinder, the connection hose, and the clamping head. Each one of these heaters is controlled independently through a



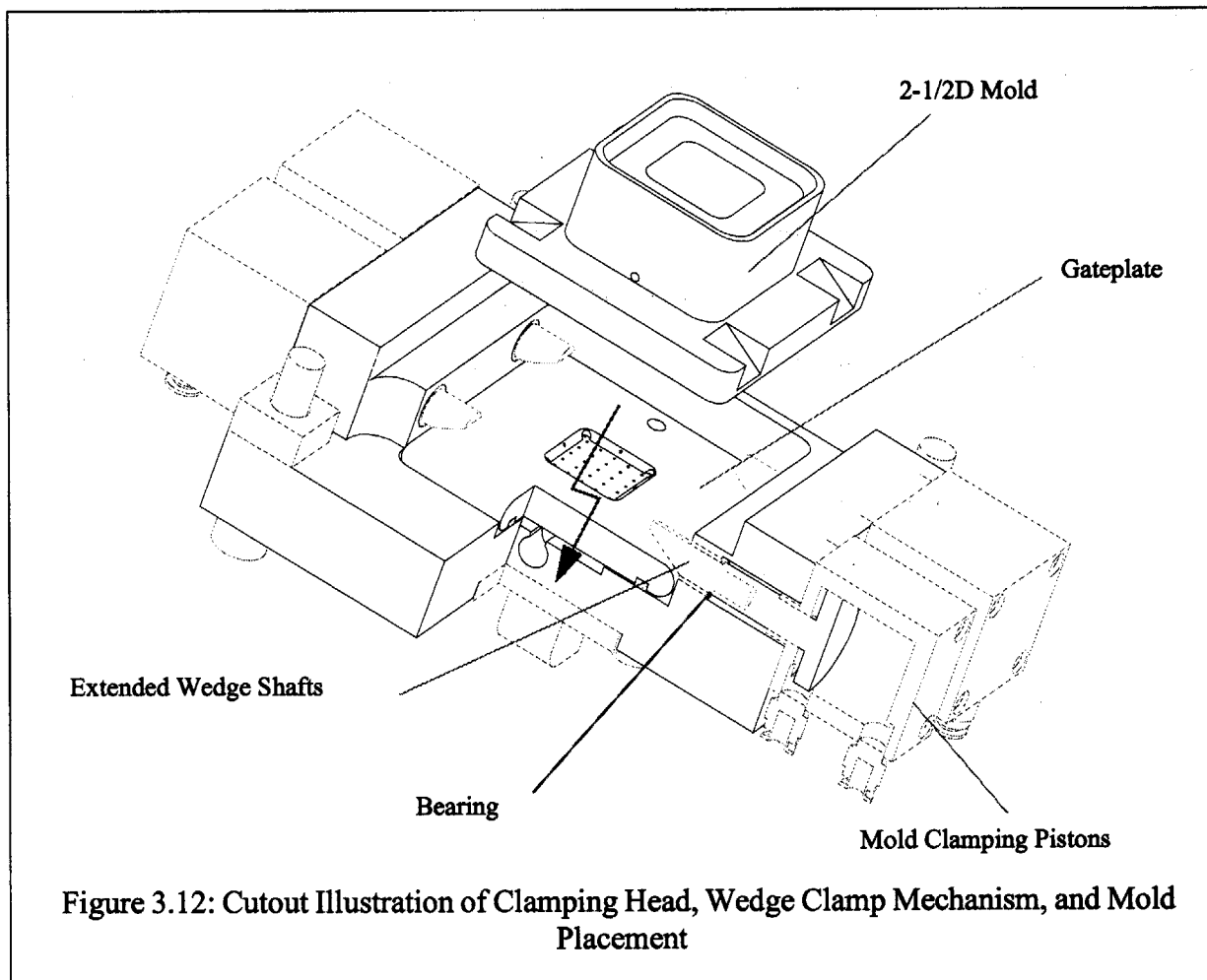


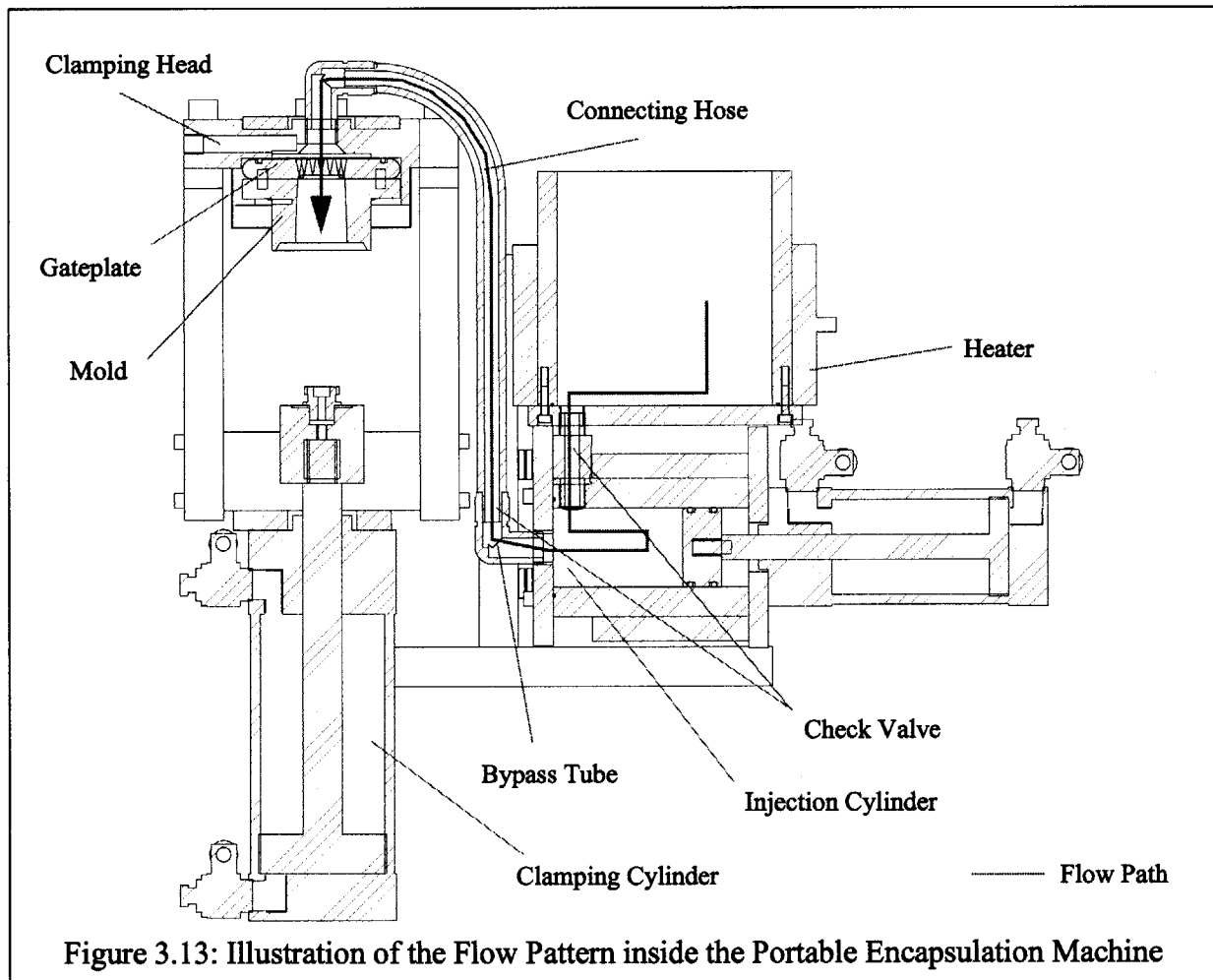
laptop PCMCIA data acquisition board readily available in industry. The pneumatics are controlled by solenoid valves, also purchased, which are themselves controlled by the same data acquisition board mentioned before.

The clamping capacity is approximately 1000lbs. It will accept molds up to 4" by 4" in footprint which shall normally be able to encapsulate a 2" by 2" piece of stock. The mold is held

in place by four pneumatic cylinders that each drive a wedge shaft into an inclined portion of the mold, transmitting an upward force, pushing the mold against the clamping head, and locking it in place. This is the same design as found on the larger machine.

The flow of the encapsulant is similar to that of the larger encapsulation machine. The portable machine has two check valves, located between the tank and the injection cylinder and between the injection cylinder and the hose leading to the clamp. Just as in its larger counterpart, injection flow is allowed primarily only in one direction, from the tank to the cylinder and then to the clamp. A small bypass valve is placed to short-circuit the second check valve in order to allow the pressure within the clamp to equalize to atmospheric after the injection piston has been retracted.





3.3 Summary

The design of the encapsulation machines present an entirely new set of hurdles and challenges for which solution can not easily be found in today's academic literature or engineering knowledgebase. For these new challenges, new technologies have been developed and incorporated into the encapsulation machines. The fundamentals of the encapsulation machines are straight-forward. They are the adaptation of technology that exist in the die casting, squeeze casting, injection molding and other molding processes. However, a new set of requirements unique to the encapsulation process requires the introduction of novel technology.

Features not found in die casting or injection molding, such as the bypass tube or the runnerless gating design, are implemented to facilitate the encapsulation process and to ensure a quality and controllable process. The next step is thus to understand how the encapsulation process performs under various process conditions. This will be discussed in the coming chapters.

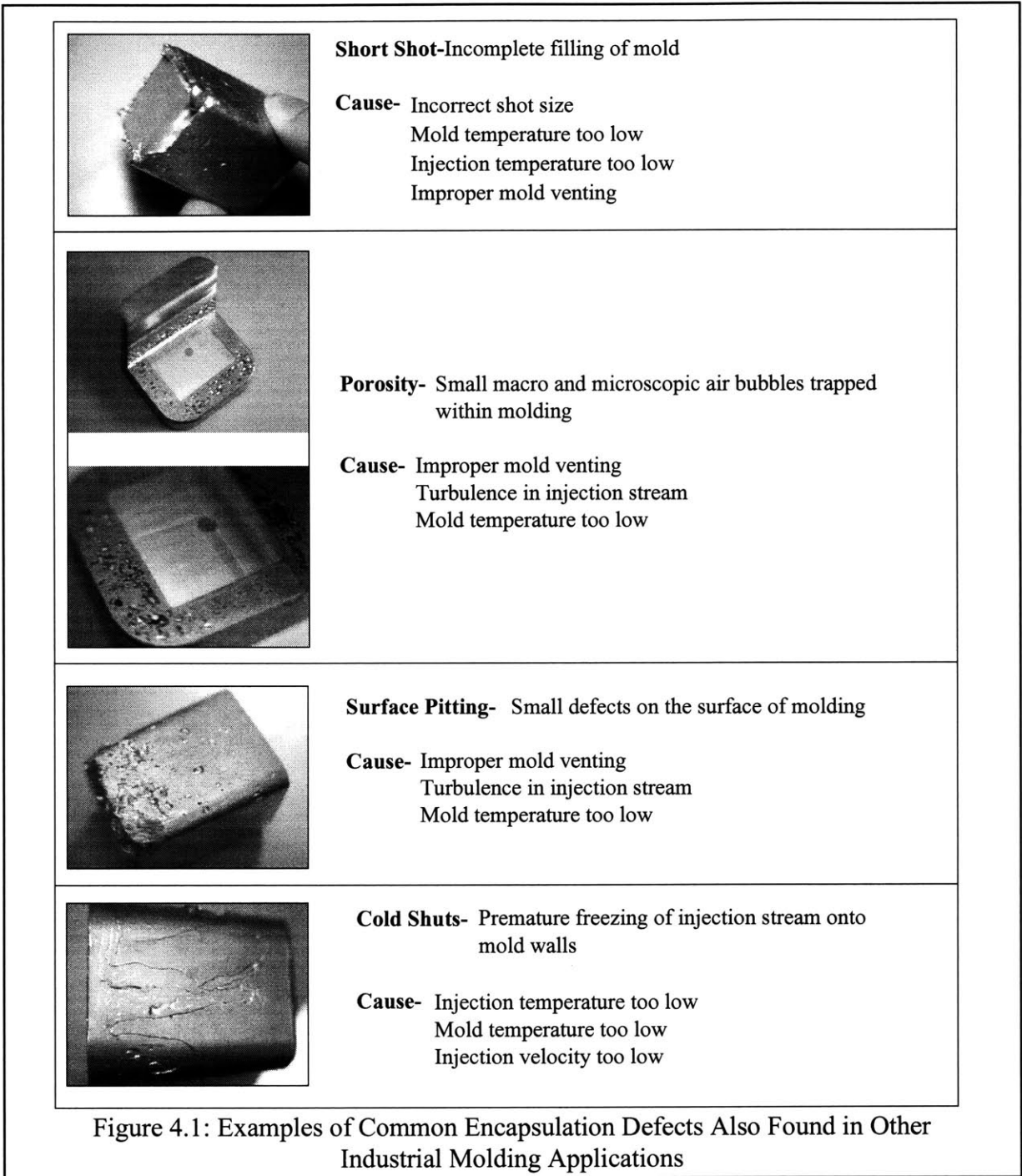
Chapter 4

Analysis of the Encapsulation Process

As in all molding and manufacturing processes, defects will occur if certain process parameters are set incorrectly. The encapsulation process is no different. In fact, many of the defects encountered in the encapsulation process are quite common and well understood in other industrial fields such as die casting, injection molding, squeeze casting, *etc.* Although it is important to understand the exact causes of these defects and to develop protocols that will minimize their effects, they will not be discussed extensively within this chapter nor within this thesis. Outside of encapsulation, these defects are already well studied and understood. Molding is an ancient practice dating back to prehistory. Its technology has been broken down and absorbed into a variety of industrial fields. Die casting and injection molding are perhaps the two most widely used form of molding. Within each field, problems, similar to those found in encapsulation, have been overcome, and these processes have been made robust and economical. As a result, our goal is to study those phenomena that are not found elsewhere and thus not well understood.

4.1 General Defects

As shown in Figure 4.1, improper encapsulations can result in a variety of defects. Short shots, porosity, surface pitting, cold shut and other defects have already been well documented in such fields as die casting [Upton 82] and they are present in encapsulation as well. Figure 4.1 lists the common causes of these defects and the most probable ways of preventing or removing these defects. Most of these are remedied by adjusting various process parameters such as the injection temperature or the mold preheat temperature. Others, such as porosity and surface pitting, are avoided by properly designing the molds and carefully planning vent locations and sizes [Bar-Meir 96].



In addition, Fan and Guevara, in their masters theses under Sarma, extensively explore these molding process parameters as they pertain to the encapsulation process. Fan derived a relationship between injection/molding pressure to the resulting encapsulation surface finish. His

work proved the necessity of pressure during the encapsulation process. He also showed that the ultra-high pressure associated with die casting and injection molding, normally in the 10's of thousands of pounds per square inch, was not necessary for encapsulation. His research claimed that performing the encapsulation under 65psi of pressure is sufficient to obtain the necessary surface finish that will allow the accurate and repeatable fixturing of the encapsulation assembly [Fan 00].

Guevara, in her masters research, explored the effects of injection temperature, mold preheat temperature, the cooling rate, the ejection temperature, the temperature at which the encapsulation is removed from molding system, packing pressure, aging, the long-term changes in the molecular structure of the encapsulation material, and alloy composition on the quality of the encapsulation process. She examined the resulting surface finish, the level of porosity and the dimensional accuracy of the encapsulation. Her results lead her to conclude that the BiSn alloy exhibited very little aging, none of which impacted the quality of the encapsulation. The cooling rate and ejection temperature, as well, was shown to have little impact on the degree of porosity, the attainable level of surface finish, and the resulting dimensional accuracy of an encapsulation. As could be expected, the dominant parameters for controlling the quality of the encapsulation are in the preheat temperature and the injection temperature [Guevara 01].

4.2 Unique Defects Found Only in the Encapsulation Process

With such extensive work already performed in developing an understanding for the general practices of encapsulation molding, this research is aimed at studying those phenomena that are unique to the encapsulation process. The goal is to add to the understanding of the encapsulation process in ways that would not be achievable by simply extrapolating the knowledge of other fields and applying it to the encapsulation process.

The encapsulation process does possess one process defect not common to other manufacturing processes. The defect is called weak rewelding. This phenomenon is similar to the weldline defects found in injection molding. However, while weldline defects in injection molding are created within one injection stream—the stream does not properly adhere to itself as it travels around obstacles and meets again—weldline defects in encapsulation are created because of improper bonding between a new encapsulation layer and the previous encapsulation layer. The dominant causes of this defect are inadequate preheating of the workpiece prior to encapsulation and the inadequate super heating of the injection stream. In order to produce a proper bond, the injection stream must melt away and dissolve the oxides which exist on the top layer of the solid encapsulation. If the injection stream temperature or the preheated mold temperature is too low, the oxide layer will not dissolve entirely. As shown in Figure 4.2, the weak rewelding results in a flawed encapsulation. As machining forces are applied to the encapsulation, the weldline does not possess enough strength to resist and breaks along the weldline, thereby destroying the effectiveness of the encapsulation material to support and immobilize the workpiece.

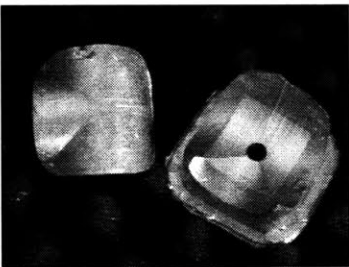
	Rewelding Weakness- Inadequate, incomplete or non-existent adhesion between the old and new encapsulation materials
	Cause- Injection temperature too low Mold temperature too low Stock temperature too low Incompatible encapsulation material

Figure 4.2: Picture of Rewelding Defect Unique to Encapsulation Molding

Material choice also plays a role in preventing or creating the weldline defect. Materials with high latent heat and high thermal diffusivity are likely to exacerbate the problem. The high latent heat requires that a large amount of thermal energy be transferred to the weldline surface to

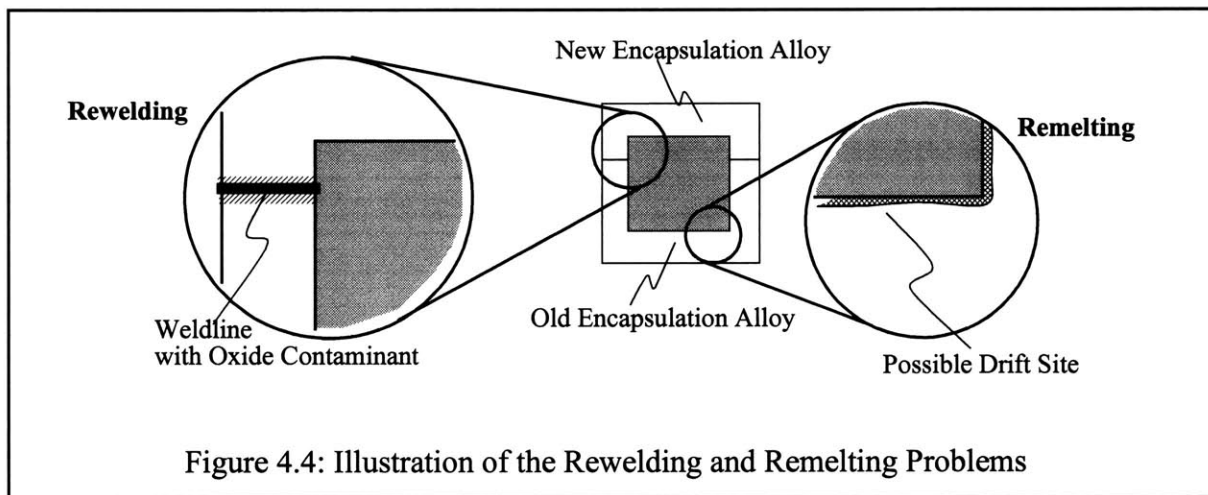
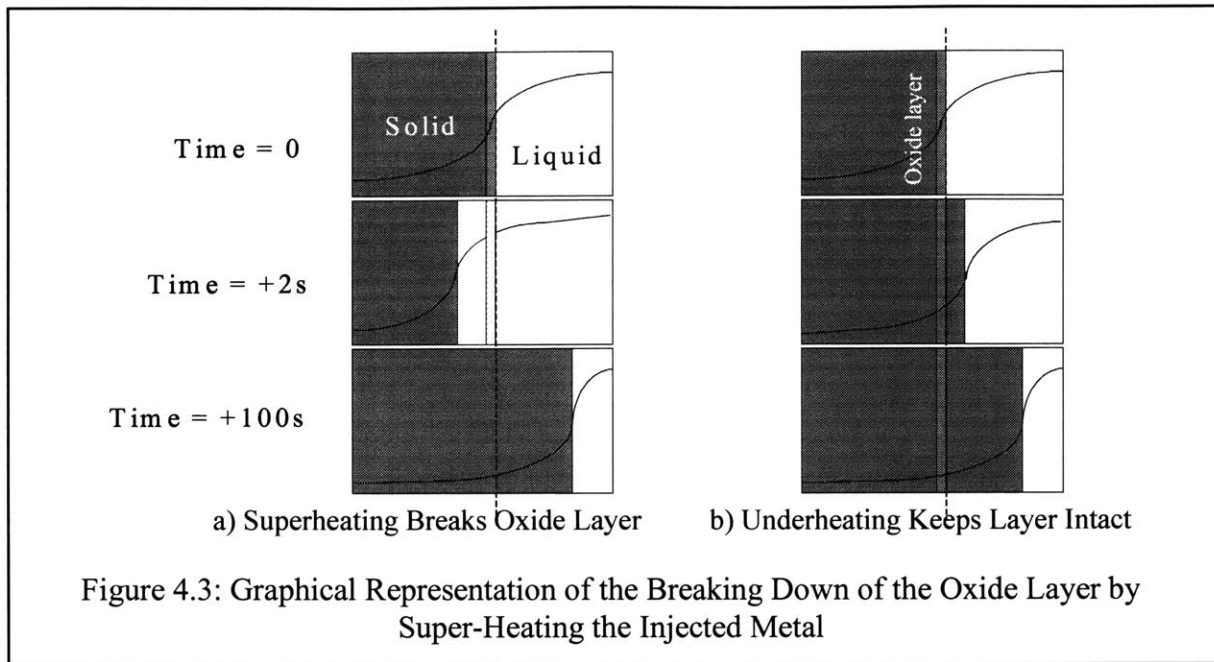
develop a melt layer, which is used to dissolve the surface oxides. The high thermal diffusivity prevents that heat energy from remaining at the surface.

4.3 The Rewelding Defect and its relationship to the Remelting Effect

In order to better understand the encapsulation process, it is necessary to obtain a more accurate picture of the solidification process of the encapsulation alloy, in our case the BiSn eutectic, after it has been injected into the encapsulation mold. Two particular issues, those of rewelding and of remelting, deserve close examination as they greatly affect the quality of the encapsulations produced.

Rewelding, as discussed above, is the bonding of the newly injected encapsulation alloy to the original alloy that is already encapsulating the workpiece. Rewelding takes place during re-encapsulation. The encapsulated part is removed from the machine tool and placed back into the encapsulation machine in order to fill the newly cut features with the encapsulation alloy and to restore the block to its original shape. In order to produce a strong encapsulation, an ample amount of rewelding must occur at the alloy/alloy interface. It is assumed that a good bond is obtained when a sufficient thickness of the old encapsulation material is liquefied and the oxide layer that once preventing welding is dissolved. With most oxide layers having a thickness ranging from 0.1 μm to 1 μm , our target melt thickness should be 2 orders of magnitude thicker, about 0.1 mm.

Remelting occurs during the same encapsulation procedure as rewelding. However, while rewelding is desirable, remelting is not. Remelting is defined as the melting of the original encapsulation alloy at the workpiece/alloy interface. Remelting is most often caused by the heating of the workpiece when new molten, superheated encapsulation alloy is introduced. Severe remelting will cause the workpiece to shift during the encapsulation process and thus destroy the accuracy of the encapsulation.



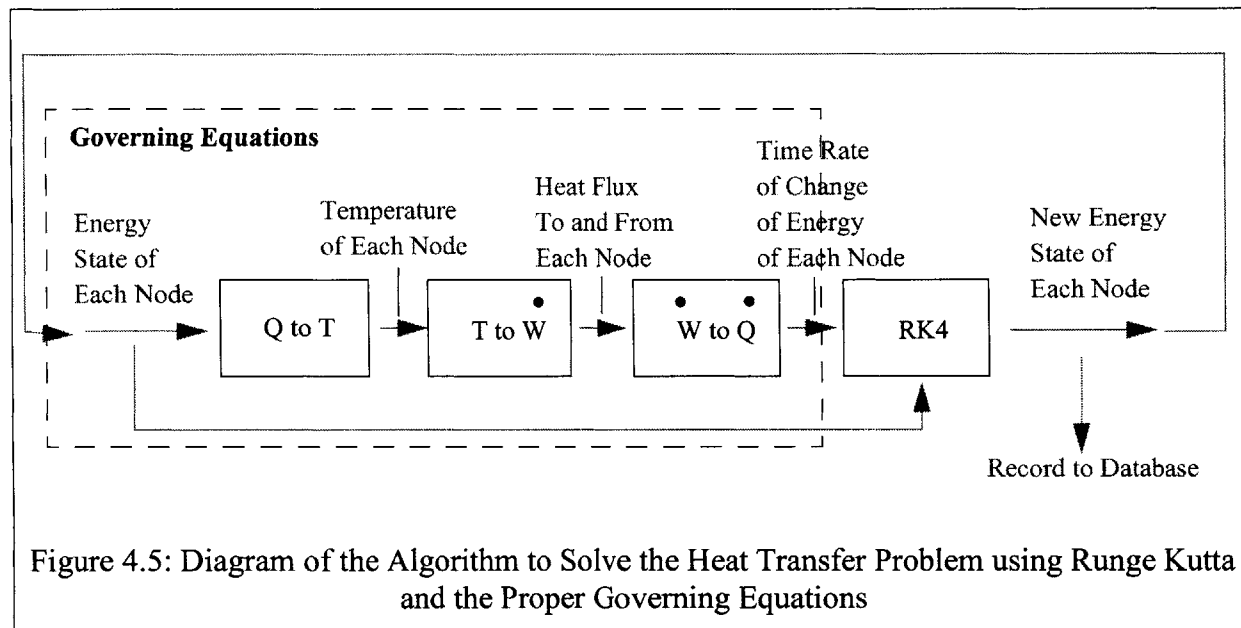
4.4 Development of a Computational Model

Because of the phase change and complex boundary and initial condition, no purely analytical solution could be found to describe the temperature profile of the encapsulation as well as the melt front movement during injection. While solutions such as the Neumann solution could describe the melt front movement and account for phase changes, it would not provide an adequate picture of the true situation because it only could provided solutions where the boundary

temperature is held constant, *i.e.* the boundary conditions must be homogeneous [Carslaw & Jaeger 65].

Therefore, a simulation has been written in Labview™, a graphical programming language, that describes the encapsulation solidification using finite element methods. The simulation uses the Runge-Kutta method of order 4 to solve for the necessary differential equation. The governing equations were written in Labview™ as well.

The Labview™ algorithm calculates the heat transfer interactions through the following steps. After the materials to be simulated are designated, the solver breaks down each layer into nodes of a specified node length. The elementary laws of heat transfer, that of heat conduction through a solid and energy exchange during phase change are applied to each node. In order to track the phase change more precisely, each node's internal energy is tracked instead of its temperature. Knowing its energy state allows one to determine not only the temperature of the node but also its phase.

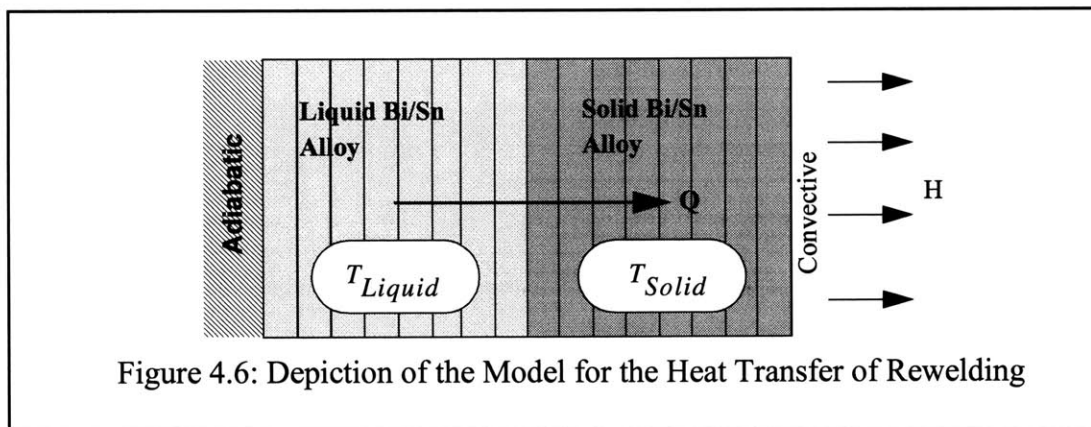


The simulation is capable of developing a temperature profile of any one dimensional, unsteady, conduction heat transfer problem. It is capable of simulating phase change with both eutectic and non-eutectic materials. The simulation can also accommodate a conduction problem where there are multiple materials, each having dissimilar thermal properties and each having different initial conditions. Lastly, on the hot end of the model, an adiabatic condition is assumed. On the other end, an ambient temperature and heat transfer coefficient can be prescribed and applied.

To optimize processing time, the time step size can be programmatically varied. It can be made small in the beginning to allow the capture of the fast changing temperature profiles that exists at the start of the model and can be made larger when the temperature profile is closer to a steady state condition so that processing time can be reduced. Stability, discussed in section 5.3, must of course be satisfied when modifying these parameters.

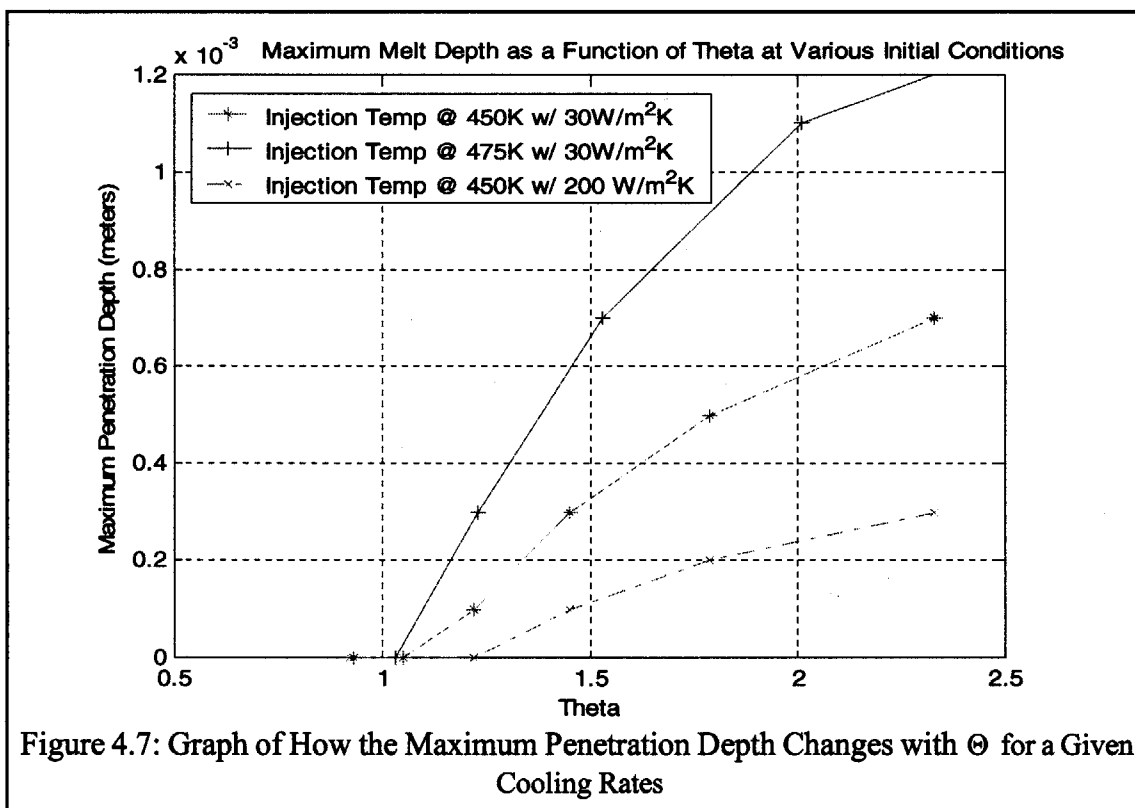
4.5 The Simulation Models and Results

4.5.1 Rewelding



As shown in Figure 4.6, the rewelding simulation consists of a 2 layer model of the BiSn eutectic. The first layer is in solid phase and the second in liquid. Each layer is 0.0127m thick

and is held at a specified initial temperature. The 2 layers are model as being brought into instantaneous contact and the heat transfer is simulated. While one end condition is an adiabatic surface, the other surface is subjected to convective cooling at a specified heat transfer coefficient. The simulation was run 10's of times varying both the injection temperature and the preheat temperature on each run. The temperature profile was tracked as it varies with time. This data was then be post-processed to show the movement of the solid/liquid interface, determine if rewelding has occurred and show the degree of rewelding.



As expected, the simulation showed that rewelding initiates when Θ is approximately unity, where:

$$\Theta = \frac{(T_{Liquid} - T_{melt})}{(T_{melt} - T_{Solid})} \quad \text{Eq. 4.1}$$

This agrees very well with the analytical model of two semi-infinite bodies of similar material placed in instantaneous contact with one another. With the thermal properties of the material in both solid and liquid form being fairly similar, the melting of the solid will begin once Θ is above unity. At unity, neither side changes phase and below unity, the liquid starts to solidify. The simulation, however, can illustrate a more complex behavior than the simple analytical semi-infinite body model. The semi-infinite model is only appropriate for either very large bodies or for very short periods of time. It cannot demonstrate a melt front coming into the solid region and then retreating, allowing the liquid to solidify. The simulation on the other hand is capable of showing the semi-infinite behavior and then at the appropriate time demonstrate the retreating of the melt front. The maximum depth for which the melt front travels into the solid is here designated as the maximum melt depth and it is the variable we are seeking to study.

From Figure 4.7, one will recognize that melting in general begins when Θ is slightly above unity. In the third case, where the convective heat transfer coefficient is higher, we see that a perceptible amount of melting does not occur until Θ is close to 1.25. One can thus conclude that for the simulated geometry, the convective end condition will affect rewelding. It is thus recommended that cooling is not begun immediately so as not to hinder remelting. From the above graph, we can also recognize that not only is the quantity Θ important in determining the maximum melt depth but the individual injection and preheat temperatures do play a role in the maximum penetration depth of the melt front. One sees that with higher injection temperatures, a greater melt depth is achieved for a given Θ . It could be surmised that the highest possible temperature for injection will provide the most benefit for the encapsulation process. However, the injection temperature must be limited by other practical considerations. For example, it has been observed that an increase in injection temperature will increase the oxidation rate of the liquid encapsulation alloy. With greater amounts of oxidation, the encapsulation alloy will not

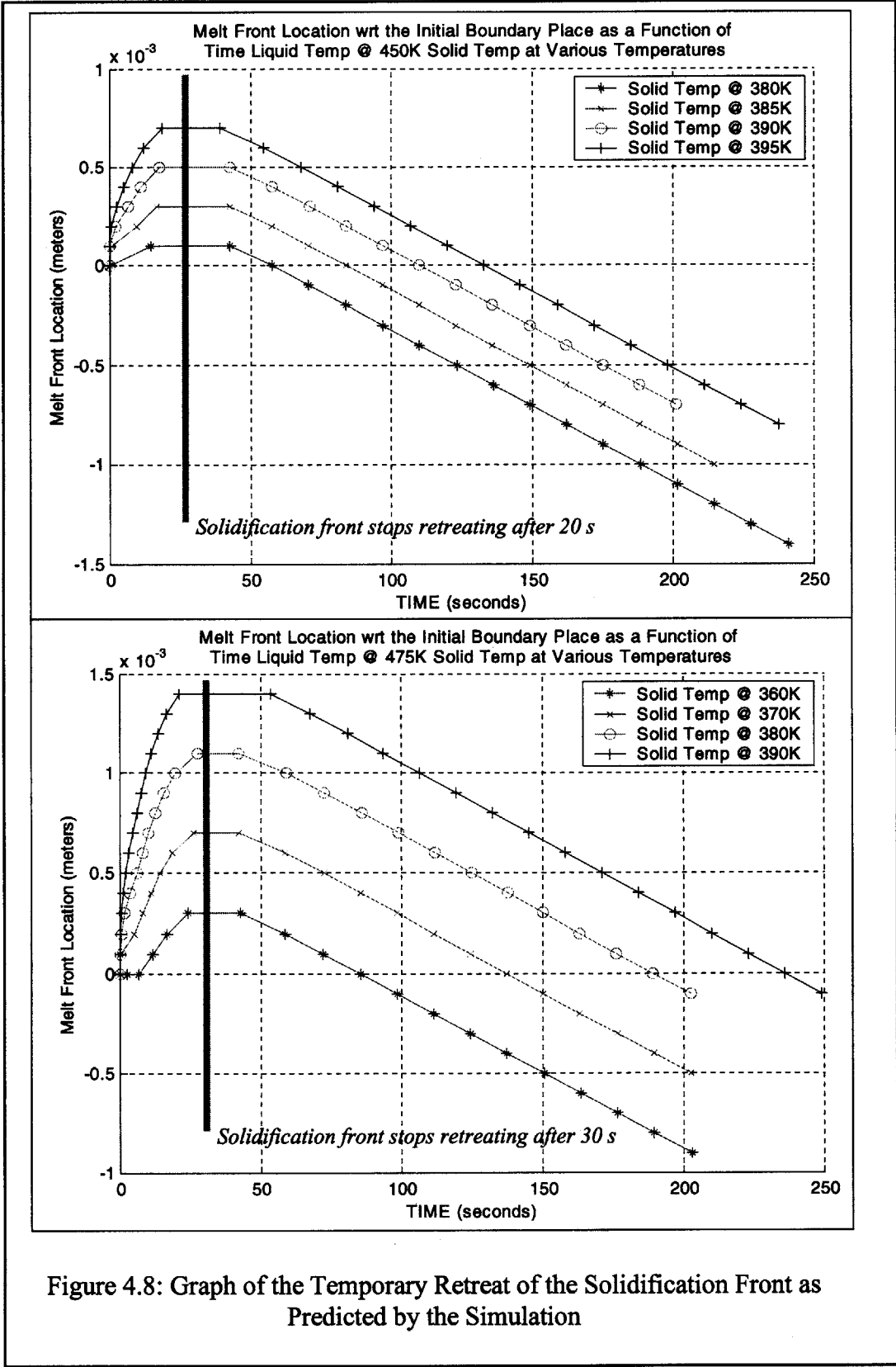
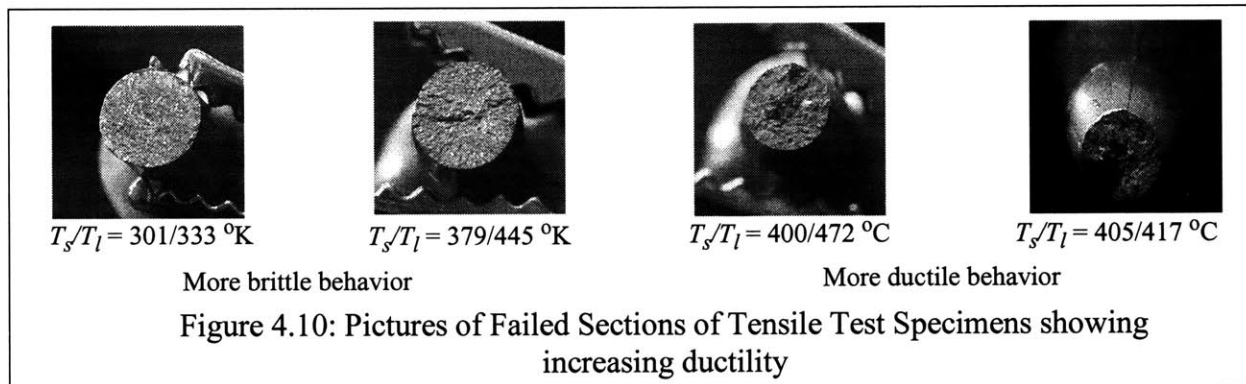
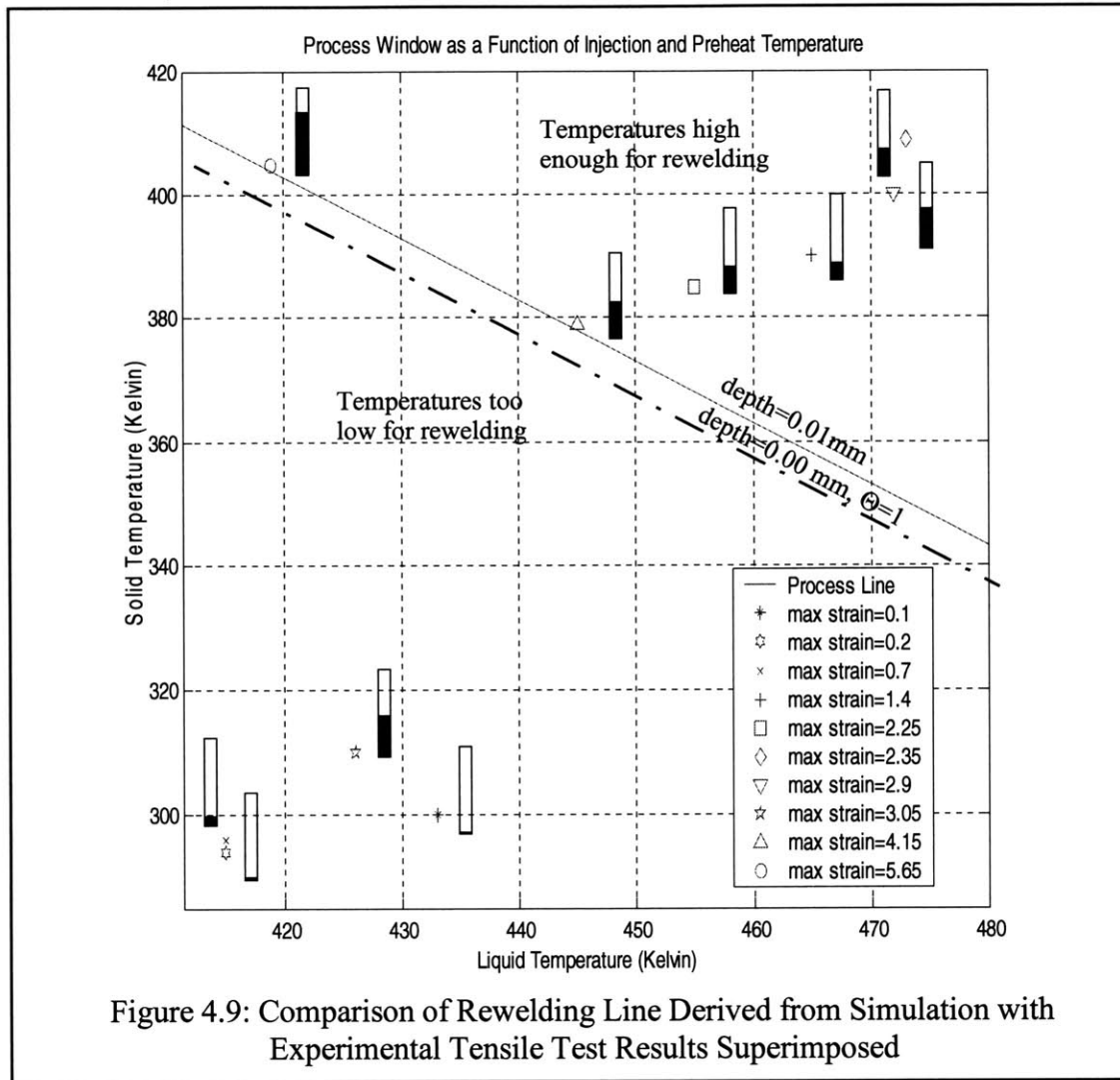


Figure 4.8: Graph of the Temporary Retreat of the Solidification Front as Predicted by the Simulation

perform well during the encapsulation process. Encapsulations become more brittle and exhibit more surface defects and porosity.

While convection cooling was previously stated to be detrimental for rewelding, one can observe from Figure 4.8 that initiating cooling 20 or so seconds after the mold has been completely fill will not impact the quality of the rewelding. After 20 seconds, the melt front has reached its maximum depth and has begun to recede. It can also be observed that after approximately 1 minute, the solidification front moves with a constant speed. This behavior can be classified as being quasi-steady state. In other words, while the temperature profile is still changing due to the solidification of the encapsulation alloy, the temperatures profile is governed only by steady state conditions and the layer thickness. The thickness of the body is merely the solid layer thickness and the boundary conditions are specified as being the melting temperature at one end and the convection heat transfer condition at the other. In this mode, heat flux through the solid is constant and is essentially the heat convected from the front end at the specified heat transfer coefficient. This should and does match the constant slope of the graph after 1 minute has passed.

Valdivia, in her masters research with Sarma, performed a variety of tensile test on weldline specimens. Figure 4.9 shows how the simulation results compare to the findings of her research. For the most part, it show that the specimens molded in condition predicted to have poor weldline strengths do exhibit less tensile strength than those molded in conditions predicted to have more favorable weldline strengths [Valdivia 00]. As can be seen in Figure 4.10, specimens that were predicted to have little or no rewelding exhibited a brittle fracture failure while those predicted to have good rewelding exhibited signs of ductile fracture.



4.5.2 Remelting

From the information generated by the simulation, one can conclude that for an injection temperature of about 450K, the solid encapsulation needs to be preheated to about 380K to achieve the desired 0.1mm of melt penetration depth. While increasing the preheat temperature

will surely increase the penetration depth, we must now examine how the preheat temperature will affect our second issue, that of remelting.

The remelting simulation consists of a 4 layer one dimensional heat transfer model. The first layer is liquid BiSn alloy, 0.0635 meter thick. The next is a piece of 0.127 meter thick of Aluminum 6061-T. It is followed by a solid layer of BiSn, 0.0635 meter thick. And lastly a 0.0635 meter thick piece of stainless steel is placed at the end. Again, the end conditions are given to be adiabatic on end and convective on the other.

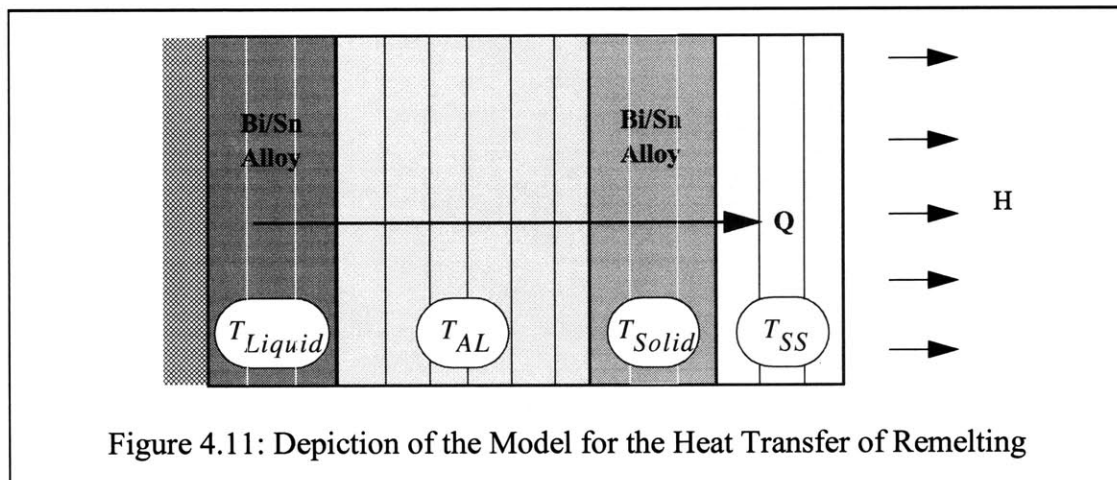
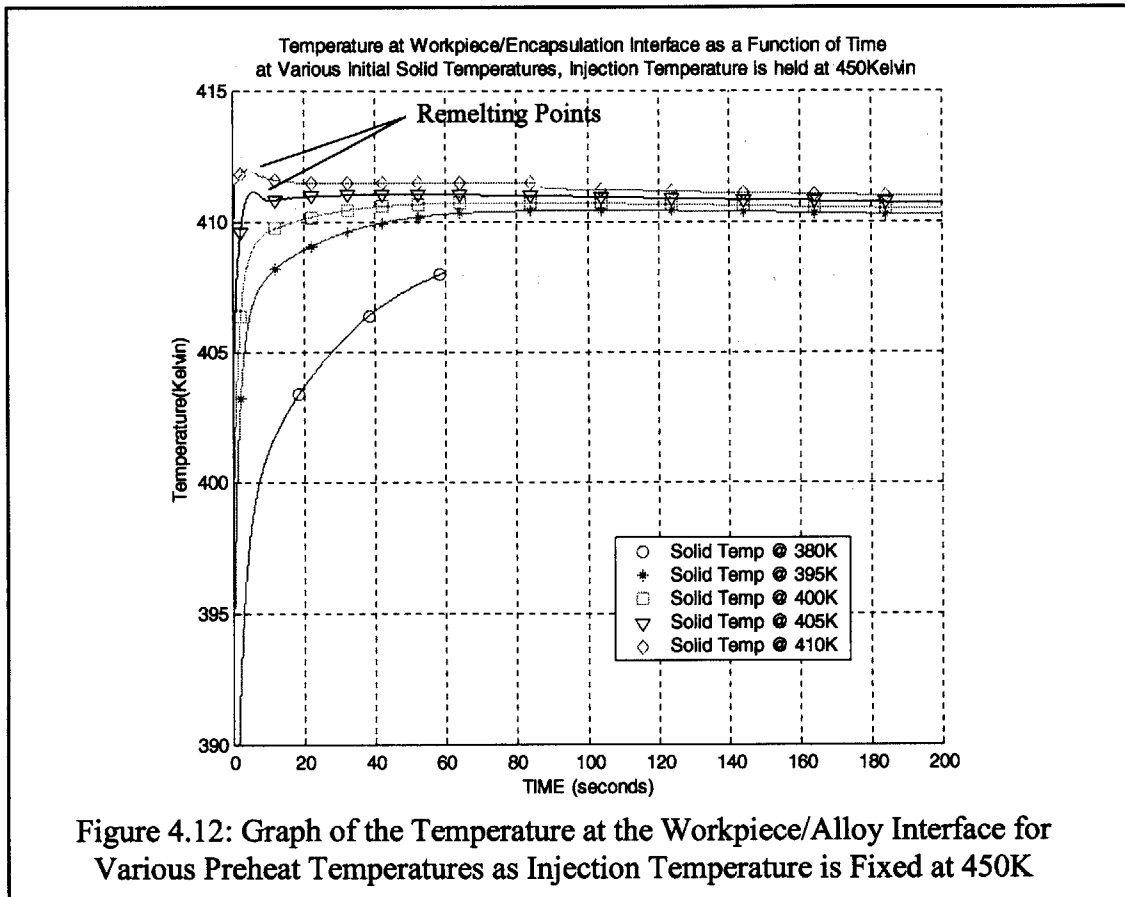


Figure 4.11: Depiction of the Model for the Heat Transfer of Remelting

Just as in the rewelding simulations, a number of remelting simulations were run using the model described in Figure 4.11. Within each run either the injection temperature or the preheat temperature was varied. The gigabytes of data that described the temperature profile of the model were then post-processed in order to develop a picture of how the workpiece/alloy temperature varied.

The graphs shown in Figure 4.12, Figure 4.13, and Figure 4.14 reveal that a preheat temperature of 380K will not initiate remelting even when the injection temperature is as high as 500K. At an injection temperature of 450K, remelting begins when the preheat temperature is

between 405K and 410K. At 475K, remelting will begin when preheat is between 400 and 405K. And at 500K, remelting begins between 395K and 405K. One observes that even with large changes in the injection temperature, the preheat temperature needed to initiate remelting does not vary that greatly. One can thus conclude that the preheat temperature is the dominant variable that controls remelting. With the melting point of the BiSn eutectic being 411.5K, one observes that remelting only occurs when the preheat temperature is very near the melting point. Thus the robustness of the encapsulation process in terms of developing a good reweld strength while preventing remelting can be considered very high. With an injection temperature of 450K, the preheat temperature can vary some 25K, from 380K to 405K, and still result in a good encapsulation.



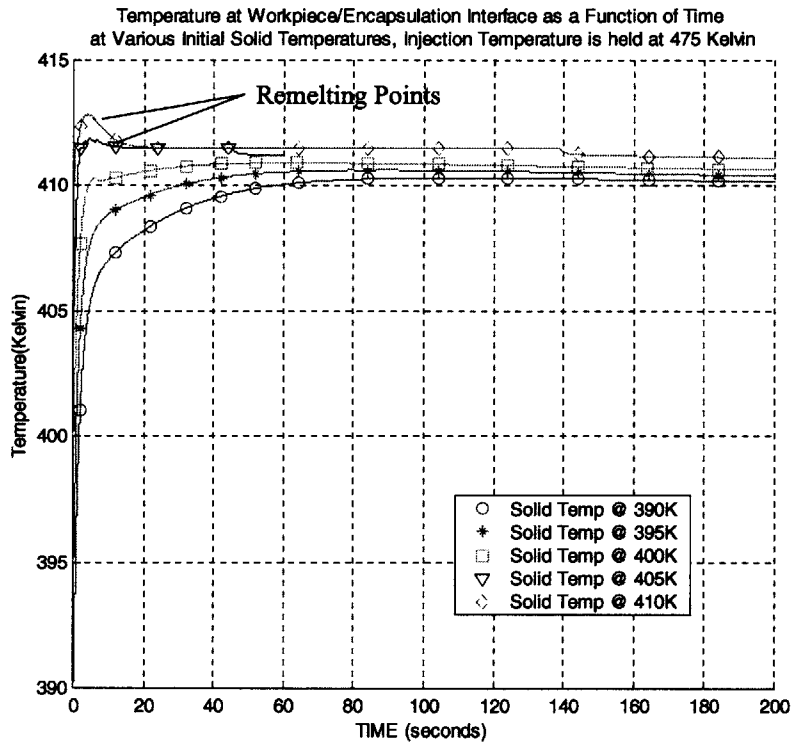


Figure 4.13: Graph of the Temperature at the Workpiece/Alloy Interface for various Preheat Temperatures as Injection Temperature is Fixed at 475K

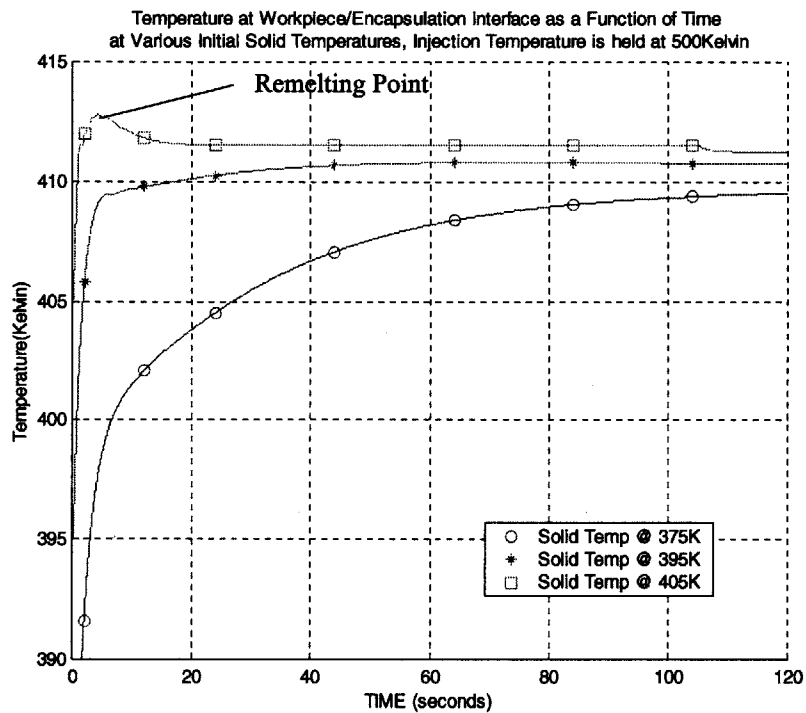


Figure 4.14: Graph of the Temperature at the Workpiece/Alloy Interface for Various Preheat Temperatures as Injection Temperature is Fixed at 500K

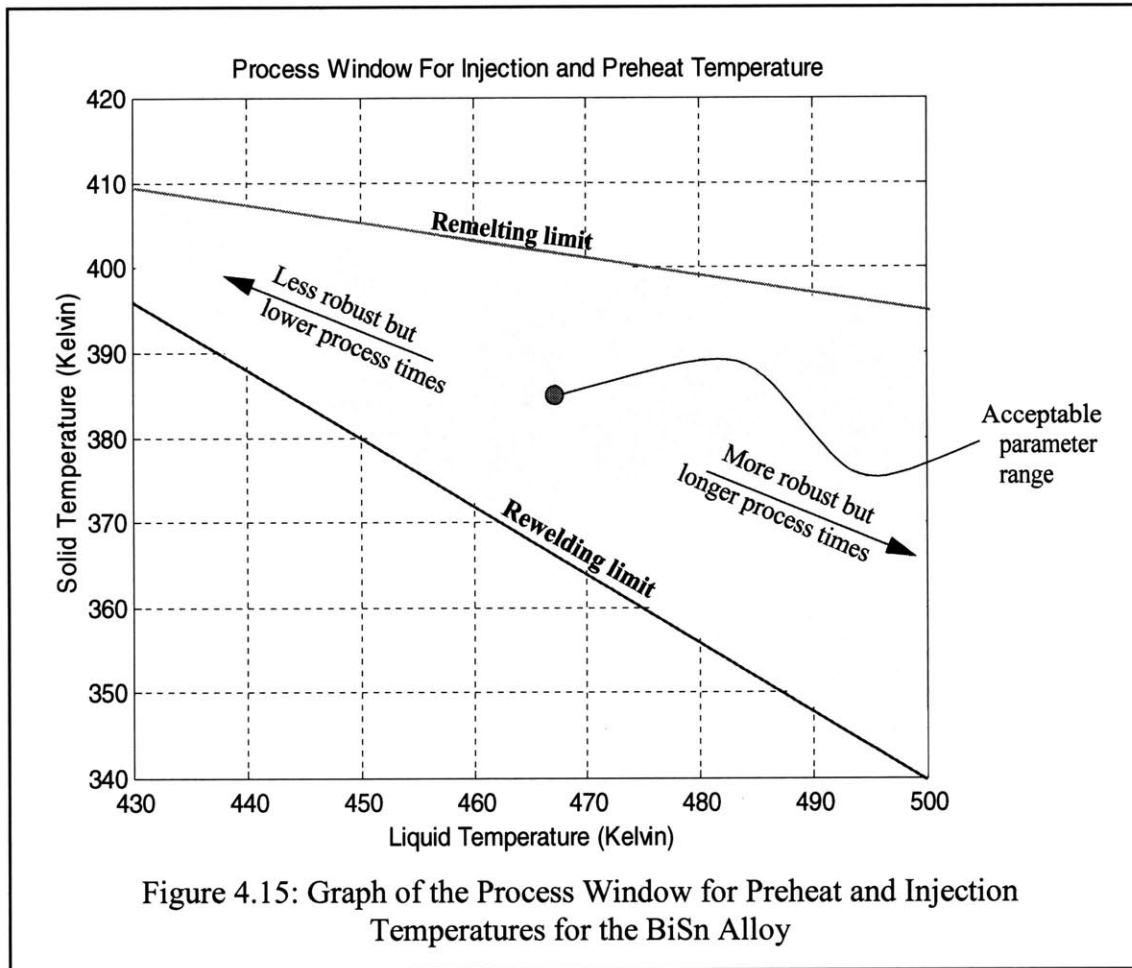
The data showed that remelting occurred as quickly as rewelding occurs. Thus, there appears to be no other way to combat the remelting problem except to modify the temperature parameters so as to avoid remelting. As stated before, additional cooling, though it would prevent remelting, would also hinder rewelding.

4.5.3 The Process Window for BiSn Eutectic

Combining the data for rewelding and remelting, it is now possible to develop a process window within which encapsulation can be performed successfully and reliably. Figure 4.15 shows that as long as the injection temperature and Preheat temperature remain within this window there should be no remelting occurring at the workpiece/alloy interface. Likewise, within this window, adequate rewelding should occur at the alloy/alloy boundaries to produce an encapsulation with adequate strength. Outside this window, the resulting encapsulation will either exhibit poor weld strength or show evidence of workpiece drift because of remelting.

The findings from this section are summarized below. They result in the composite temperature process window shown in Figure 4.15, and also significantly affect the design of the process equipment.

- Re-welding can be assured by a combination of a high injection temperature and a high solid preheat temperature, which result in an initial retreat of the solidification front.
- Sufficient retreat of the solidification front is usually achieved within the first 20 seconds.
- Drift can be virtually eliminated by keeping the solid preheat temperature below 400K.



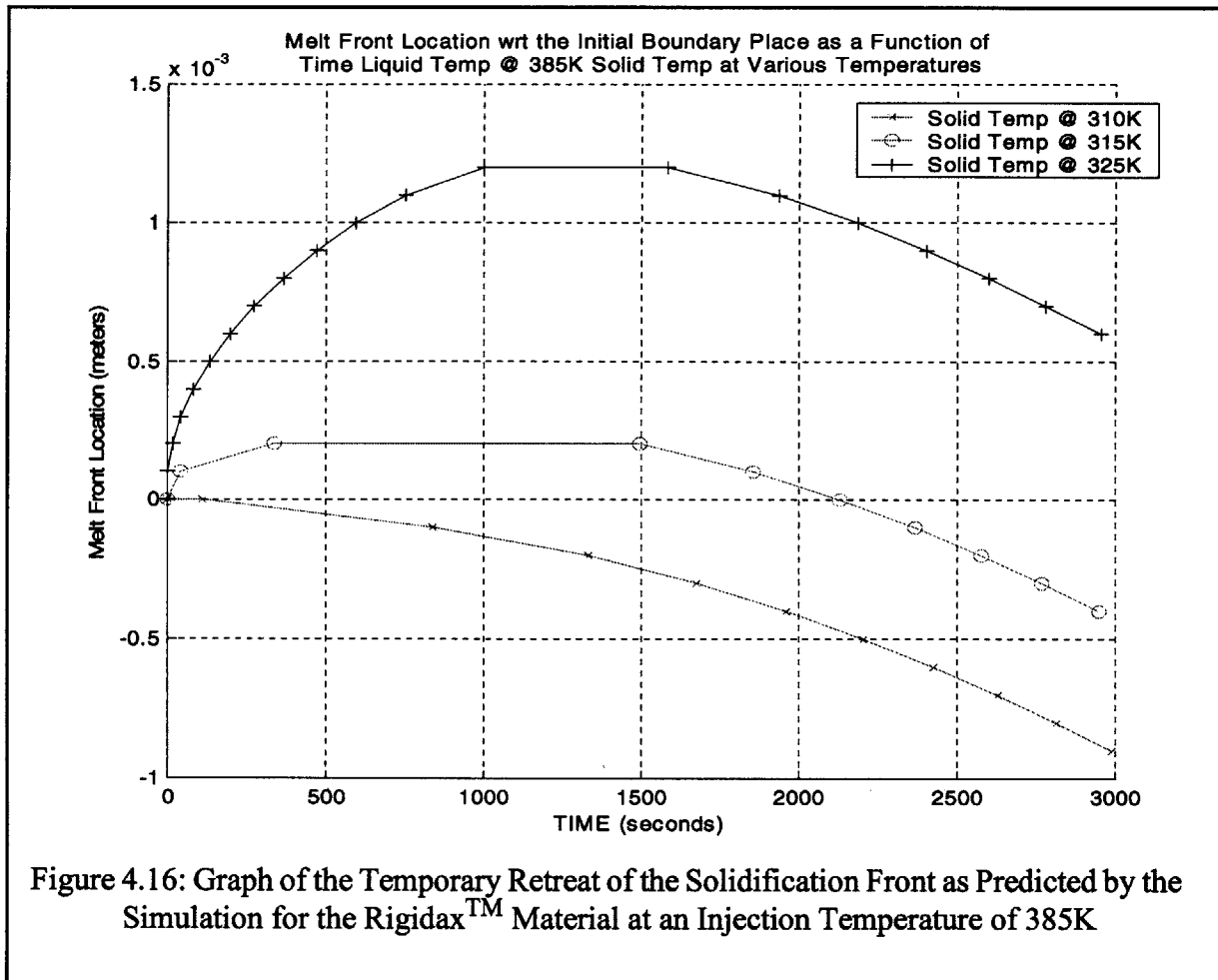
4.6 Simulation on the Rigidax™ Material

The same rewelding and remelting simulations were performed substituting the material properties of Rigidax™ for that of the BiSn eutectic alloy. The results of the simulation, as expected, reflect the difference in thermal properties between the 2 materials. For comparison, the material properties for Rigidax™ and the BiSn eutectic are listed in Table 4.1. The cooling rates for the Rigidax™ simulation are much slower than those of the BiSn eutectic. The rewelding melt front movement are orders of magnitude slower in Rigidax™ than in the BiSn eutectic. However, these findings, though important, are not the primary focus of this second set of simulation

Table 4.1: Material Properties of BiSn and Rigidax™

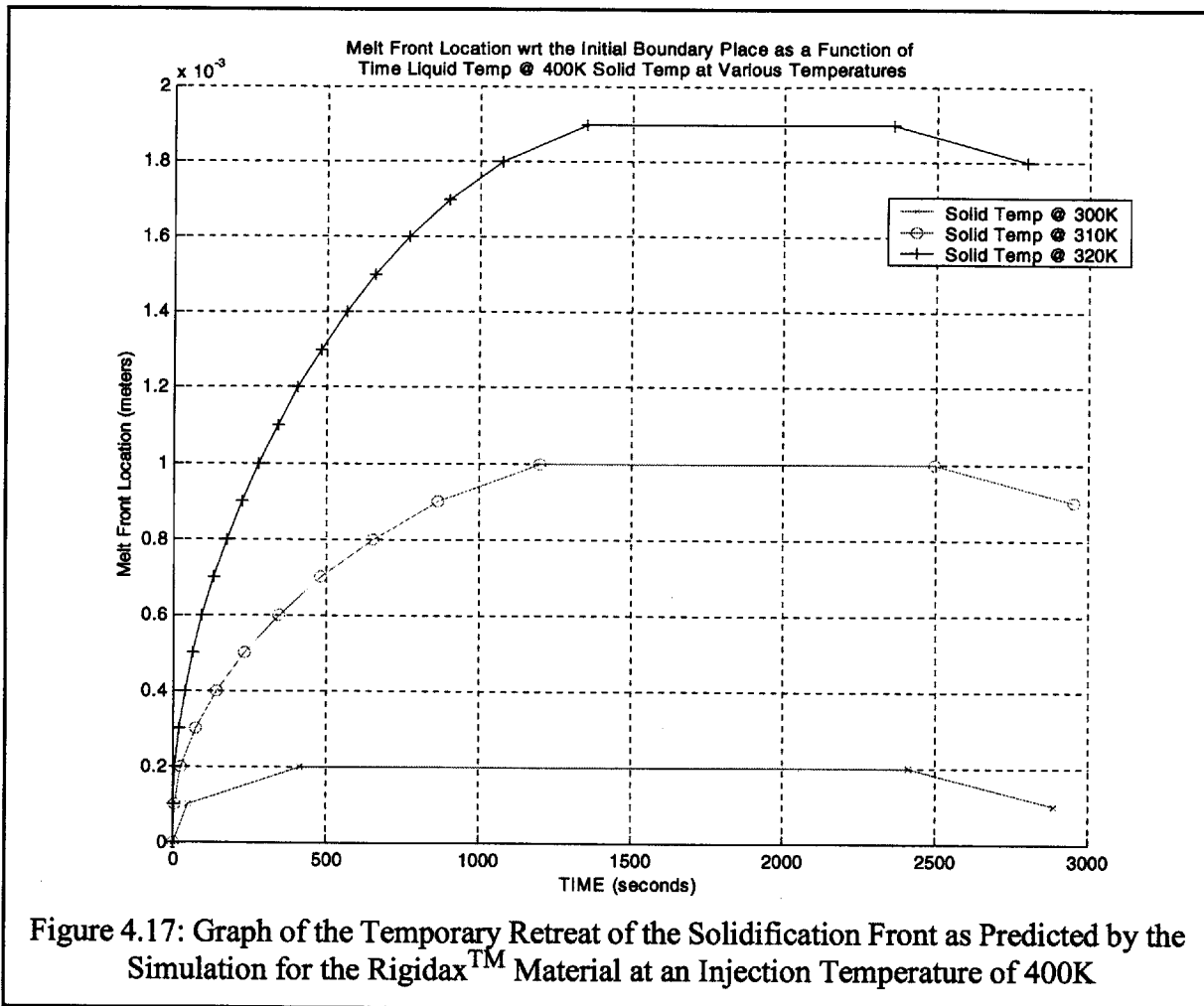
	BiSn	Rigidax™	dimensions
Specific Heat	155	2250	J/(kg K)
Latent Heat of Fusion	4.91e4	1.93e4	J/kg
Density	8580	1830	kg/m ³
Thermal Conductivity	1.39e-5	1.58e-7	W/(m K)
Viscosity	7.5e-3	1.0e-2	kg/(m s)
Thermal Diffusivity	1.39e-5	1.58e-7	m ² /s
Melting Temperature(s)	411.5	325-347	K
Coefficient of Thermal Expansion	1.5e-5	4.0e-4	1/K

The goal of running the simulation on the Rigidax™ material was to determine the effects of a melting range on rewelding and remelting behavior. It was hypothesized that a non-eutectic material would adversely impact encapsulation quality. Because of the non-eutectic nature, Rigidax™ required that it be heat far beyond its melting temperature to reduce viscosity and ensure that proper rewelding occurred. The elevated temperature would, of course, further exacerbated the remelting condition. It was suspected that a non-eutectic material, which softens as it approached its melting range, would allow small forces to easily shift the workpiece held within at temperatures far lower than that required to obtain successful rewelding.



4.6.1 Rewelding and Remelting Results

The results of the rewelding simulation are shown in Figure 4.16 and Figure 4.17. The two graphs plot the movement of the melt front for a variety of preheat temperatures. The melt front was deemed the position of the node which was at the upper most point of the melt range, 347K. For an injection temperature of 385K, rewelding is predicted by the simulation to initiate when the encapsulation is preheated to a temperature between 310K and 315K. At an injection temperature of 400K, the preheat temperature necessary to initiate rewelding is between 295K and 300K.



Remelting simulations for the Rigidax™ material were carried out as well, using the identical procedures as those used for the BiSn eutectic. Figure 4.18, Figure 4.19 & Figure 4.20 record the temperature variation at the workpiece/Rigidax™ interface. From those graphs, the condition which cause remelting can be determined. It was deemed that a remelting condition was present when the temperature of the node at the workpiece/Rigidax™ interface reached the lowest point of the melt range, 325K.

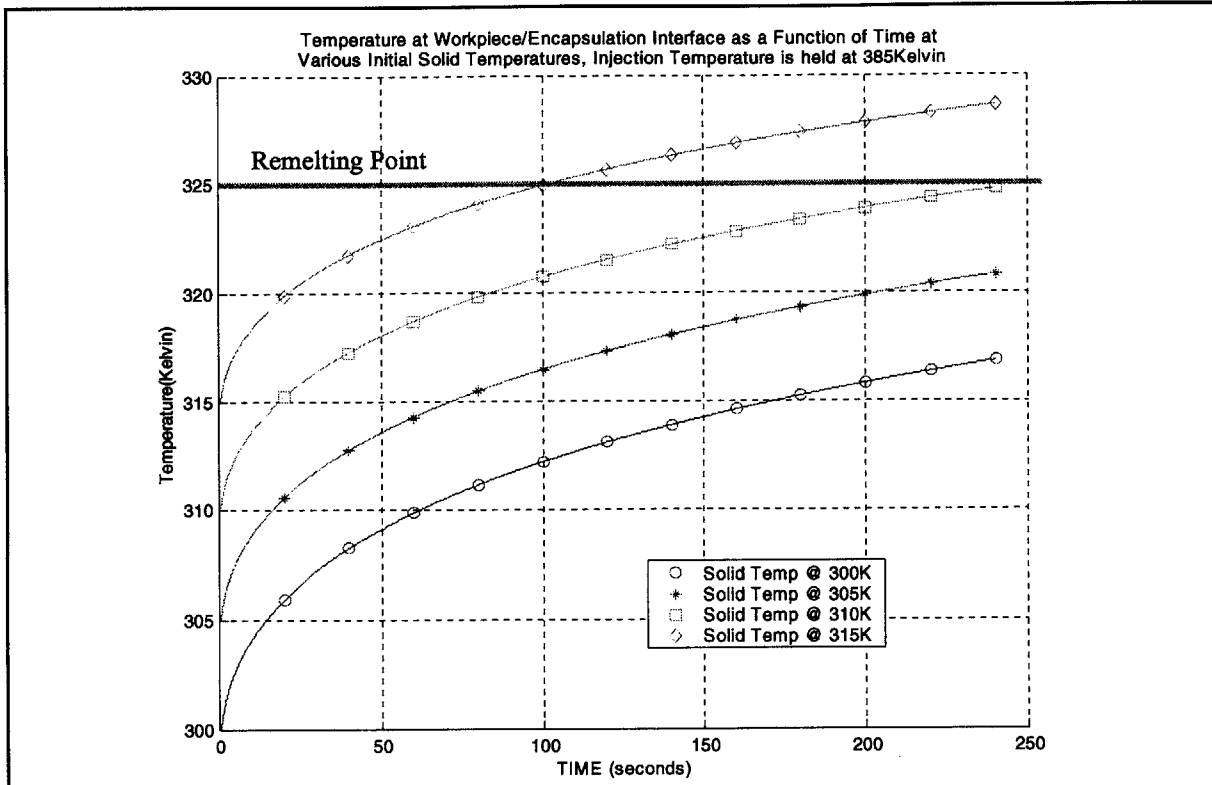


Figure 4.18: Graph of the Temperature at the Workpiece/Rigidax™ Interface for Various Preheat Temperatures as Injection Temperature is Fixed at 385K

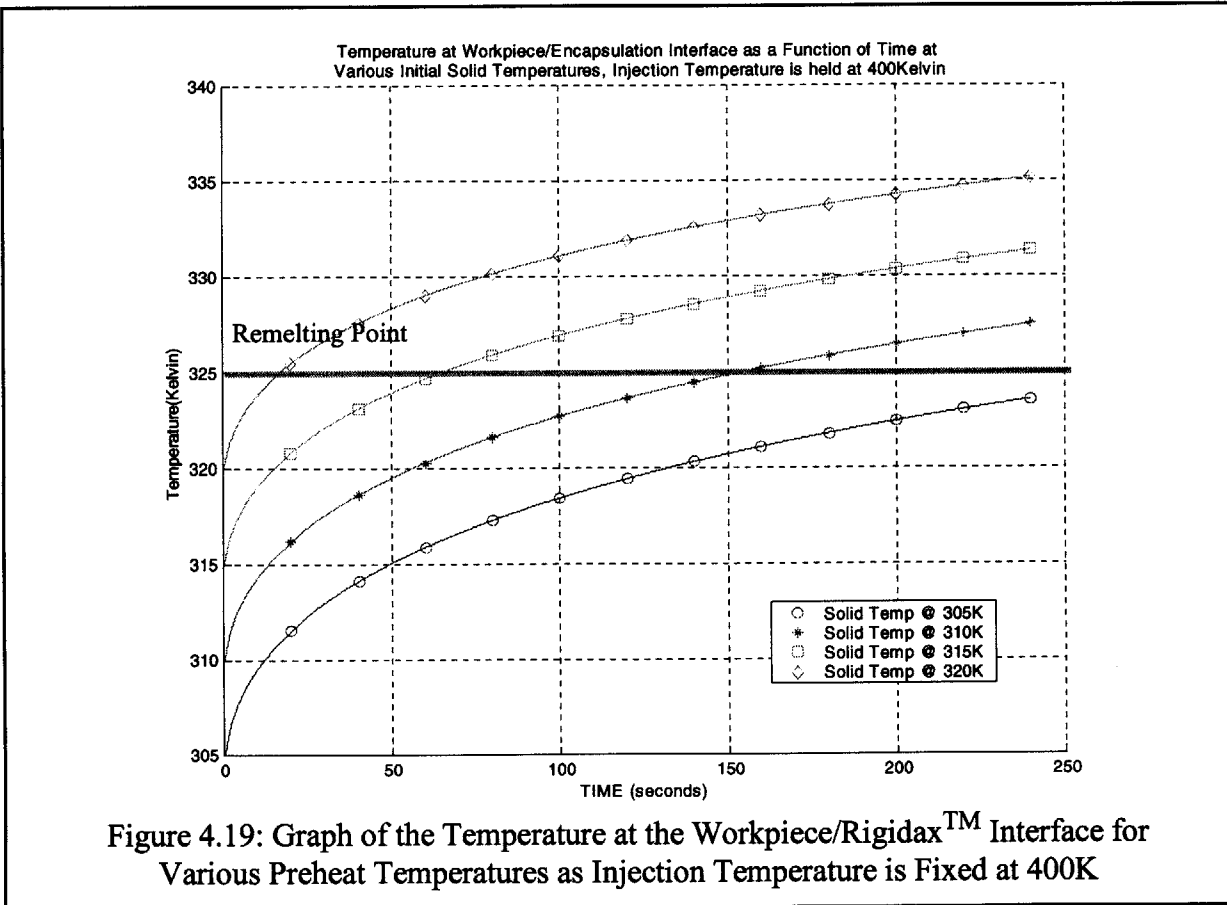
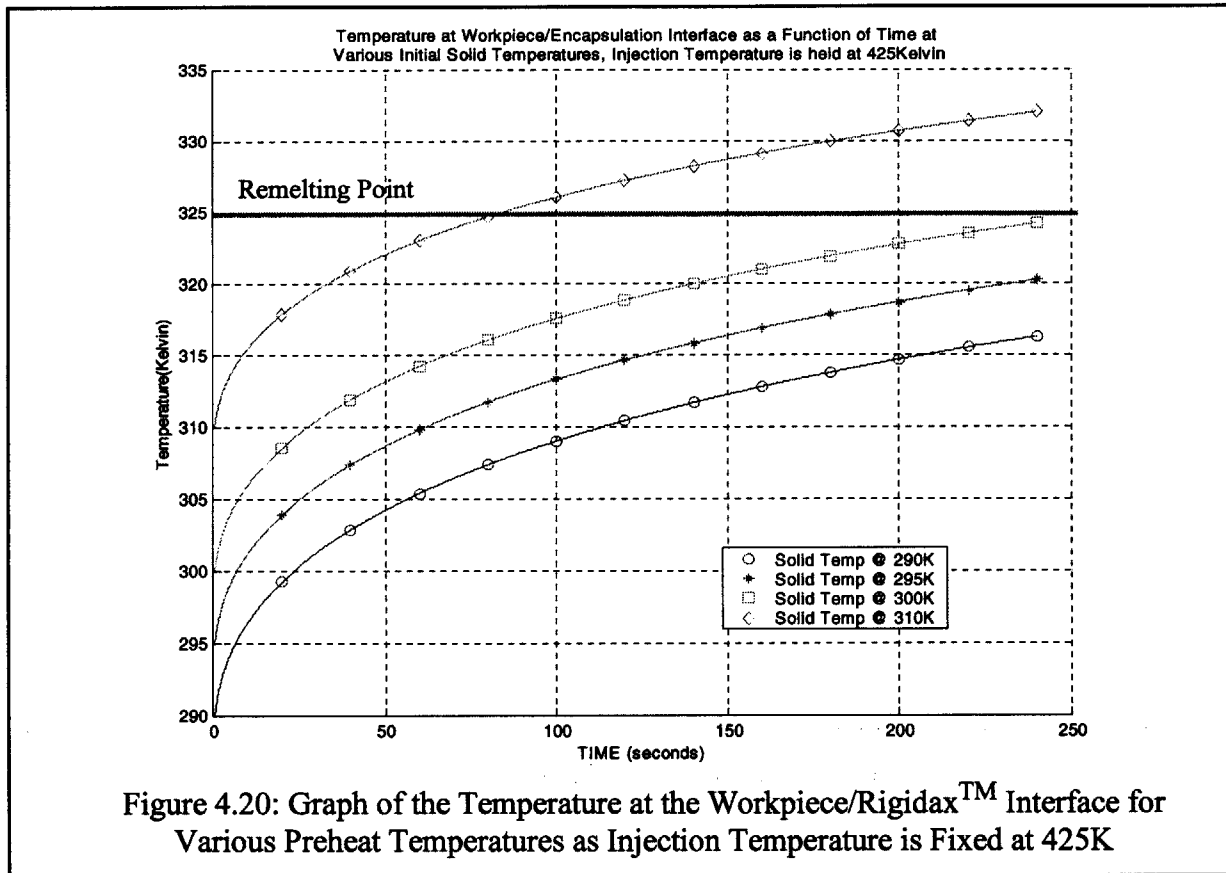


Figure 4.19: Graph of the Temperature at the Workpiece/Rigidax™ Interface for Various Preheat Temperatures as Injection Temperature is Fixed at 400K



To summarize, at an injection temperature of 385K, a remelting condition was present when the preheat temperature was set above 310K. For an injection temperature of 400K, it was necessary to set the preheat temperature to less than 305K in order to avoid remelting. And likewise, for an injection temperature of 425K, the preheat temperature recommend by the simulation is 300K or less.

4.6.2 Development of a New Process Window for Rigidax™

Figure 4.21 shows the process window for the Rigidax™ material. It was developed through the same technique as described above for the BiSn eutectic. Figure 4.22 plots both the BiSn eutectic process window and that of the Rigidax™ material. It shows that, though in different temperature regions, their shapes are actually quite similar. It is not apparent that the non-eutectic nature of the Rigidax™ material has a negative impact on process controllability. It can be

conjectured that the low thermal diffusivity of Rigidax™ and latent heat of fusion counteract any problems that could be potentially created by the non-eutectic nature of the material.

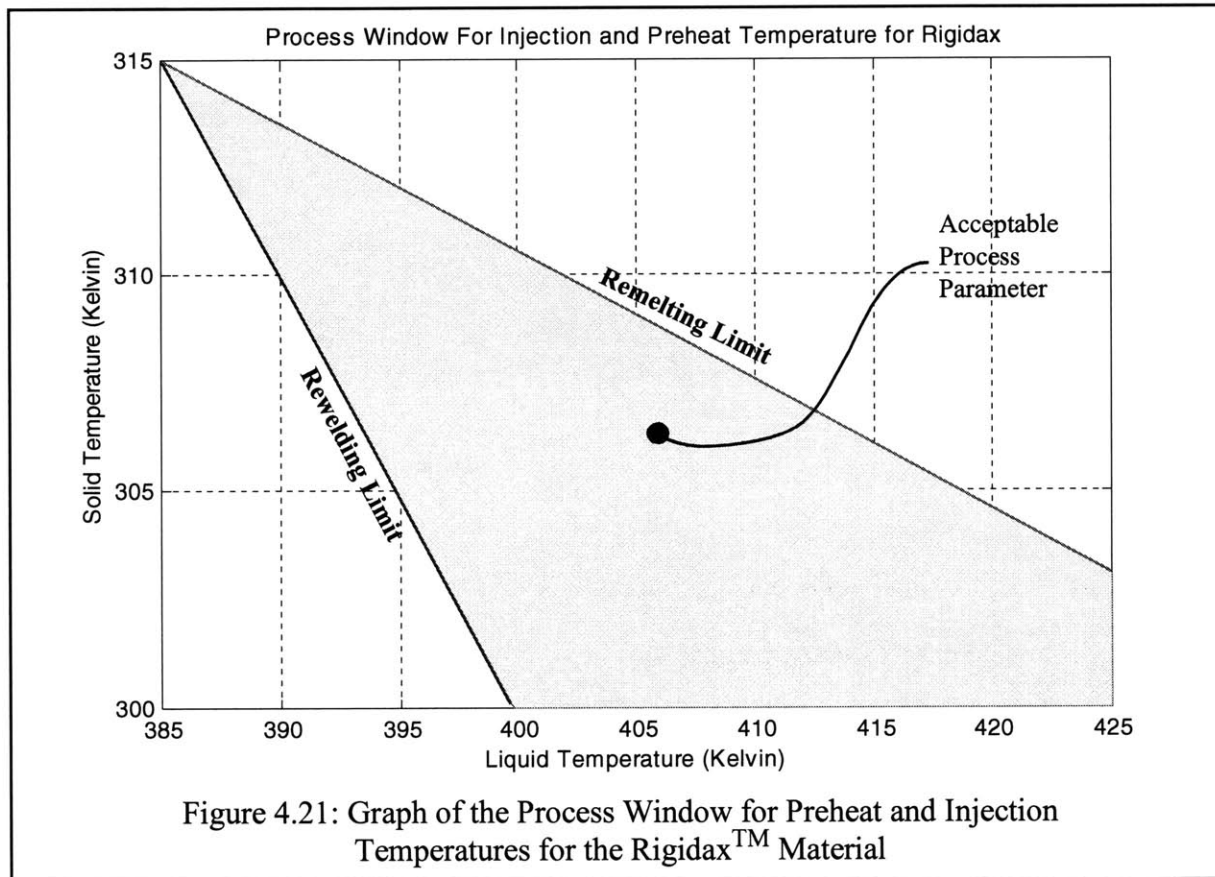
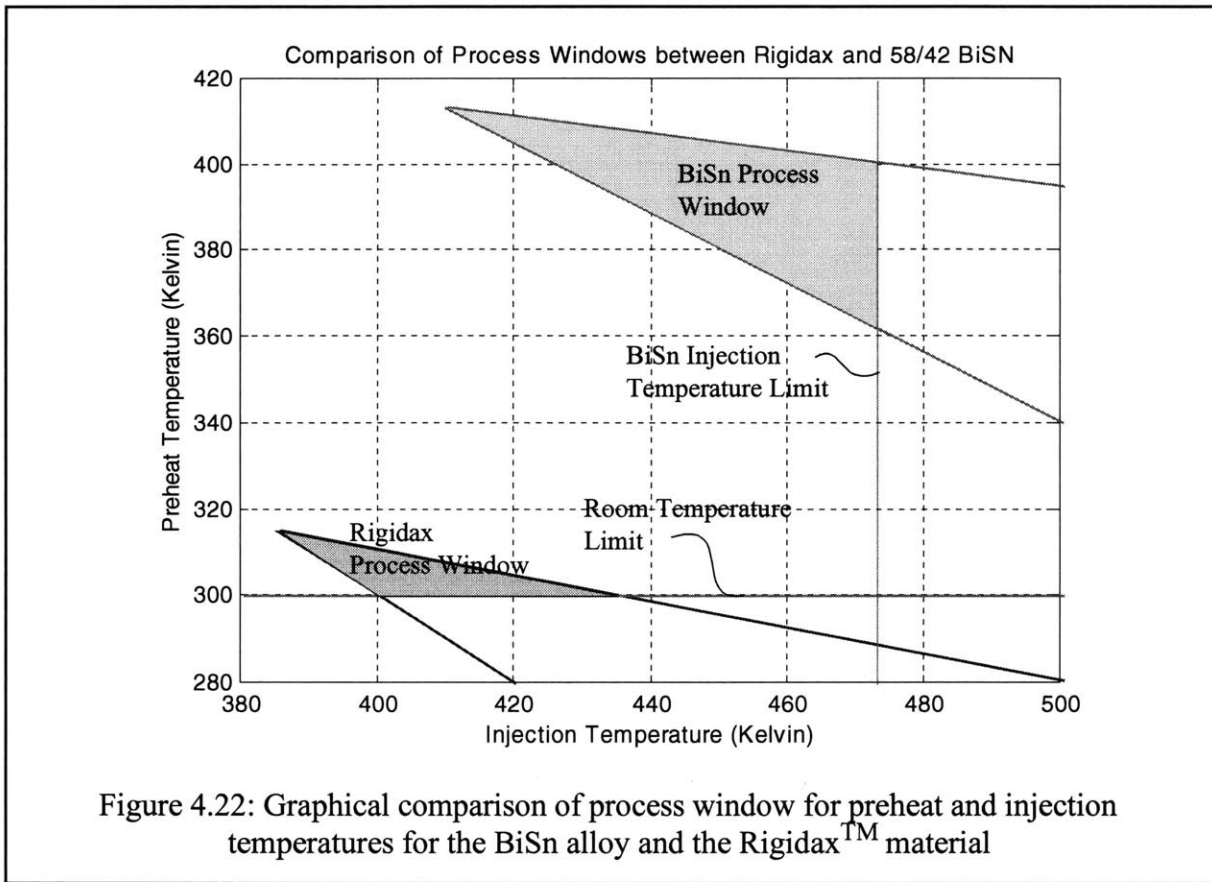


Figure 4.22 also displays the physical limitation the preheat and the injection temperatures are subjected to. The injection temperature of the BiSn eutectic alloy is limited to 500K. Above this temperature, it has been observed that the alloy begins to oxidize rapidly. Consequently, the encapsulation machines have been designed to deliver the encapsulation material at a maximum injection temperature of 500K. There is also a minimum preheat temperature imposed. Below 300K, room temperature, refrigeration equipment would be needed to cool the mold and the workpiece. In an effort to avoid complicating the encapsulation process, the use of such equipment has been avoided.



4.7 Summary: The Process Window of RFPE

The resulting process windows show that the BiSn eutectic allows for a more controllable and robust process. The process window is wide enough to accommodate any irregularities or disturbances. The Rigidax™ material, however, lacks that robustness. Its process window is thin and narrow. However, it can be stated that the Rigidax™ material is a more convenient material to use. Without requiring any preheating, a Rigidax™ encapsulation, left at room temperature, can be successfully re-encapsulated even if the injection temperature were to vary 30K. The preclusion of preheating will reduce encapsulation setup and cooling time. This does assume that the encapsulation's temperature is fixed at 300K. If the encapsulation temperature were 5K higher, the acceptable process range for the injection temperature drops from 30K to 20K.

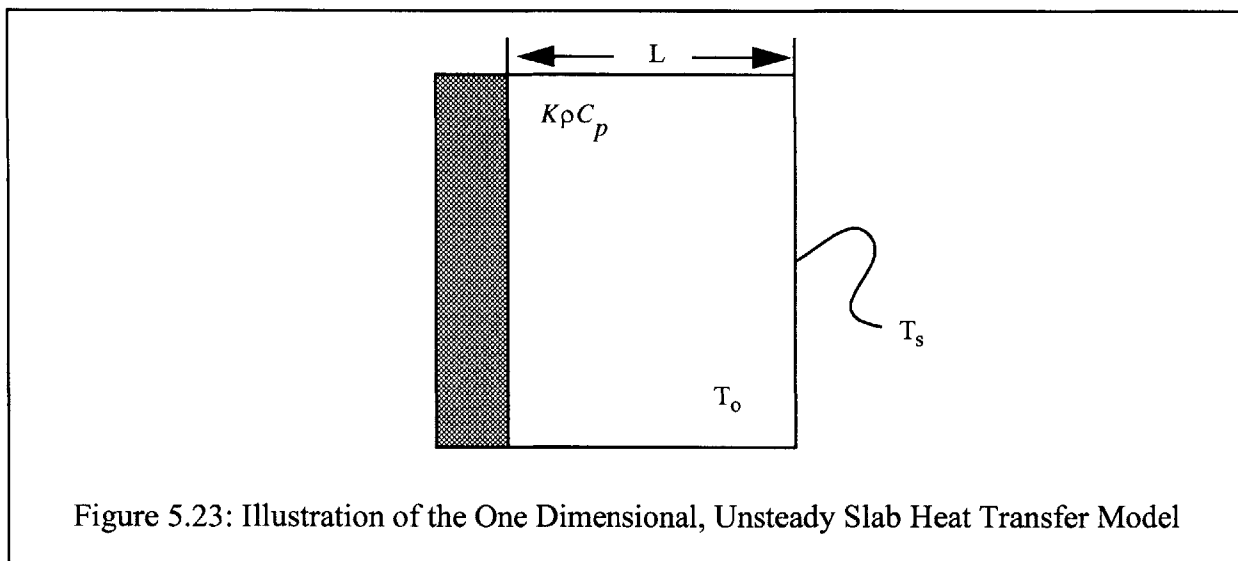
Chapter 5

Verification of the Runge Kutta Simulation

In order to verify the validity of the Runge Kutta algorithm, two analytical models that have closed form solutions were used as comparisons. The first model is an unsteady, one dimensional slab model with a fixed, uniform initial temperature. The model is subjected to a constant temperature on one side and adiabatic condition on the opposite side. This model does not possess any phase change characteristics and thus is not used verify that part of the code dealing with phase change. The second model is a set of two, one dimensional, unsteady heat conduction problems. The arrangement of the model has been modified to include phase change and is thus used to verify the phase change portion of the simulation.

5.1 Analytical Model of the Slab

The model of the slab's heat transfer is quite elementary, as illustrated in Figure 5.23.



where K is the thermal conductivity, ρ is the density, and C_p is the specific heat of the material.

The solution for this mold is easily obtained through separation of variables. It is as follows:

$$\frac{T - T_s}{T_o - T_s} = \sum_{n=0}^{\infty} \frac{2(-1)^n}{\left(n + \frac{1}{2}\right)\pi} e^{-\left(n + \frac{1}{2}\right)^2 \pi^2 F_o} \cos\left(n + \frac{1}{2}\right)\pi \frac{x}{L} \quad \text{Eq. 5.2}$$

where T_s is the surface temperature, T_o is the initial temperature, L is the slab thickness, and the Fourier number is defined as $F_o = \frac{\alpha t}{L^2}$, the thermal diffusivity multiplied by the time divided by the slab length squared.

Two materials, aluminum 6061-T6 and stainless steel 304, were simulated and compared with their analytical counterparts. The solution to the infinite series was calculated by programming Labview™ to calculate each term sequentially until the solution arrived at a convergence condition. The convergence condition was set so that the final answer would be 1% of the supposed answer. For both cases, no more than 10 terms were needed to arrive at convergence. In order to obtain the data from the simulation, a one dimension, single layer model was created with identical boundary conditions as shown in Figure 5.23. The temperature profile was tracked and a postprocessor program was written in Labview™ to capture the temperature profile of the at prescribed times. The simulation results were then compared to those obtained from the analytical model.

As shown in Figure 5.24, the analytical and simulated results agree very closely if not exactly. From these results, it can be concluded that general unsteady heat transfer and conduction component of the Runge Kutta simulation produces highly accurate results. These results, however, say nothing about the dependability of the phase change component of the Runge Kutta simulation. This will be examined in the next model.

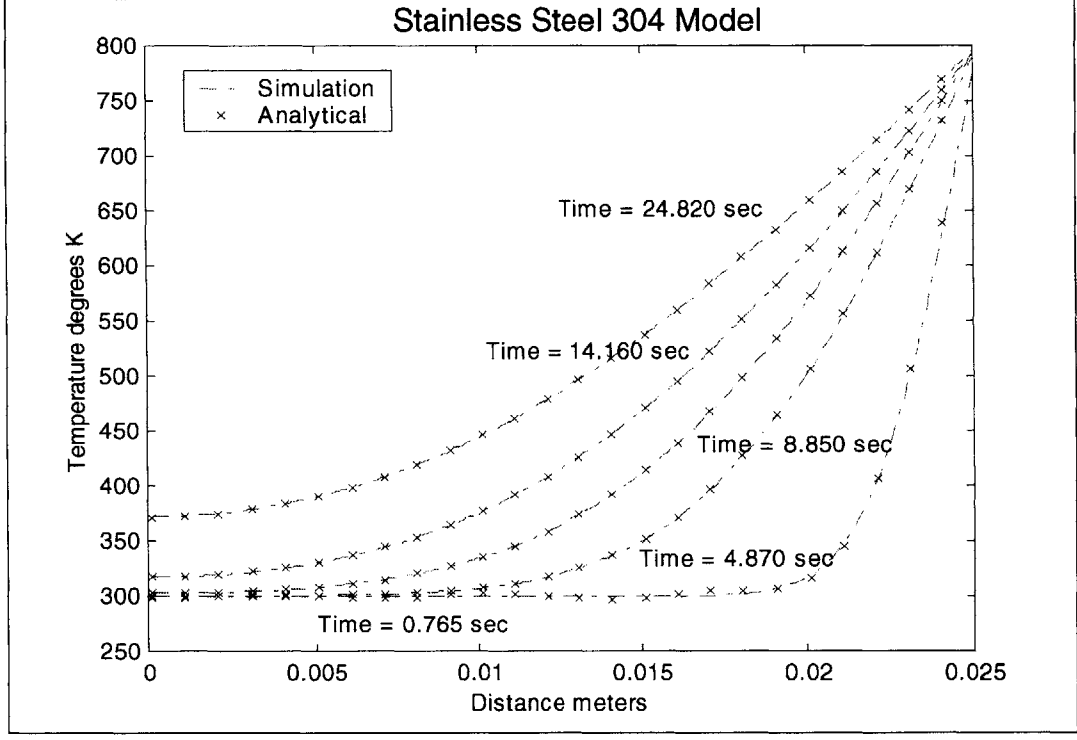
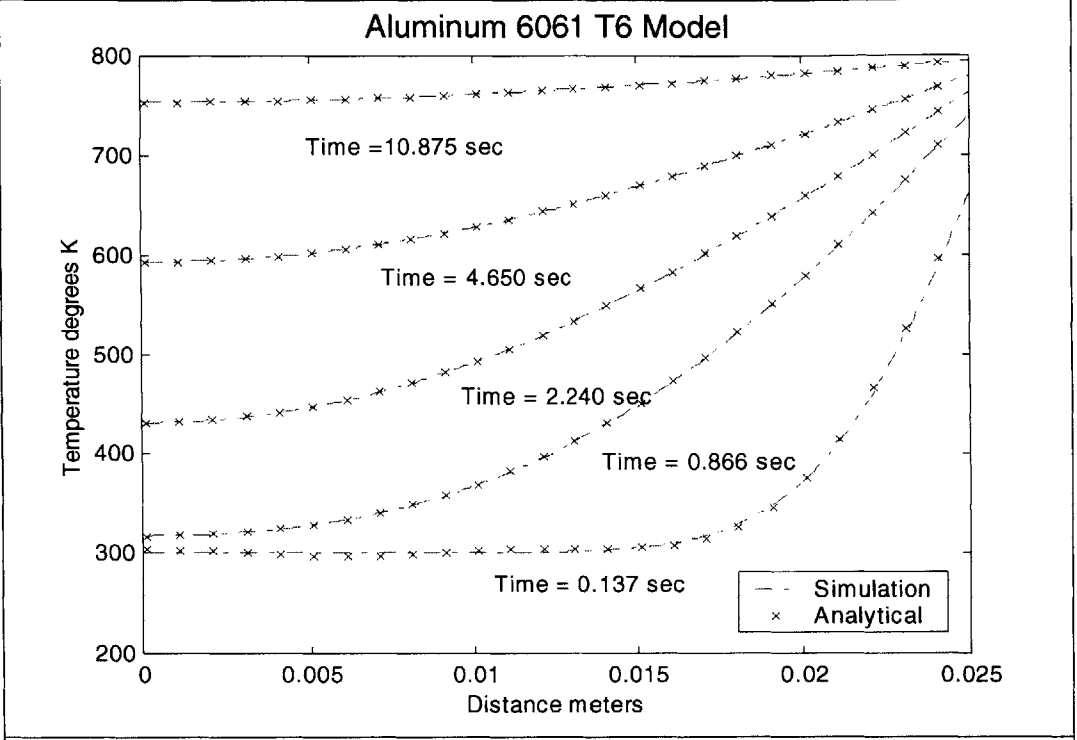
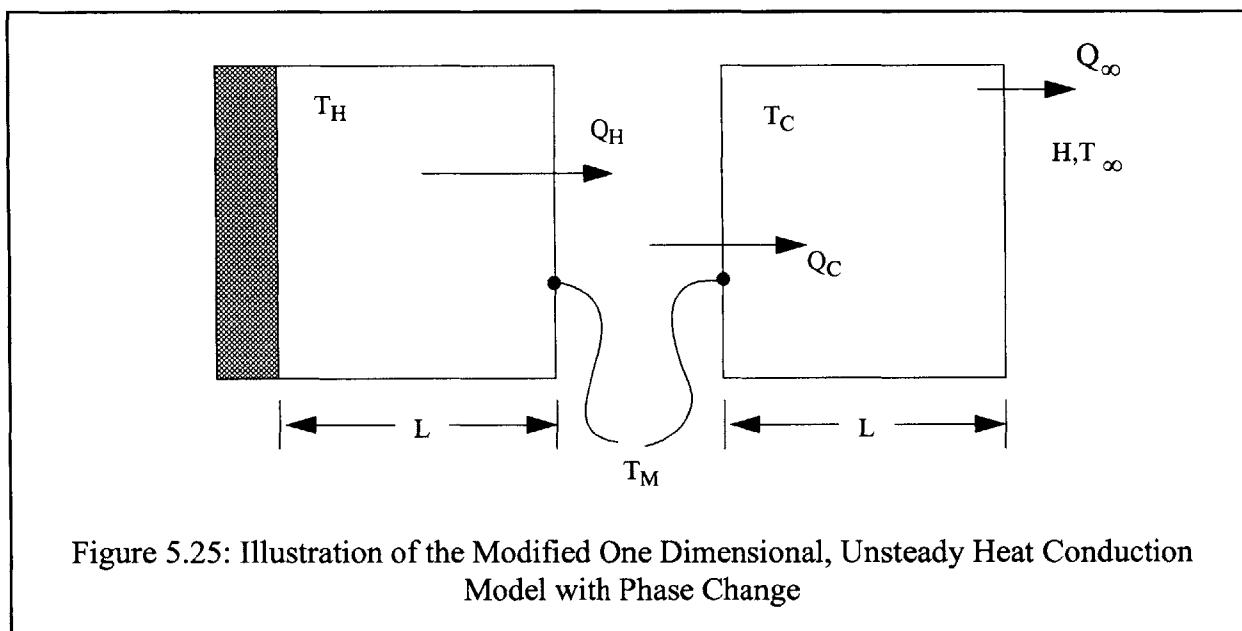


Figure 5.24: Verification of 4th Order Runge Kutta Simulation to Closed Form Solutions of a Unsteady Slab Conduction Model

5.2 Analytical Model Which Includes Phase Change

This analytical model is developed with the rewelding conditions in mind. Like the rewelding simulation model, this analytical model is also composed of two layers, a liquid layer and a solid layer. However, to determine the melt front movement, the two layers are not modeled as being brought into instantaneous contact with one another. Instead, a constant temperature, that of the melting point of the material, is imposed on the respective mating surfaces and the resulting time dependent heat flux is calculated for both layers. The cold layer will receive the heat energy, while the hot layer will lose the heat energy. The time dependent difference between the two heat flux will determine the movement of the melt front. This is illustrated in Figure 5.25. There is also an adiabatic condition imposed on the opposite end of the liquid layer and a convective condition imposed on the opposite end of the solid layer. This is identical to the simulation environment.



T_H is the initial temperature of the liquid layer, T_C is the initial temperature of the solid layer, T_M is the melt temperature of the material, T_∞ is the exterior temperature, and H is the convective heat transfer coefficient.

To determine the movement of the melt front, it is necessary to impose a conservation law at the two layer interface. It is obvious that if Q_H , the heat energy leaving the liquid layer, is not equal to Q_C , the heat energy entering the solid layer, there must be energy absorbed or released at the interface, caused by phase change. Knowing the amount of addition heat energy created or absorbed will thus provide an equation for the melt front movement. It can be described as follows:

$$Q_H - Q_C = \rho h_{fg} (\delta x) A \quad \text{Eq. 5.3}$$

In the one dimensional case, A , the cross-sectional area of each layer, is taken to be 1. h_{fg} is the latent heat of fusion, ρ is the density and δx is the thickness of layer that has undergone phase change. Differentiating Eq. 5.3 with respect to time,

$$q_H - q_C = \rho h_{fg} V \quad \text{Eq. 5.4}$$

V is the melt front velocity. Thus, by determining q_H and q_C , we can now approximate the melt front velocity and thus develop a function which described the melt front location with respect to time.

It is important to note that this model is an approximation of the actual condition that occur during rewelding. The model assumes that the layer thicknesses remain fixed. This is obviously untrue since the phase change will allow one layer to eat into the other. It is, however, a valid approximation if the phase change layer thickness, or the maximum melt depth, is much smaller than that of each layer. From the results above, we can assume that the maximum melt depth is on the order of 1 mm. To follow the same parameters as those in the simulation, the model layers are set to 12.7 mm thick. Thus, while the ratio of model layer thickness to melt layer thickness is not

extremely large, one can expect a reasonably accurate result. Since the layer thickness is held constant, this analytical approximation does over-estimate the heat flux which is transmitted to from the liquid layer to the solid layer. Thus one can expect the analytical model to also over estimate of the maximum melt depth and predict a faster than realistic melt front movement.

The solution to this unsteady conduction problem is broken down into two parts, one for the liquid layer and one for the solid layer. Each layer is solved independently and, though Eq. 5.4, combined to develop an expression for the melt front movement. That is:

$$X(t) = \int v dt \quad \text{Eq. 5.5}$$

$$X(t) = \int \frac{(q_H - q_C)}{\rho h_{fg}} dt \quad \text{Eq. 5.6}$$

Since the liquid layer model corresponds directly to the first verification model, the solution can be taken from Eq. 5.2,

$$\frac{T - T_M}{T_H - T_M} = \sum_{n=0}^{\infty} \frac{2(-1)^n}{(n + \frac{1}{2})\pi} e^{-\left(n + \frac{1}{2}\right)^2 \pi^2 F_o} \cos\left(n + \frac{1}{2}\right)\pi \frac{x}{L} \quad \text{Eq. 5.7}$$

$$q_H = -K \frac{dT}{dx} \quad x = L \quad \text{Eq. 5.8}$$

$$q_H = 2 \frac{K(T_H - T_M)}{L} \sum_{n=0}^{\infty} e^{-\left(n + \frac{1}{2}\right)^2 \pi^2 F_o} \quad \text{Eq. 5.9}$$

While the solid layer is a slightly more arduous to solve mathematically, the same techniques, those of separation of variables, are used to solve for the temperature profile which varies with time. The solution obtained is by separating the solution into its homogeneous solution and its particular solution.

$$T(x, t) = T_1(x) + T_2(x, t) \quad \text{Eq. 5.10}$$

$$T_1(x) = \frac{H(T_\infty - T_M)}{HL - K} x - T_M \quad \text{Eq. 5.11}$$

$$T_2(x, t) = \sum_{n=0}^{\infty} C_n \sin\left(\alpha_n \frac{x}{L}\right) e^{-\alpha_n^2 F_o} + T_M \quad \text{Eq. 5.12}$$

where α_n must satisfy the following condition:

$$\tan(\alpha_n) = -\frac{\alpha_n K}{LH} \quad \text{Eq. 5.13}$$

and

$$C_n = 2 \left(\frac{\left(\frac{\sin(\alpha_n) - \alpha_n \cos(\alpha_n)}{\alpha_n} \right) \ominus + (T_M - T_C)(\cos(\alpha_n) - 1)}{\alpha_n - \cos(\alpha_n) \sin(\alpha_n)} \right) \quad \text{Eq. 5.14}$$

where:

$$\Theta = \left(T_M - T_C - \left(\frac{(T_M - T_C) \frac{K}{L} + (T_\infty - T_C) H}{\left(\frac{K}{L} + H \right)} \right) \right) \quad \text{Eq. 5.15}$$

By differentiating with respect to x , with $x = 0$, as was done in Eq. 5.8, it is now possible to develop an expression for q_C . It is as follows:

$$q_C = -K \left(\frac{H(T_\infty - T_M)}{HL - K} + \sum_{n=0}^{\infty} C_n \frac{\alpha_n}{L} e^{-\alpha_n^2 F_o} \right) \quad \text{Eq. 5.16}$$

Inserting Eq. 5.16 and Eq. 5.9 into Eq. 5.6 allows the completion of the analysis, providing a closed form solution describing the melt front movement as a function of time. Figure 5.26 plots the solution for two different injection temperatures as the preheat temperatures is varied. The results of the simulations run under the same condition are plot over the analytical results. The results show that the analytical results predict a greater maximum melt depth than what is developed from the simulation, as expected. It also shows that the heat transfer rate is slightly faster in the analytical case than in the simulation as shown by the faster times to peak. Figure 5.27 graphs the predicted maximum melt depth for both simulation and analytical model. The analytical model predicts about a 30% higher maximum melt depth. Since the results of the simulation fall on the lower side of those of the analytical model, the more realistic side, the trends of the analytical model seem to support that the results of the simulation are accurate. Thus, it can be said that the simulation is validated by this analytical model.

The obvious question here is why not use this analytical model instead of the simulation to predict maximum melt depths. Calculating the infinite series using a computer program, in this case a LabviewTM program was written to do so, is orders of magnitudes faster than using finite element methods to simulation the heat transfer reactions. In practice, an analytical model would

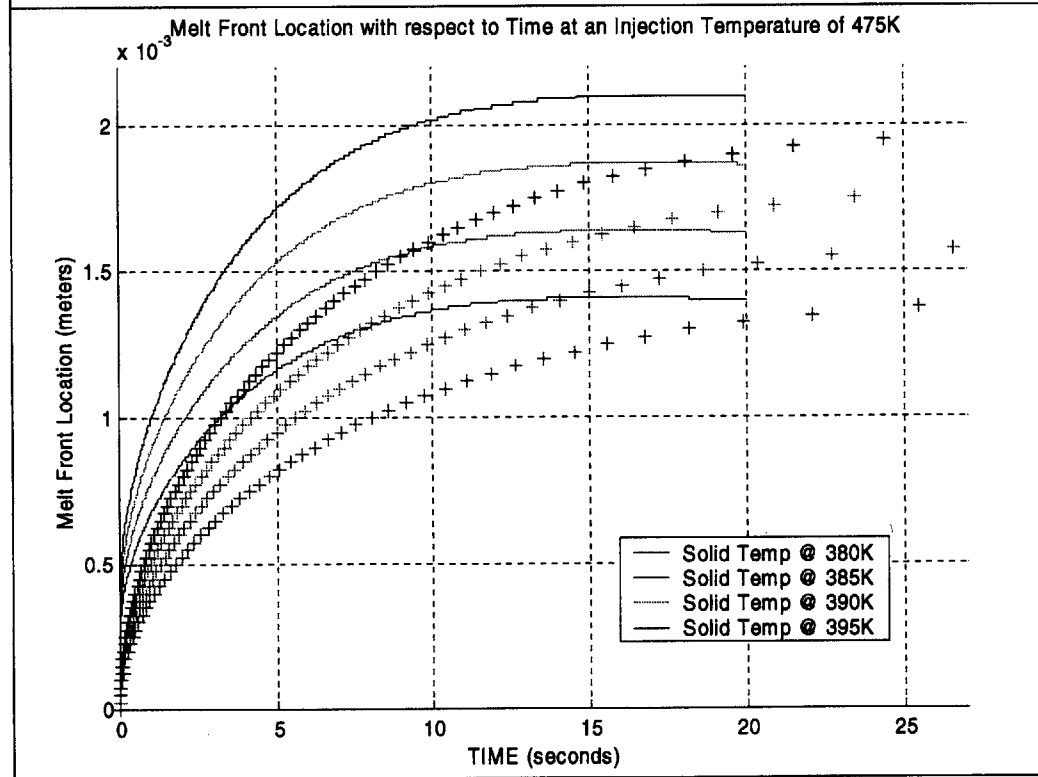
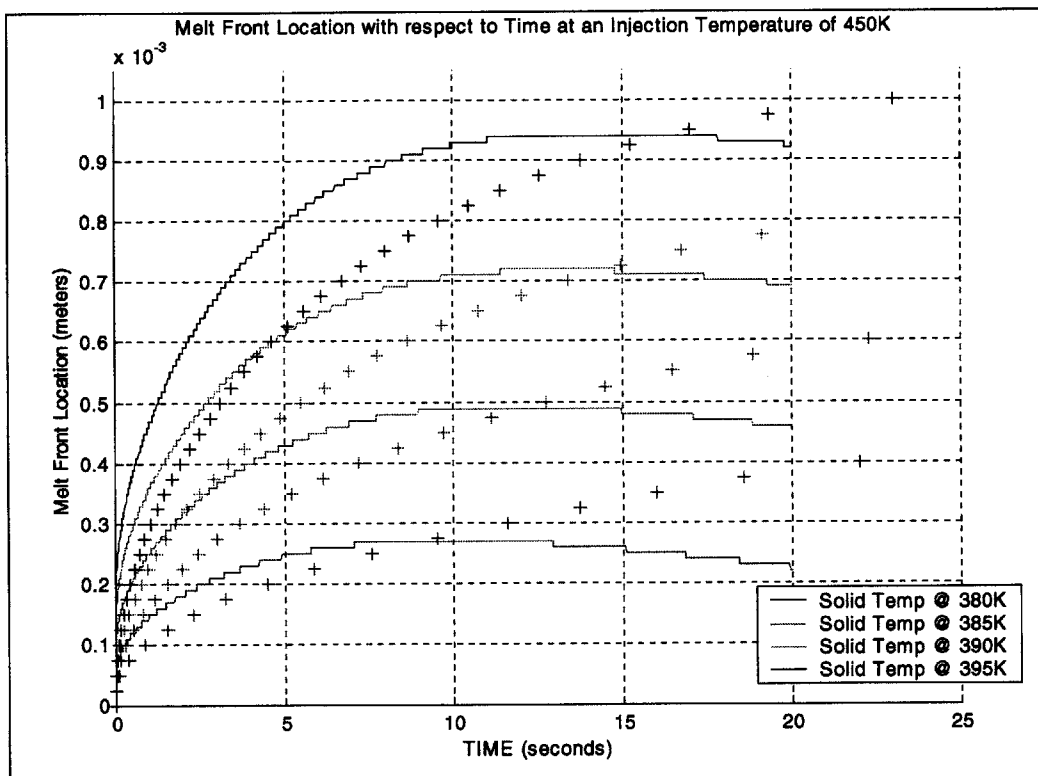


Figure 5.26: Comparison of Results of Melt Front Location as Plotted with Time Derived by an Infinite Series Solution (solid lines) and by the 4th Order Runge Kutta Simulation (points)

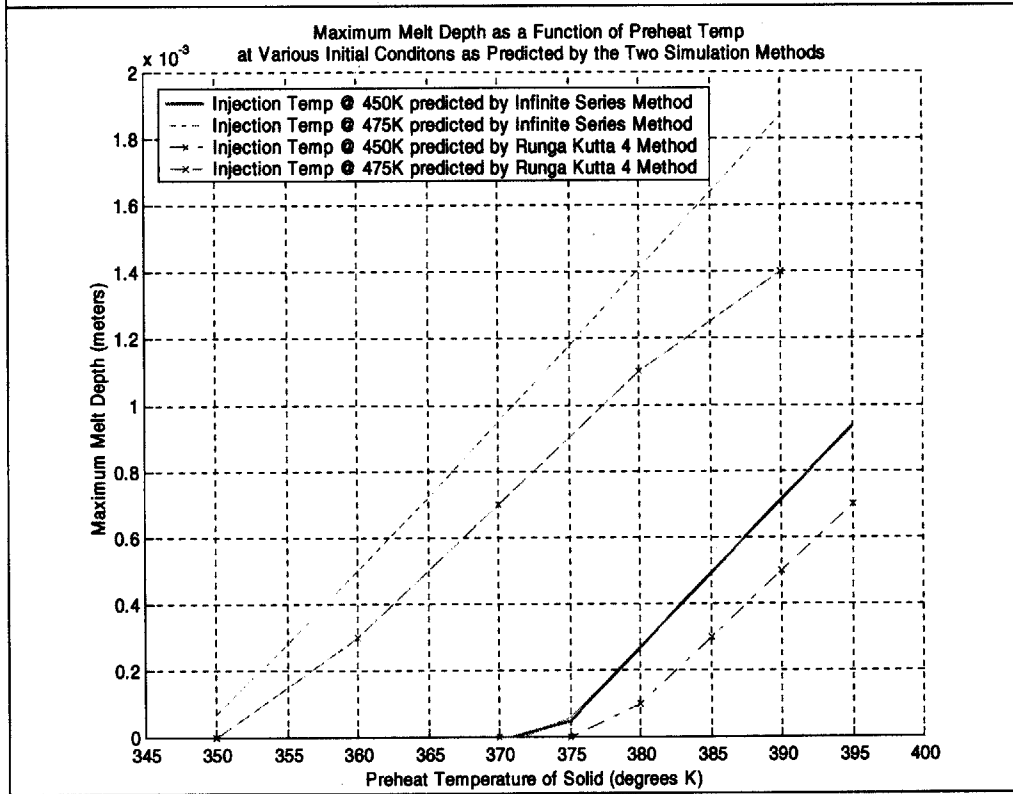
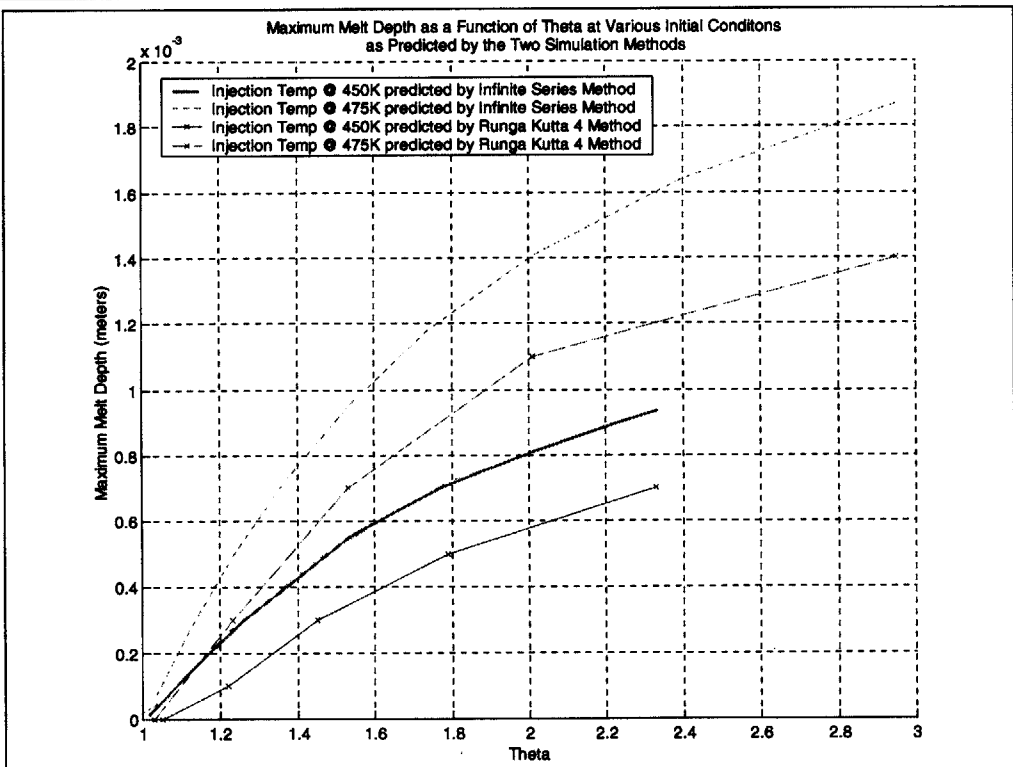


Figure 5.27: Graphical Comparison of the Maximum Melt Depth as Predicted by Both the Simulation and the Analytical Model

require approximately 2 hours to complete a run while the finite element simulation would require 30 hours. Clearly, the analytical model has the advantage of speed. However, the simulation has the advantage of flexibility. The simulation is written to be able to account for non-eutectic materials. The analytical model is incapable of including those features. Also, the simulation can be run for any one dimensional unsteady conduction problem, regardless of the number of layers involved or the different initial conditions prescribed. The analytical model solution is suitable for only a two layer model.

The closed-form solutions could be resolved to include these additional intricacies. However, this would require writing an entirely new program to calculate the resulting infinite series. Thus, while the analytical model provides utility in studying the rewelding behavior, the simulation was solely relied upon to study the remelting behavior.

5.3 Stability of the Runge Kutta Simulation

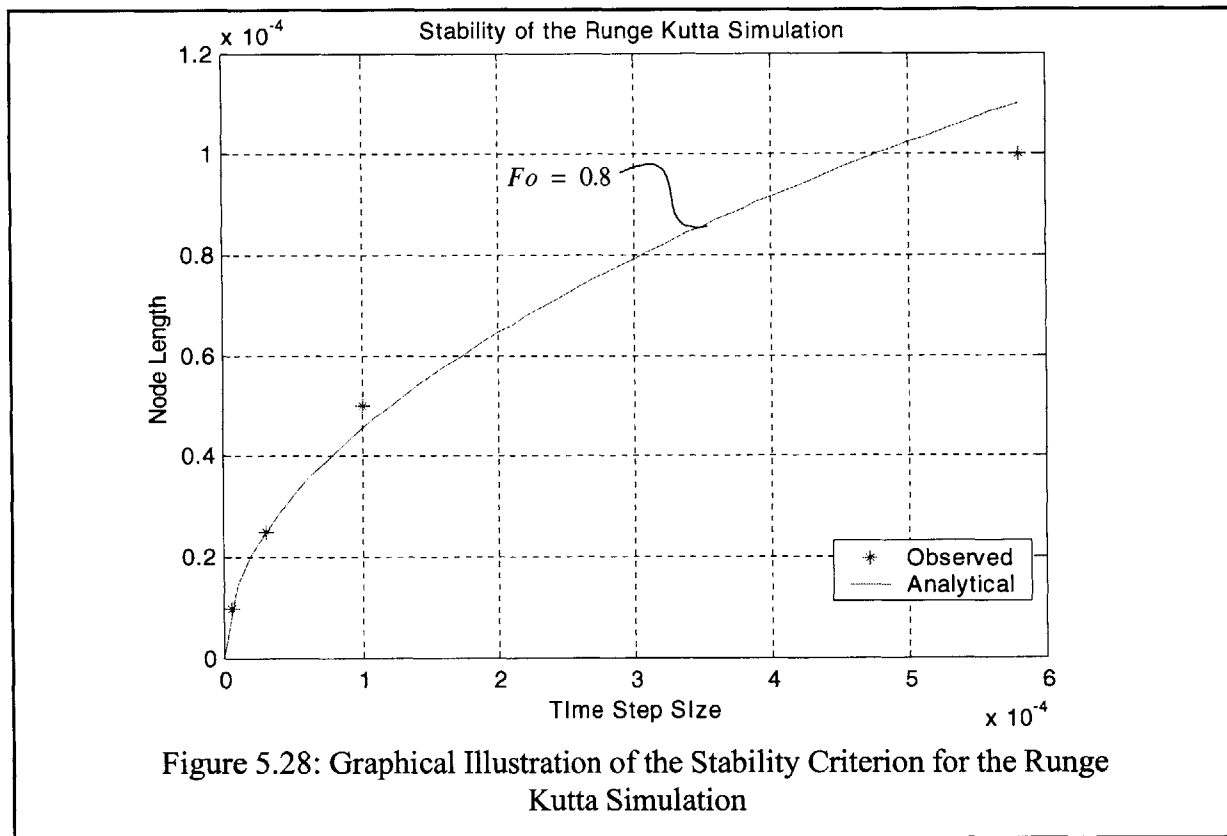
While running the Runge Kutta simulation, it was observed that the simulation would become unstable and not converge when the equivalent Fourier Number was greater than 1.0. The equivalent Fourier Number is defined by Eq. 5.17.

$$Fo = \frac{\delta}{\sqrt{a_t t}} \quad \text{Eq. 5.17}$$

where δ is the node length, a_t is the thermal diffusivity, and t is the time step size. Through a number of simulation trials, it was seen that the simulation would run stably and reliably only if the equivalent Fourier Number was lower than unity.

For a given node length, the time step size was varied to find the stability boundary. It was observed that as node length increased, the time step size necessary to satisfy stability increased. As shown in Figure 5.28, four stability points were taken and plotted. The equivalent Fourier

number of 0.8 was plotted as well and represents a good match to the measured points. It can be thus seen that stability becomes the limiting constraint that prevents the simulation from being completed at shorter times. In general, one would think that by increasing the time step size, one could decrease the time to complete a simulation. However, the stability criterion shows that in order to decrease the time to complete a simulation one must decrease resolution in the model, *i.e.* increase the node length. One can not simply increase the time step and hold the node length fixed. That would eventually lead to an unstable run. Once at the stability boundary, one must increase the node length with increases to the time step size. The stability thus shows that there is a trade-off between speed and resolution.



The stability criterion can be further explained by examining the heat transfer between the nodes themselves. It is evident that the heat energy transferred between nodes can not result in a

situation where the temperature of one node becomes higher or lower than the initial temperature of its adjacent nodes. Put another way, Eq. 5.18 must always be satisfied.

$$(\Delta T_H C_p \delta \rho = \Delta T_L C_p \delta \rho) \leq K(T_H - T_L) \frac{t}{\delta} \quad \text{Eq.5.18}$$

It can be assumed that:

$$\Delta T_H \cong \Delta T_L \cong (T_H - T_L) \quad \text{Eq. 5.19}$$

Thus, Eq. 5.18 can be simplified to be:

$$\frac{C_p \rho}{K} \leq \frac{t}{\delta^2} \quad \text{Eq. 5.20}$$

$$1 \geq \frac{\delta^2}{\alpha t} \quad \text{Eq. 5.21}$$

$$Fo \leq 1 \quad \text{Eq. 5.22}$$

Eq. 5.22 is the stability criterion. It thus shows that the stability criterion is in fact grounded in the basic laws of heat transfer. The stability criterion prevents the simulation from transferring energy through the nodes faster than what is physically possible.

5.4 Summary

Two analytical models have been used to successfully verify the validity of the Runge Kutta finite element simulation written to specifically investigate the rewelding and the remelting

phenomenons. It has been shown that the simulation results contain a high degree of reliability. While the simulation is computationally intensive, it provides the flexibility to model an assortment of heat transfer conditions. Programmed to be fully automatic, the simulation model can be easily input into the simulation and allowed to run overnight. While the length of the runtime is dependent on the size of the model and the desired simulation time and detail of the results, the average runtime is approximately 30 hours on a Pentium III class process. The simulation algorithm has proven to be invaluable in the study of the rewelding and the remelting phenomenon. With such versatility, other applications for the program surely exist.

Chapter 6

Industrial Application Experiment

In order to develop a better understanding of the effectiveness of RFPE fixturing, a test part has been obtain from the Ford motor company. The test part, known as a body mount, is described in Figure 6.1. In normal production the part is punched and stamped to its final shape, encapsulated in an elastomer and installed in an automobile between the frame and chassis. Its function is to aid in dampening higher frequency road vibrations, preventing the “road noise” from being felt by passengers within the vehicle.

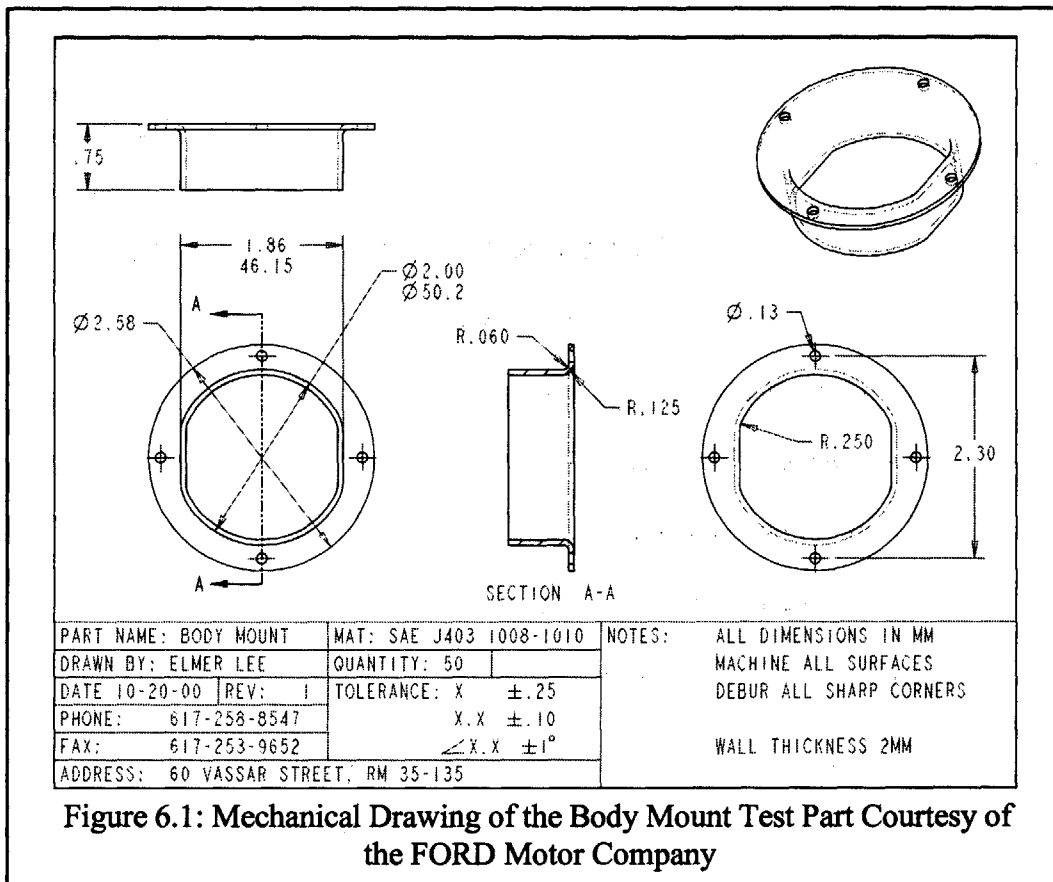


Figure 6.1: Mechanical Drawing of the Body Mount Test Part Courtesy of the FORD Motor Company

6.1 Three Fixturing Strategies and Their Machining Procedures

To compare and evaluate the RFPE fixturing performance with those of other tooling, the test part was also machined using two other conventional fixturing setups. The first tooling setup used what is known in industry as soft tooling. Soft tools are fixturing tools manufactured from “soft” aluminum as opposed to harden steel. Such tooling is normally designed for short runs where no more than 100’s of parts are produced. The soft tool is specifically designed with features that allow it to locate the test part quickly and grip the workpiece securely. The tooling can not completely support flexible members of the workpiece during. Therefore there is a strong likelihood that slender members of the workpiece will deform under machining forces. The upfront work needed to create the soft tool is high. However, if the quantities justify this expenditure, the soft tooling will greatly reduce per part setup time and, in the long run, reduce piece cost.

The second tooling setup uses make-shift tooling. Composed mainly of a rudimentary two-jaw vise, the makeshift tooling has the benefit of being fast and inexpensive. It will simply secure the part to the machining environment. Once loaded into the machining environment, the workpiece must be manually located by an operator using analog or computerized indicators. There is very little upfront planning and development of tooling for this situation. This is counterbalanced, however, by the larger per piece setup time needed to position, secure and locate the part. If quantities are low, then, even though per piece setup time is large, the piece cost can still be relatively low.

The RFPE fixturing system can be seen as a mating between the best of the two situations described above. The tooling will provide support and immobilize the workpiece and can be used to quickly and automatically locate the workpiece once inside the machining environment. What’s more, there is very little upfront setup time and development cost associated with this scheme if the proper RFPE system is already

implemented. The RFPE process still has hard tooling. The molds and the fixtures are specifically designed for RFPE usage. However, because of the generic nature of the RFPE process, the tooling can be reused for other parts, thus amortizing the tooling cost and time over a larger part piece cross-section.

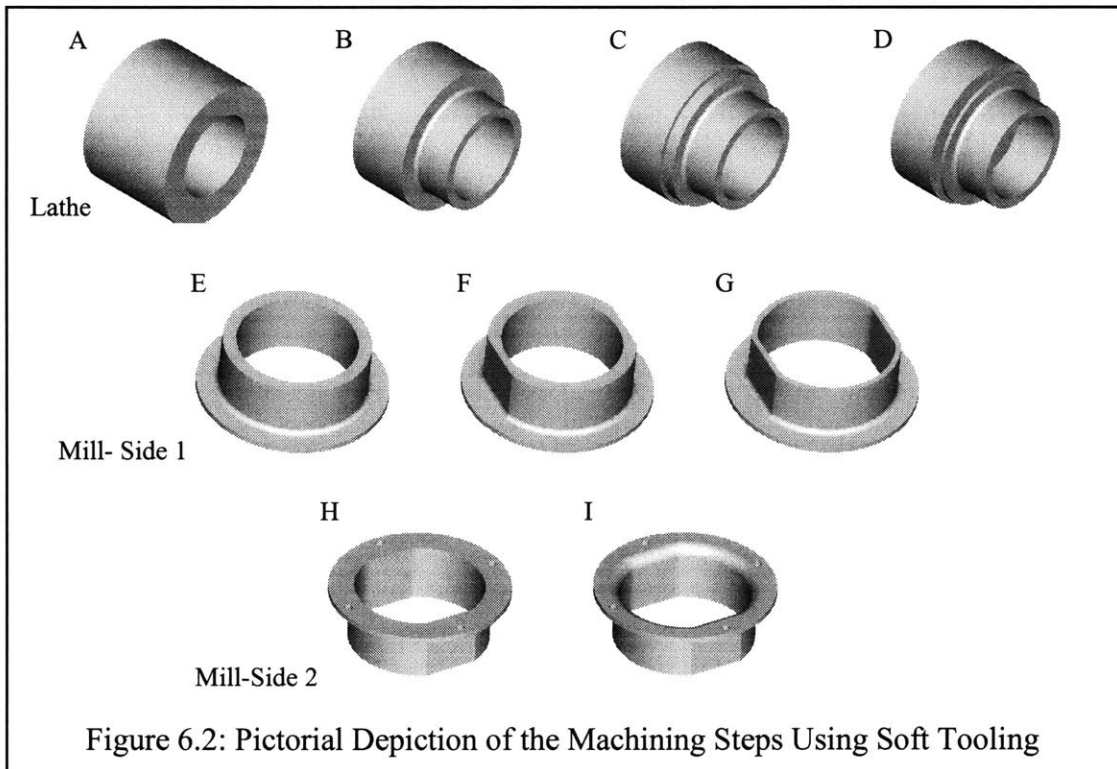
6.1.1 Soft Tooling

The soft tool fixturing scheme utilizes a lathe and a milling machine. There is one setup on the lathe in which the part will be held and located using a conventional lathe chuck. Within the milling machine, there are two setups, one to machine features located on the front side and the next to machine features on the back side. The tooling is machined from a block of 6061-T6 aluminum. It is manufactured in two pieces which when finished will be mounted on either side of a two-jaw vise. The tooling has 2 main features. The first is a semi-circular pocket that will mate with the outer diameter of the flange on the workpiece. The second consists of flats that will be used to align and orient the workpiece when machining its back side.

The machining procedures are illustrated in Figure 6.2.

- A) Round hollow stock is loaded into a lathe. The front side is lathe to ensure that it is flat and square to the workpiece
- B) Both the outer diameter and the inner diameter are turned to the appropriate size.
- C) The flange diameter is turned.
- D) The workpiece is parted from the rest of the stock.

- E) The workpiece is loaded into the milling machine. The specifically designed tooling grabs the workpiece around the flange diameter.
- F) Flats are milled into the outer diameter.
- G) Flats are milled into the inner diameter.
- H) The workpiece is flipped upside down. The flats previous machined are now used to aligned the part to the tooling. Four holes are drilled into the flange.
- I) Lastly, a radius is milled on the inner diameter to finish the prototype part.



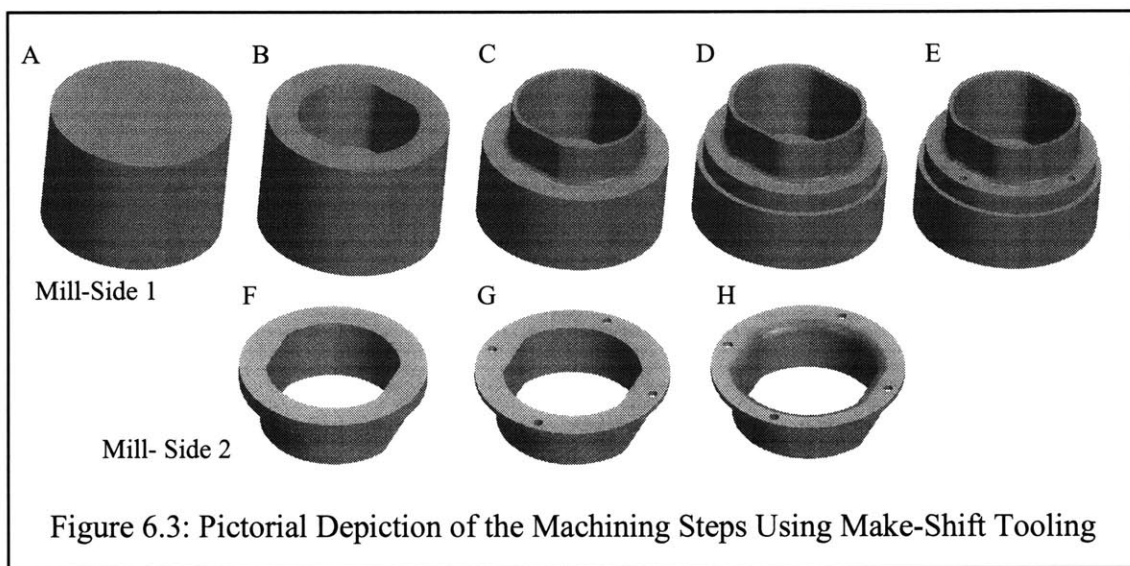
6.1.2 Make-Shift Tooling

The makeshift tooling scheme uses only a milling machine to manufacture the test part. Although the material removal rate is superior in a lathe, the setup of a second machine and the transport of parts from one machine to the next increase piece cost if the quantities to be manufactured are small. Within the milling machine, two setups are required. A conventional two-jaw vise is used to hold the workpiece. No other specifically design tooling is used. The machining procedures are illustrated in Figure 6.3.

- A) A piece of solid round stock is loaded into the milling machine and clamped down tightly in the two-jaw vise. Hollow stock could have been used instead. However, since hollow stock is not as commonly found, it would need to be specially ordered. For small quantities, this simply is not economical. The stock is roughly indicated to determine the center of the workpiece. The top side is milled flat and represents the zero in the z-direction.
- B) The internal bore with flats is milled into the stock.
- C) The outer diameter is milled into the stock as well. A bull-nose endmill is used to machine in the radius.
- D) The flange diameter is milled in.
- E) Four holes are drilled into the flange.
- F) The part is removed from the mill and installed into a horizontal bandsaw. The workpiece is chopped off and returned to the mill. The workpiece is now held in the two-jaw vise which clamps down on the flats that were previously machined. To

provide support. a wooden block is quickly sanded down to size and wedged into the internal core.

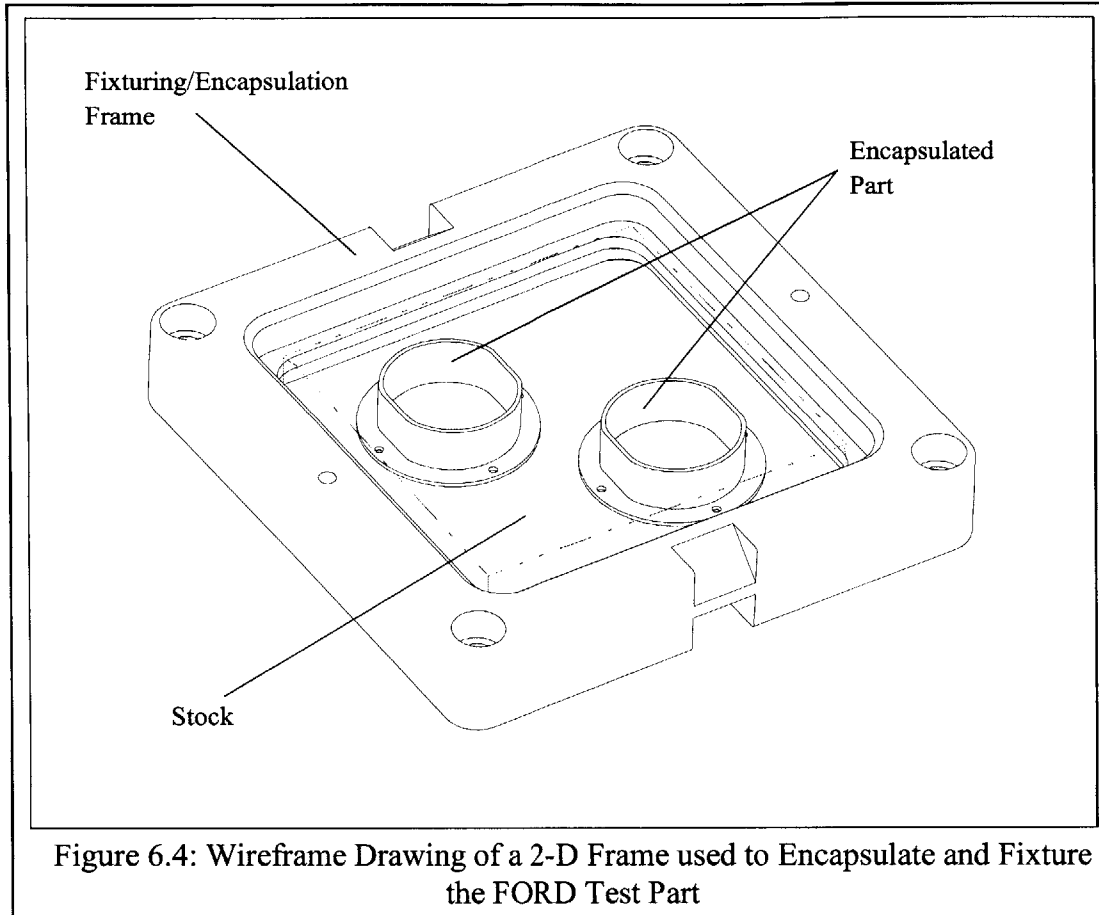
- G) The top side is then machined down to give the flange the correct thickness.
- H) Finally, a radius cutter is used to machine in the round.



6.1.3 RFPE Fixturing

The test part can be easily fixtured using a 2-D RFPE encapsulation method. Figure 6.4 shows the stock encapsulated in the 2-D frame. Refer to Appendix B for more details of the encapsulation procedures. In the 2-D case, the encapsulation material provides support and helps to immobilize the workpiece. The location of the workpiece is however relied upon through features found on the 2-D frame surrounding the stock. The frame is also used to mold the encapsulation. Two dowel pin holes are used to locate the frame in the X & Y-planes and since the thickness of the frame is accurately known, the horizontal

surfaces are used to locate the workpiece in the Z-plane. Within the 6" frame, there is enough space to machine two test parts.



The machining procedures using the RFPE fixturing system is illustrated in Figure 6.5. It depicts only one part being machine and excludes all detail of the 2-D frame.

- A) A square plate stock is encapsulated in the 2-D frame. In ideal conditions, pre-encapsulated stock would be stored on a machine shop floor and taken out to be used when necessary.
- B) The first machining procedure is to mill a circular pocket on the top face.

- C) The internal bore is milled including the flats.
- D) A radius is cut into the sharp edge of the internal bore.
- E) Four holes are drilled into the flange.
- F) The flange diameter is milled in.
- G) The workpiece is flipped and the opposite side is milled so the part has the correct height.
- H) The workpiece is removed from the milling machine and returned to the encapsulation machine. There, the machined featured are filled with the encapsulation alloy .
- I) Returned to the milling machine, the workpiece is mounted with the second side up. The outer diameter is cut to the correct depth using a bull nose endmill to create the proper radius.
- J) The workpiece is, again, removed from the milling machined and moved to the melting unit where the encapsulation alloy is liquefied.
- K) The part is extract and cleaned.

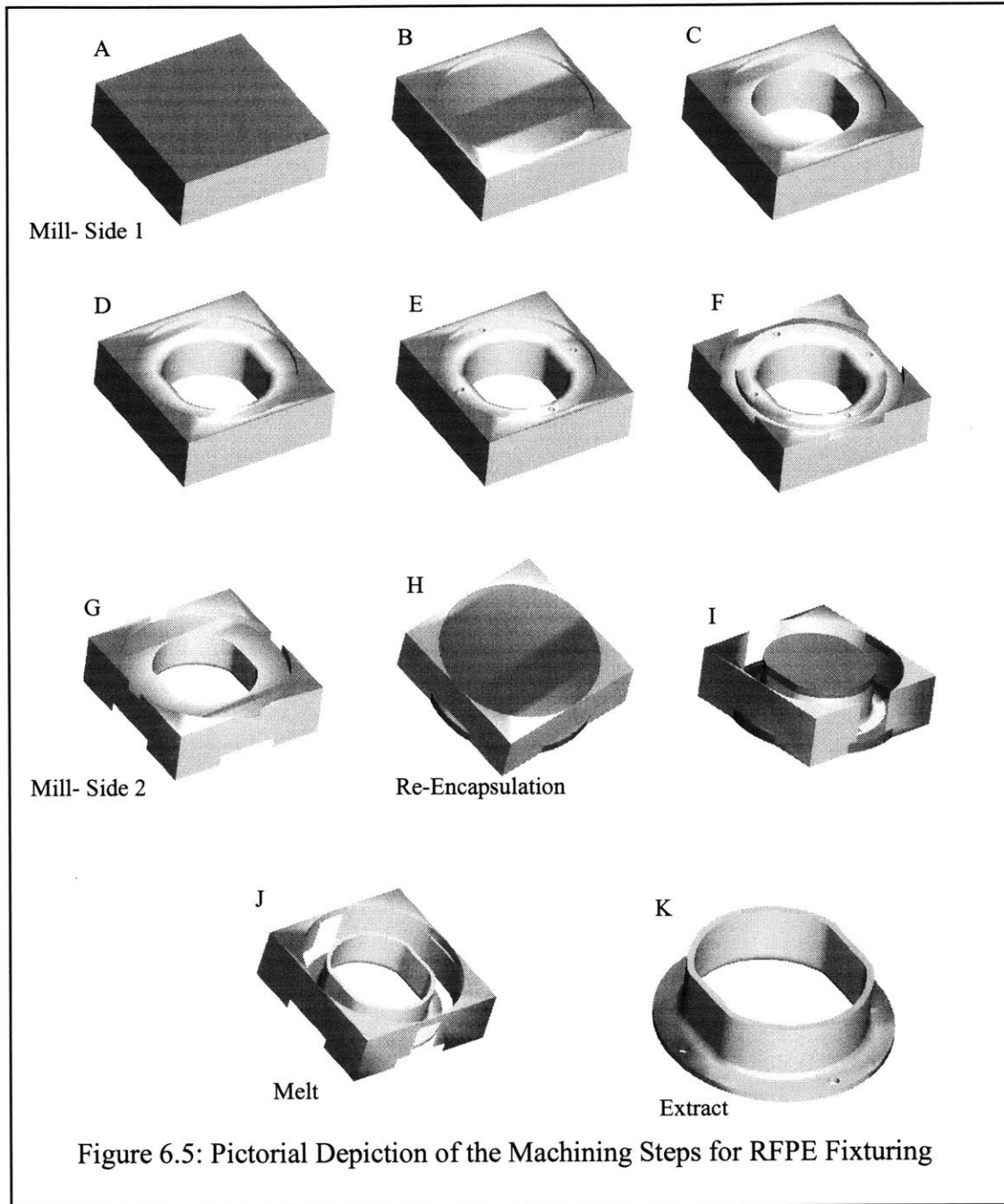


Figure 6.5: Pictorial Depiction of the Machining Steps for RFPE Fixturing

6.2 Results

The machining and setup time data for the three fixturing schemes are tabulated in Table 6.1, Table 6.2, and Table 6.3. They show what is not unexpected. The dedicated soft tooling results in considerably more upfront planning and is thus not well suited for single part production. From Figure 6.6, one can see that almost 75% of its single part production time is spent developing the dedicated tool. When compared to that of make-shift tooling, in which only about 45% of its single part production time is dedicated to setting up the machine and fixturing, it is obvious that make-shift tooling will be superior for single part production. If there is a need for multi-part production, dedicated tooling quickly becomes more economical at around 2 to 3 pieces, as shown in Figure 6.8. What makes dedicated tooling more economical is not because of an increase in machining proficiency. Figure 6.7 shows that the machining times for all processes are relatively similar. The gain is mainly because of the considerably less per part setup time needed for the dedicated tooling than for the make-shift tooling, 15 minutes as opposed to 30 minutes.

The question remains how RFPE fixturing performs when compared to these two fixturing schemes. Figure 6.7 shows that RFPE fixturing has the least time spent on per part setup. It clearly rivals that of dedicated tooling. Its one time setup time is equally impressive, rivaling that of make-shift tooling. There is, of course, a slight trade off. Machining times in the RFPE fixturing situations are slightly longer than the two other cases. This is primarily attributed to the increased amount of material that needs to be removed. While the encapsulation alloy can be easily machined. Cuts as deep as 0.50" with feedrates at 10ipm are made with little trouble. However, it is inadvisable to cut this quickly because while cutting encapsulation alloy, endmills will occasionally encounter the workpiece material. While CAD models can easily describe and predict when and

where these encounters will come, CAM packages are currently incapable of automatically adjusting cutter velocity to adapt to these changes. It is thus prudent to run the cutter at velocities that would be guarantee safety and reliability. It is clear that machining performance under RFPE fixturing can be further optimized. Nonetheless, the result of this case study show that RFPE fixturing will out perform these two other fixturing methods under certain conditions and when a certain number of part need to be machined.

Table 6.1: Machining and Setup Time for Soft Tooling

Conventional (10+ parts)			<u>Time(hours)</u>
Programming			1.50
Setup		<u>occurs</u>	
	pass 1	initial	0.25
	pass 2	every run	0.08
	pass 3	initial	0.50
	pass 4	every run	0.08
	pass 5	every run	0.00
	pass 6	every run	0.08
Machining		<u>description</u>	
	pass 1	Lathe-turning	0.08
	pass 2	Lathe-Parting	0.02
	pass 3	Milling-Outer Flats	0.17
	pass 4	Mill-Inner bore and Flats	0.42
	pass 5	Mill-Drill	0.02
	pass 6	Mill back Face and Cut Radius	0.25
Tooling			
	design		1.00
	programming		1.00
	machining		0.50
	total machining time		0.95
	total one time setup time		4.75
	total setup time during machining		0.25
	Total		5.95
	Cost	at \$50 dollars per hour for a single piece	297.33

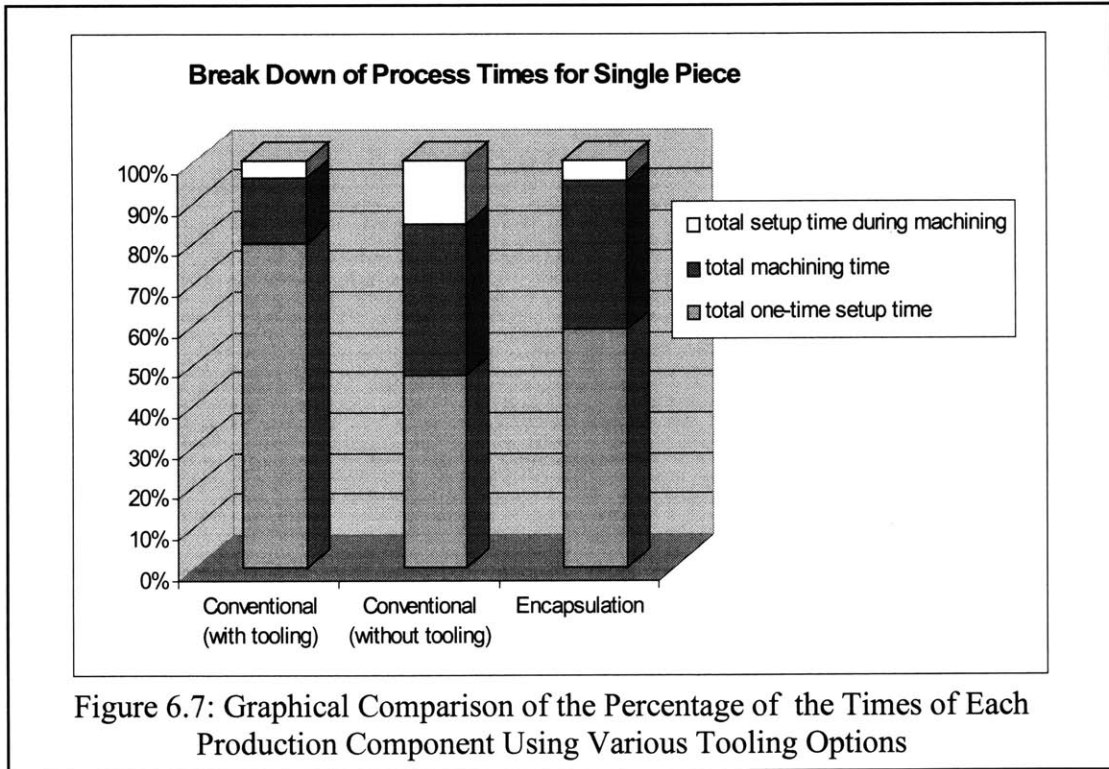
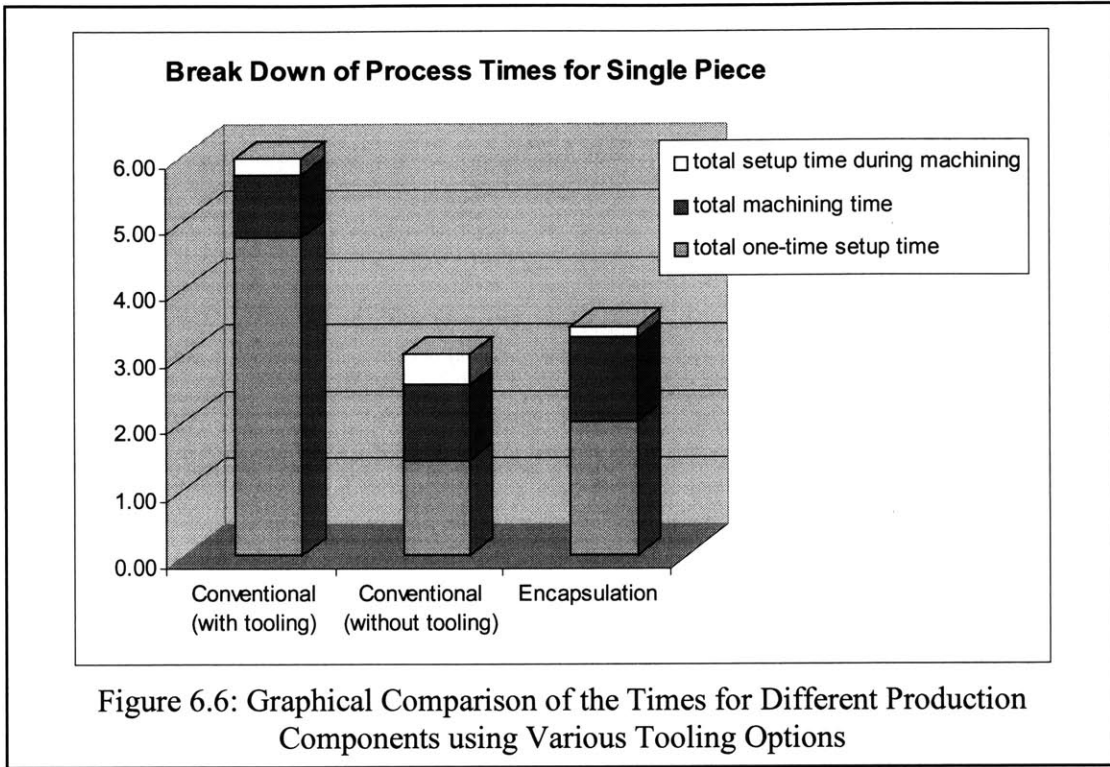
Table 6.2: Machining and Setup Time for Make-Shift Tooling

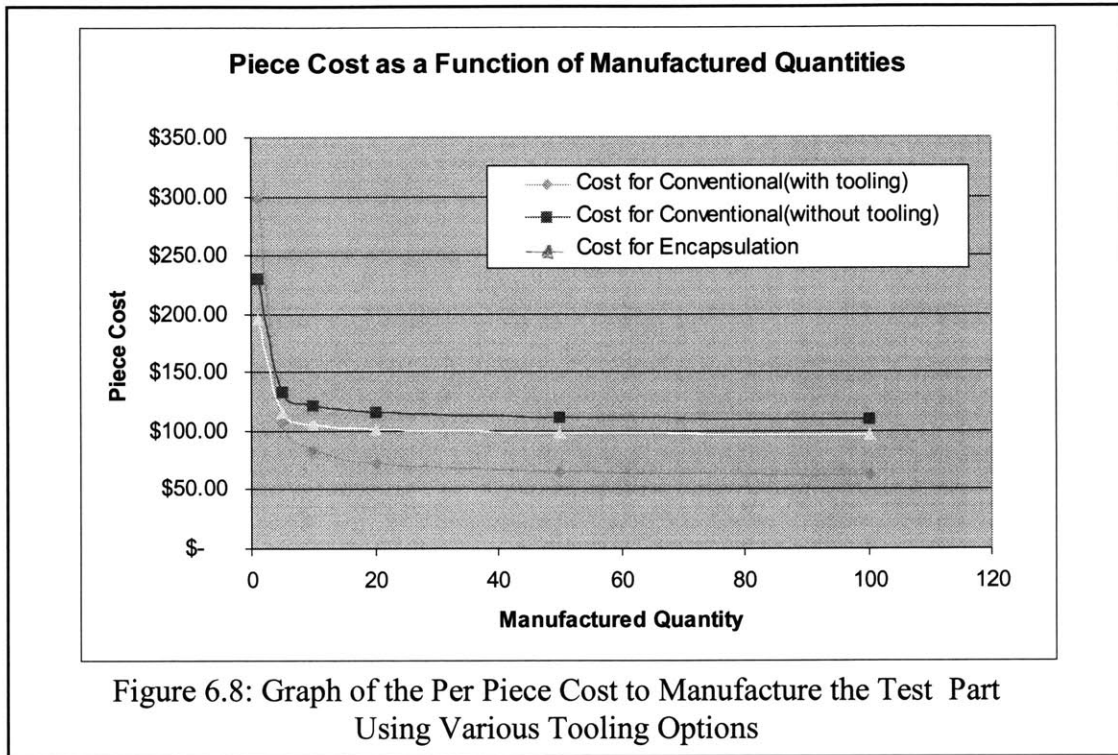
Conventional (1-10 parts)		<u>Time(hours)</u>
Programming		1.00
Setup		
	<u>occurs</u>	
pass 1	initial only	0.25
pass 2	every run	0.13
pass 3	every run	0.00
pass 4	every run	0.00
pass 5	every run	0.00
pass 6	every run	0.00
pass 7	every run	0.00
pass 8	every run	0.00
pass 9	every run	0.00
pass 10	every run	0.00
pass 11	every run	0.08
pass 12	every run	0.25
pass 13	every run	0.00
Machining		
	<u>description</u>	
pass 1	band saw stock	0.08
pass 2	mill top surface flat	0.05
pass 3	drill clearance hole for inner bore	0.03
pass 4	rough mill inner bore	0.12
pass 5	rough mill outer tube	0.08
pass 6	rough mill outer flange circumference	0.05
pass 7	finish mill inner bore	0.13
pass 8	finish mill outer tube	0.13
pass 9	finish mill outer flange circumference	0.05
pass 10	drill bolt circle	0.03
pass 11	band saw stock	0.17
pass 12	mill back side to thickness	0.13
pass 13	mill radius into back	0.05
Tooling		
design		0.08
programming		0.00
machining		0.08
total machining time		1.12
total one time setup time		1.42
total setup time during machining		0.47
Total		3.00
Cost	at \$85 dollars per hour for a single piece	255.00

Table 6.3: Machining and Setup Times for RFPE Fixturing

Encapsulation			<u>Time(hours)</u>
Programming			1.50
Setup		<u>occurs</u>	
	pass 1	initial only	0.50
	pass 2	every run	0.08
	pass 3	every run	0.08
Machining		<u>description</u>	
	pass 1	mill internal bore, mill back flat, cut radi	0.50
	pass 2	outer diameter and mill front flat	0.50
	pass 3	flange	0.25
Tooling			
	design	none	0.00
	programming	none	0.00
	machining	none	0.00
Encapsulation Cost			
	Cost per operations		25.00
	total machining time		1.25
	total one time setup time		2.00
	total setup time during machining		0.17
	Total		3.42
	Cost	at \$50 dollars per hour for a single piece	195.83

Because of RFPE has the ability to be automated, less skilled operators are needed to man a machine with the RFPE fixturing system incorporated within. The situation will be similar to that of soft-tooling. From interviews with a variety of job shops, it was determined that \$50 an hour would be billed in the soft tooling situation, and \$85 for the make-shift tooling situation. For the RFPE case, the hourly rate was set at \$50 and a per part encapsulation fee was set at \$25. This rate was derived from the total machine cost, estimated at about \$25,000, being amortized over a single year of use. It also includes an addition of 10% to the machine cost for maintenance and upkeep [Jezowski 01].





6.3 Conclusion

It can be concluded that RFPE fixturing offers some production performance benefits for this particular part. Yet, from its design, the test part is not considered by most as a complex geometry. Fixturing this part using conventional methods proves to be fairly trivial. All machinists interviewed had little trouble designing tooling for this part within minutes. Had the test part geometry been more complex, fixturing complexity would have played a greater role in the manufacturing of this part. As a result, the effects of RFPE fixturing would be more dramatic. In this case, the break even production size using RFPE fixturing is approximately 5 to 7 parts. Had the geometry been more complex, one can easily imagine the break even point and the cost benefits of encapsulation fixturing to be more significant.

Chapter 7

Research Conclusions

7.1 Machine Design

Neither encapsulation machines have been extensively and rigorously tested to discover their potential failure modes. The testing thus far has been limited to ensuring that the components of each encapsulation machine function within their design specifications. No analysis has been conducted on the long term wear characteristics of the linear guide bearings. No examination has been made to understand the response of the structural members of the clamping unit to the stresses induced by the thermal cycling. Nor has the encapsulation machine design been optimized for production, assembly, or maintenance. These task are left to future researchers.

The encapsulation machines have been tested to demonstrate that phase change fixturing techniques can be modified to the RFPE guidelines and result in an operable automated and universal fixturing system. These results are present in the following sections.

7.1.1 Machine Components and Sample Encapsulations

Encapsulation tests have been conducted on the large encapsulation machine using the 2-D encapsulation technique. On the portable machine, tests have been performed using the 2 1/2-D setup. The 3-D encapsulation technique, though fully conceptualized, has yet to be implemented and tested.

The figures below illustrate the 2-D and the 2 1/2-D molds and the encapsulation assemblies produced by them. The mold components are machined from stainless steel 304 alloy. All features are manufactured using a CNC milling machine with the exception of the cavity for the 2 1/2-D mold. The cavity was manufactured by means of wire EDM. The cost of the 2 1/2-D mold

is roughly \$3,000. The mold cavity is large enough to encapsulate a block with a 1" x 1" cross-section. The cost for the 2-D mold is roughly \$4,000. It is capable of encapsulating a 1" thick plate, 6" x 6" large. It is evident, that the lack of any wire EDM work allows the cost of the 2-D mold to be substantially reduced relative to the size of stock it is capable of encapsulating.

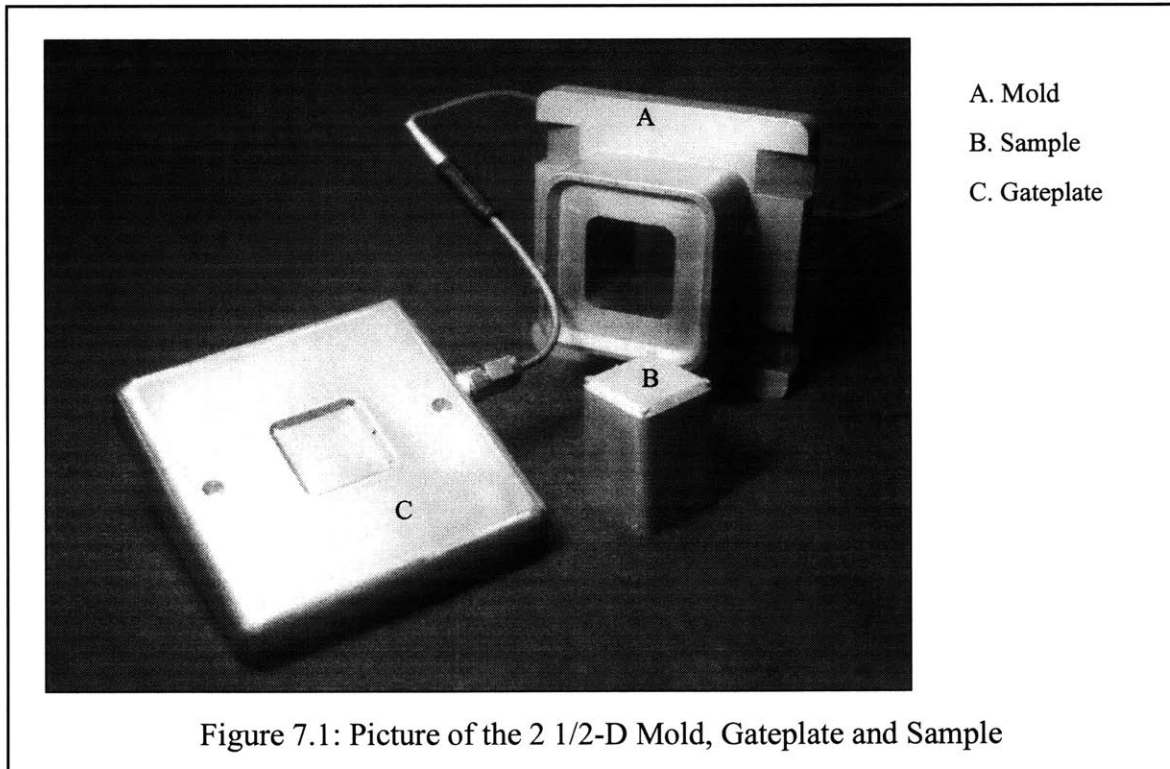
Figure 7.2 show the successful encapsulation of a 2 1/2-D workpiece. Figure 7.3 displays the encapsulation as it is being machined. The feeds and speed of the machine procedures follow those recommended for the workpiece encapsulated within. The encapsulation alloy offers very little machining resistance. The chips produced are very fine and splitter size. Because location is solely a function of the embedded fixture devices, encapsulation accuracy was not as important. However, it was measured that, upon re-encapsulation, the newly encapsulation surfaces were flush with the previous encapsulation layer by within 0.002".

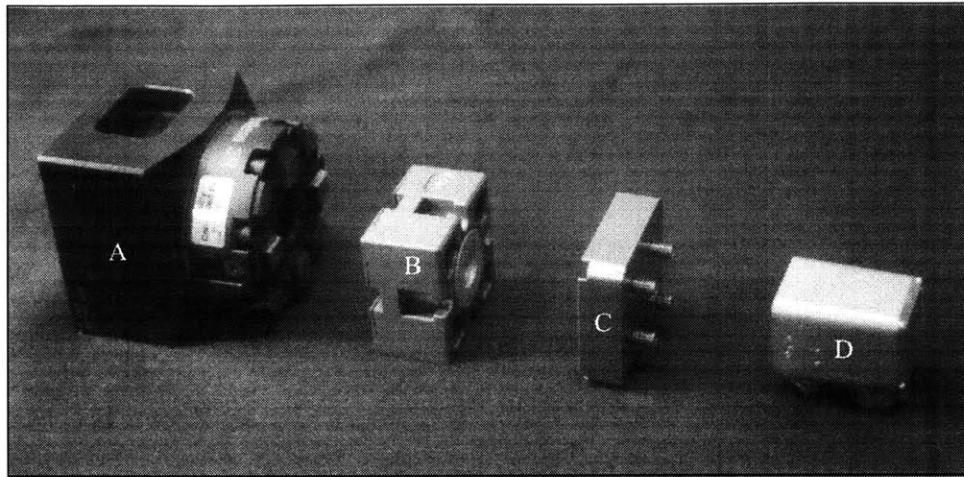
The cooling cycle is the most dominant part of the overall encapsulation cycle time. Ten's of minutes are needed to achieve full solidification when only air convective cooling is applied. There is an obvious need to increase the cooling rate. This will be an important part of future research. Liquid cooling through a low viscosity oil can greatly increase cooling rates. It is suggested that a heat exchanger be set up between the clamping system and a mold preheating station. In this way, as the newly encapsulated workpiece is being cooled within the clamping system, its heat can be absorbed and used to preheat another workpiece that awaits encapsulation. This arrangement can increase the energy efficiency of the encapsulation system with minimal additional cost to the overall system.

We have shown that encapsulation machines need not be extremely expensive in order to successfully perform the RFPE procedures. The large encapsulation machine cost approximately \$25,000 to build and the portable machine, about \$10,000. On the production scale, these

machines will most likely be less expensive to produce. We are able to cut costs by not requiring the components of the encapsulation machine to be manufactured with high degrees of accuracy. Instead, the precision is built into the mold. It is estimated that when built, the 3-D mold will cost approximately \$15,000 to \$20,000.

The cost of the machines are further reduced by choosing to actuate the clamping and injection stages with pneumatics. Pneumatics are far less expensive to purchase, maintain and service than a hydraulic system. What's more, pneumatic sources are readily available in the environment the encapsulation machine is designed to operate. Machine tools and other equipment rely on pneumatics to operate subsystems. Hydraulics, on the other hand, are not readily found on the machine shop floor and would thus require the installation of a compressor, delivery lines, and a host of other support equipment.





A. 3R Fixture B. 3R Fixture Plate C. Adapter Plate D. Encapsulation Sample

Figure 7.2: Picture of the 2 1/2-D Fixturing Assembly

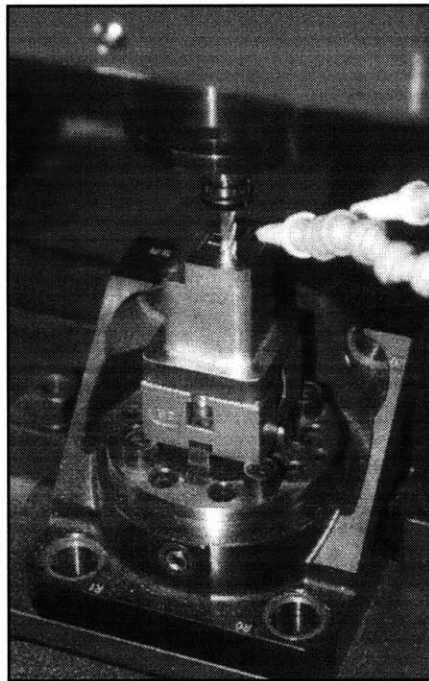
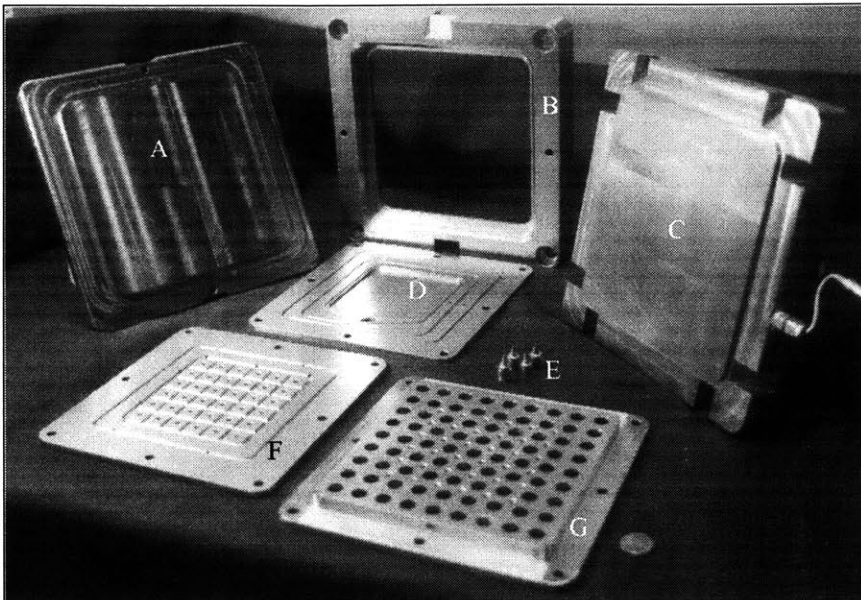


Figure 7.3: Picture of 2 1/2-D Encapsulation Assembly Installed in a Machine Tool



- A. Bottom Plate
- B. Fixture
- C. Gateplate
- D. Gate Plug Plate Cover
- E. Gate Plugs
- F. Gate Plug Distributor Plate
- G. Gate Plug Housing Plate

Figure 7.4: Picture of the 2-D Mold Components

- A. 2 D Encapsulation Frame
- B. Encapsulation Alloy
- C. Workpiece

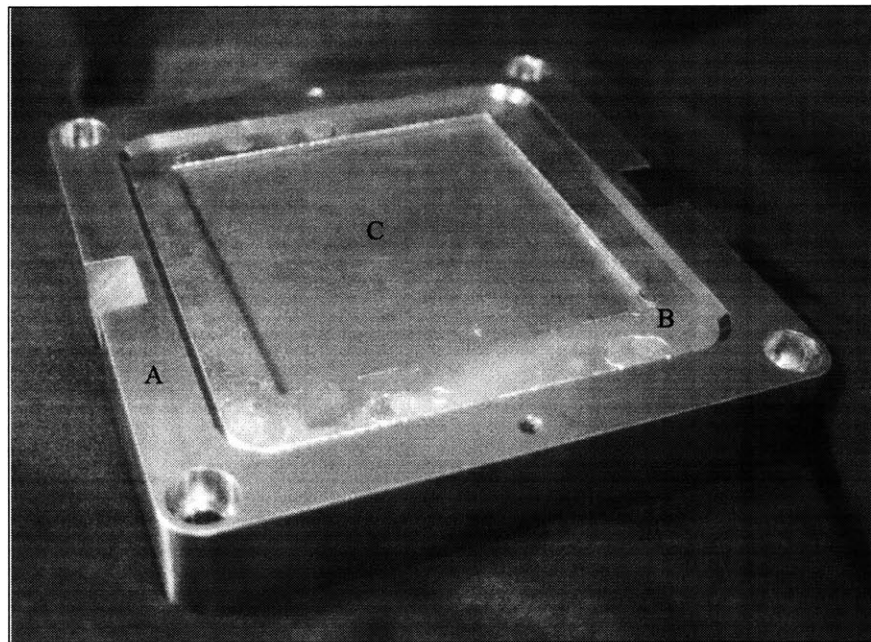


Figure 7.5: Picture of the 2-D Encapsulation Assembly

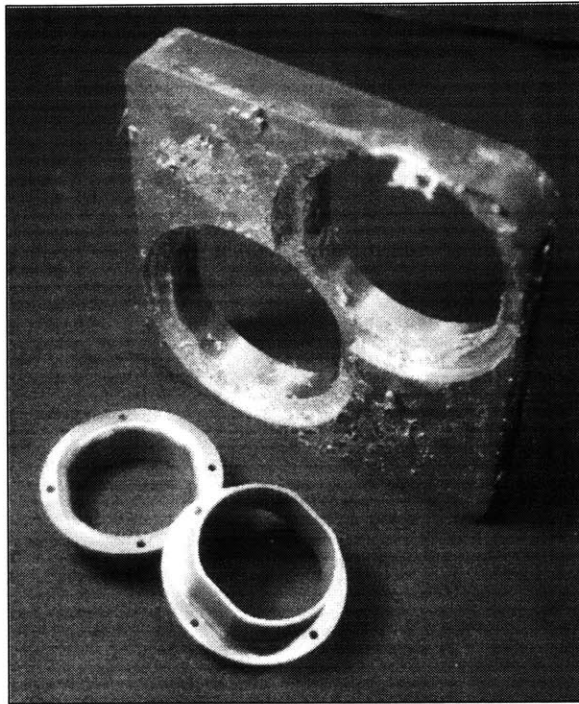
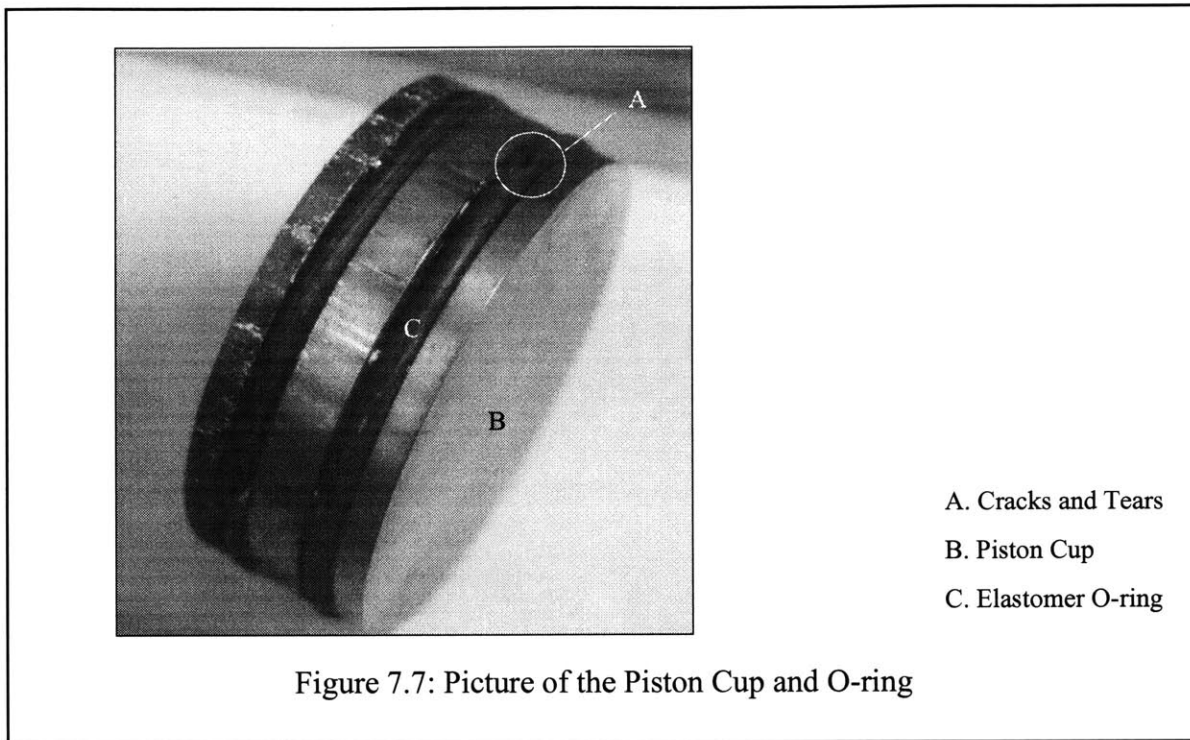


Figure 7.6: Picture of the Melted Encapsulation Assembly with the Finished Parts and Excess Stock Shown

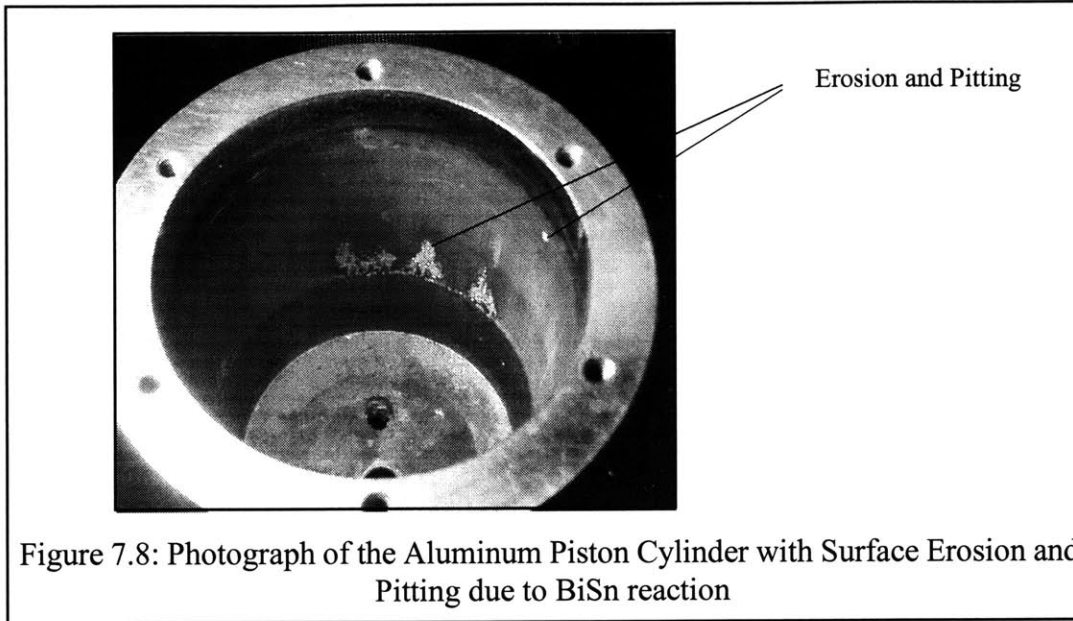
7.1.2 Failure Modes

In the course of the preliminary testing conducted, it has been observed that O-ring failure is the most common break down the encapsulation machines suffers. While the VitonTM O-rings used in all of the sealing surfaces of the machine are rated to withstand temperatures as high as 500K, there is evidence of cracking and splitting in those areas wear dynamic seals are installed. For example, the O-rings of the piston cup found inside the injection piston exhibited failure. After approximately 100 hours of use, the O-ring have become torn and brittle. The piston is operated in a temperature range of 390K to 400K. What's more, similar O-rings, held at the same temperature, but not subjected to movement remained intact within the encapsulation machine. It is conjectured that the combination of high heat and stresses induced by the friction of the piston



movement, and perhaps even some chemical interaction with the encapsulation material, created a failure mode which ultimately cause the O-ring to crack.

A second mode of failure was also observed. It was discovered that the BiSn eutectic material will stain aluminum alloys. Mild staining results only in discoloration, turning the aluminum alloy from a bright silver color to a dull grey. Staining only occurs when contact between the aluminum and the liquid BiSn alloy is held for durations in excess of an hour. Severe erosion, however, does occur with durations of contact in excess of days. It was observed that the injection piston cylinder, initially manufactured from aluminum 6061-T6, developed pits approximately 0.010" deep after 100's of hours of use. Subsequently, all machine components which came into direct contact with the encapsulation alloy and were subjected to friction wear were replaced with stainless steel 303 components. Those which came into contact with the alloy but involved no



moving parts were simply nickel plated. After such precautions were implemented, no signs of component erosion surfaced.

7.2 Immediate Applications for RFPE Fixturing

2-D encapsulation fixturing is the most simple form of RFPE fixturing. Through the testing described in Chapter 6, it has been shown that it can be used to reliably, quickly and efficiently fixture parts. While 2-D machining may appear to have very limited applications in industry, it is apparent that parts manufactured through stamping and pressing, and through injection molding bear the same type of feature topography. A majority of sheet metal part and plastic injection molded parts only have features found on two opposite sides.

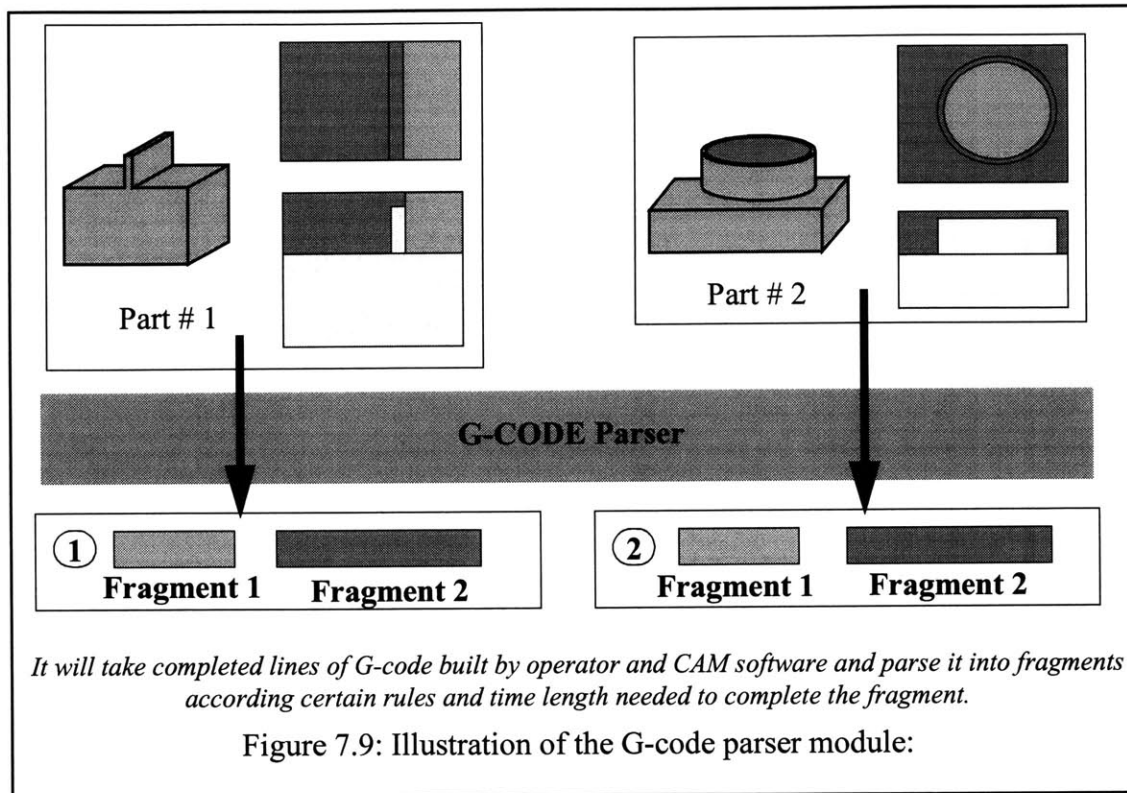
While the throughput of machining with the RFPE fixturing system would never be able to compete with the production efficiency of injection molding and sheet metal stamping machines in a mass production environment, it can easily compete and dominate when placed in a sheet metal or injection molding prototyping environment. Since tooling cost of injection molds and stamping dies are so high, prototyping parts through these processes is inconceivable. Most of

industry turn towards a machining process to prototype these types of parts. However, since the growing trend in product development is to place as many features within a single part in order to lower part count in an assembly, elements such as hinges, flexures and membranes have found their way into injection moldings and sheet metal stampings. Because of the thin walls and flexible members, fixturing these elements without an encapsulation process would be extremely challenging. Add to that the small production size, the resulting tooling can become a very sizeable portion of the overall part cost. In these cases, RFPE fixturing becomes a very appealing alternative. There is an obvious need to study this application further and to identify possible routes through which RFPE fixturing can be made useful.

7.3 Future Work

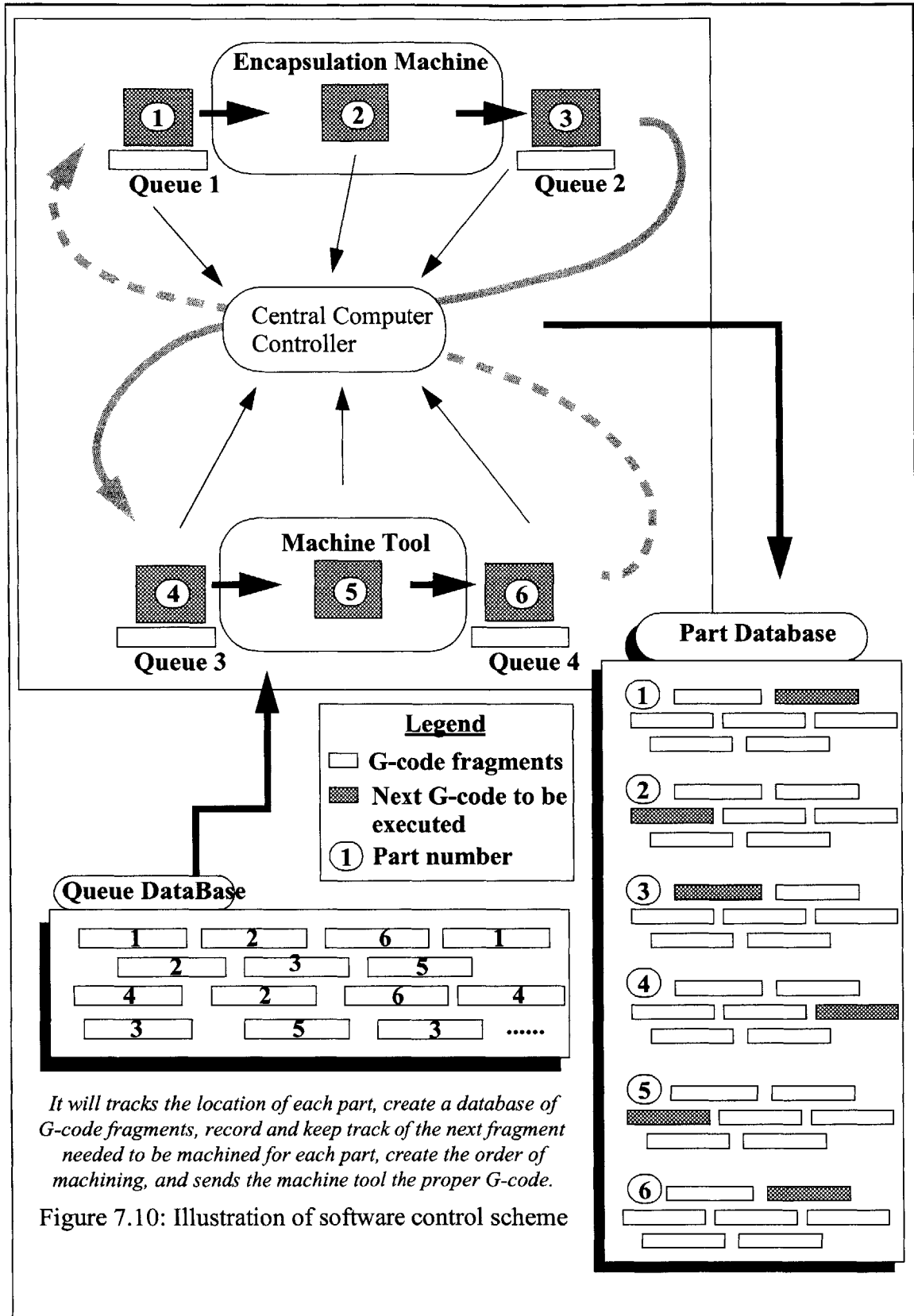
It is the hope of this researcher that the RFPE fixturing system, while demanding a significant investment in terms of equipment, training and adjustment of the current manufacturing mentality, will be seen as a plausible solution for rapid prototyping for these applications. It our belief that the understanding of RFPE fixturing has reached a level of demonstrable feasibility. This research has shown that encapsulation is capable of fulfilling the functions of fixturing, that of part location, immobilization and support, that it is capable of becoming automatable, and finally that, though it would not be able to adapt to every single fixturing need imaginable, RFPE fixturing does possess the flexibility and the adaptiveness that, when coupled with intelligent operators, can yield remarkable fixturing performance.

The next step is integration. Any piece of automation is only as useful as the programming that runs it. The universal fixturing system would only be a collection of unusual hardware without an overall control system that allows each part to communicate with the others. The goal of this research has always been to create a fully integrated, automated machining process. This



certainly would not be possible if the software used to control our fixturing system was not equally integrated and automatable.

The software would have two primary tasks. The first would be to parse G-code created by operators and CAM packages into discrete segments, between which refills would be scheduled. The software should be able to automatically take hundreds and thousands of lines of G-code needed to completely and successfully machine a given part and determine the most optimal places to stop the machining and schedule a refilling. These segment would need to be balanced by the length of time of each G-code segment. Too long of a G-code segment will increase the average leadtime of parts going through the process. Too short of a G-code segment increases the number of setups needed to finish a part and thus decreases the throughout of the machining process.



The second task would be to queue and track each part as it travels through the system. In our automated environment, 10's if not 100's of parts can be in the queue at once, each waiting to be machined, waiting to be delivered to the encapsulation center, waiting to be refilled, and waiting to be transported back to the machining center once refilled. The software must be able to identify each part, determine what has been done to it, and what next needs to be machined into it. For all the blocks in the system, the programming must be able to order the G-code segments and schedule each block for the correct procedures. It is a non-trivial problem that involves tracking each part, managing a database of all the operations needed for each part and marking all the processes that have been completed for each part. A list of rules and guidelines must be developed within the software that will allow it to determine the optimal dissection of G-code and the optimal scheduling of machining time and refilling time. The goal is to maximize throughput in the system while minimizing the increase in the average leadtime of parts through the system, just as it would be for any mass production cell.

The maximum throughput is achieved when there is zero downtime for each of the machining centers. The minimum leadtime for a given part can be taken as the total machining time necessary to completely machine the part, ignoring refill, transport and queuing times. From these two quantities, we can then define process efficiency as:

$$\eta = \frac{\textit{Actual}}{\textit{Maximum}} \quad (\textit{Throughput}) \quad \text{Eq.7.1}$$

and the fixturing effectiveness as:

$$\varepsilon = \frac{\textit{Minimum}}{\textit{Actual}} \quad (\textit{MachineTime}) \quad \text{Eq.7.2}$$

The task is thus to determine the manner in which RFPE fixturing can be implemented so that η and ε are both well optimized.

7.4 The Future of RFPE

The level of understanding of the RFPE fixturing process is at its maximum in the academic arena. We have shown, through this research and those performed by students also working with Sarma, that the RFPE techniques does yield a successful fixturing system. We have shown that this system is automatable and, though not universal in the true sense of the word, RFPE fixturing can be applied to many applications with positive results. We have shown that we understand the encapsulation process. We have performed analysis on the process and understand the the environment in which RFPE can be performed sucessfully. Lastly, we have shown that it is possible to develop machines to perfrom the RFPE process. In creating these machines, we have introduced new technology and combined it with knowledge derived from other molding processes.

If this understanding is to grow further, development of the RFPE fixturing process must be moved out of academia and into industry. It is only there that the process can be further refined and allowed to mature. The challenge lies not in ensuring that the encapsulation process itself works. This has been accomplish. The challenge lies in developing the support systems that will further optimize the RFPE fixturing process. Automated material handling, computerize tracking and queueing of various parts while in the machining/encapsulation cycle and a variety of CAD/CAM innovations, these are the backbones on which RFPE must be supported in order to show its full strength.

Appendix A:

Detailed Specifications of the Large and Portable Encapsulation Machines

Large Encapsulation Machine

Specifications:

Maximum mold footprint:

8"x8"

Clamping Capacity:

10,000lbs

Power Requirement:

7,200 watts

Pneumatic Requirement:

75 psi

Number of Independently Controlled Heating Zones:

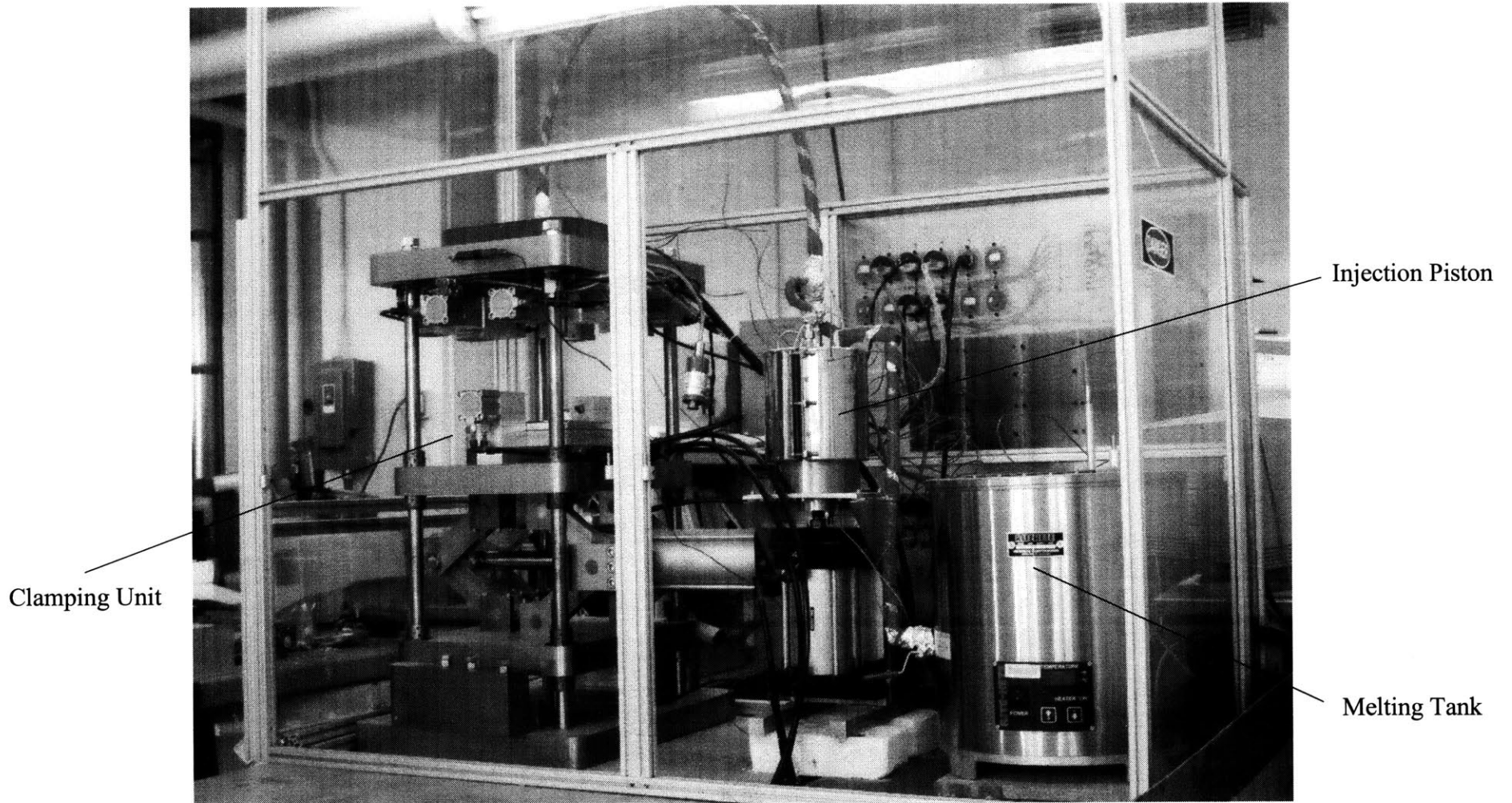
7

Number of thermocouples installed:

14 J-type

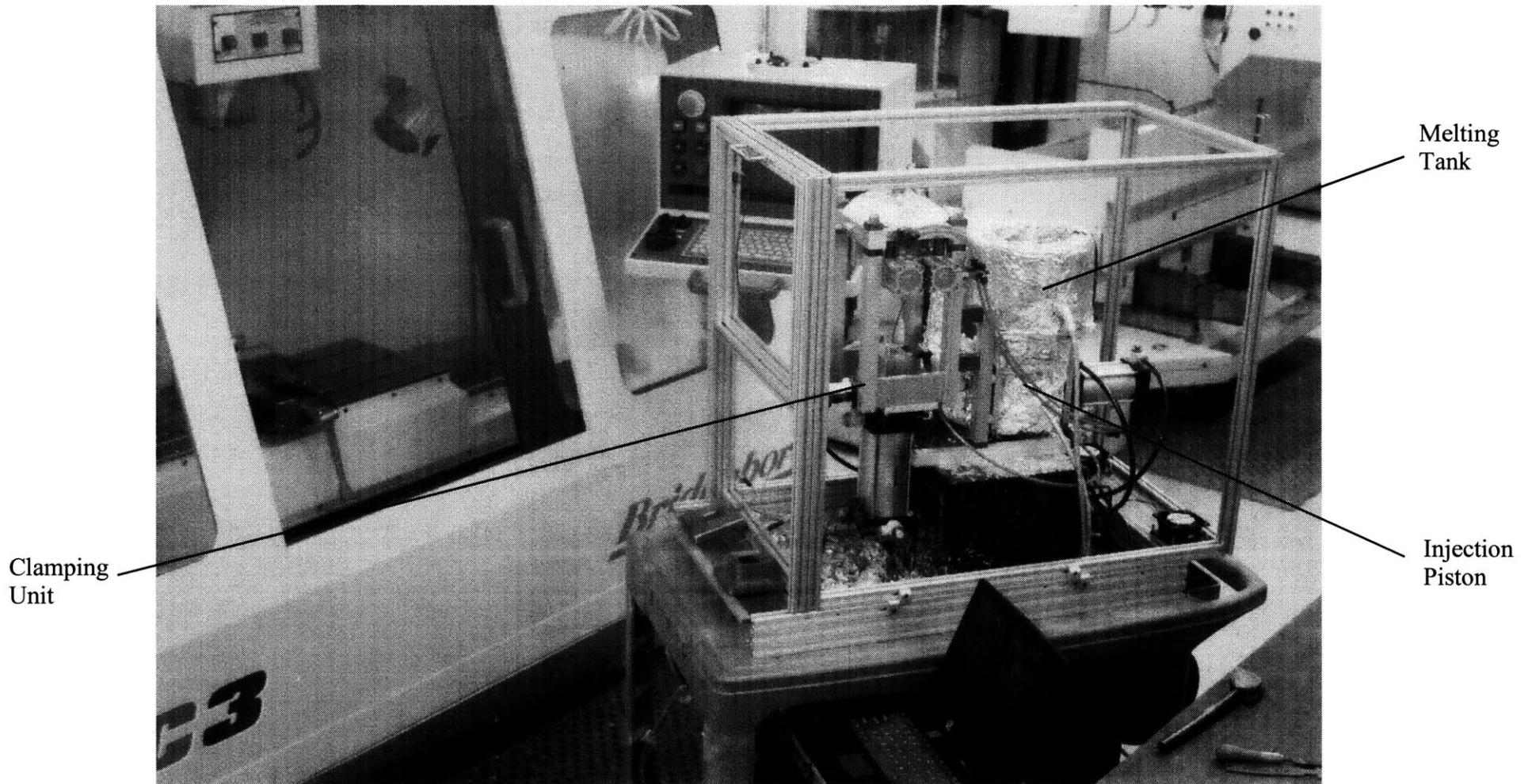
Control System:

PC controlled with DIO and DAQ cards



Mini-Portable Encapsulation Machine

Specifications:	
Maximum mold footprint:	4"x4"
Clamping Capacity:	1,000lbs
Power Requirement:	2,400 watts
Pneumatic Requirement:	75 psi
Number of Independently Controlled Heating Zones:	4
Number of thermocouples installed:	8 J-type
Control System:	Laptop controlled with PCMCIA DIO and DAQ cards



Appendix B:

Pictorial Demonstration of the Automated Fixturing System on the FORD test part

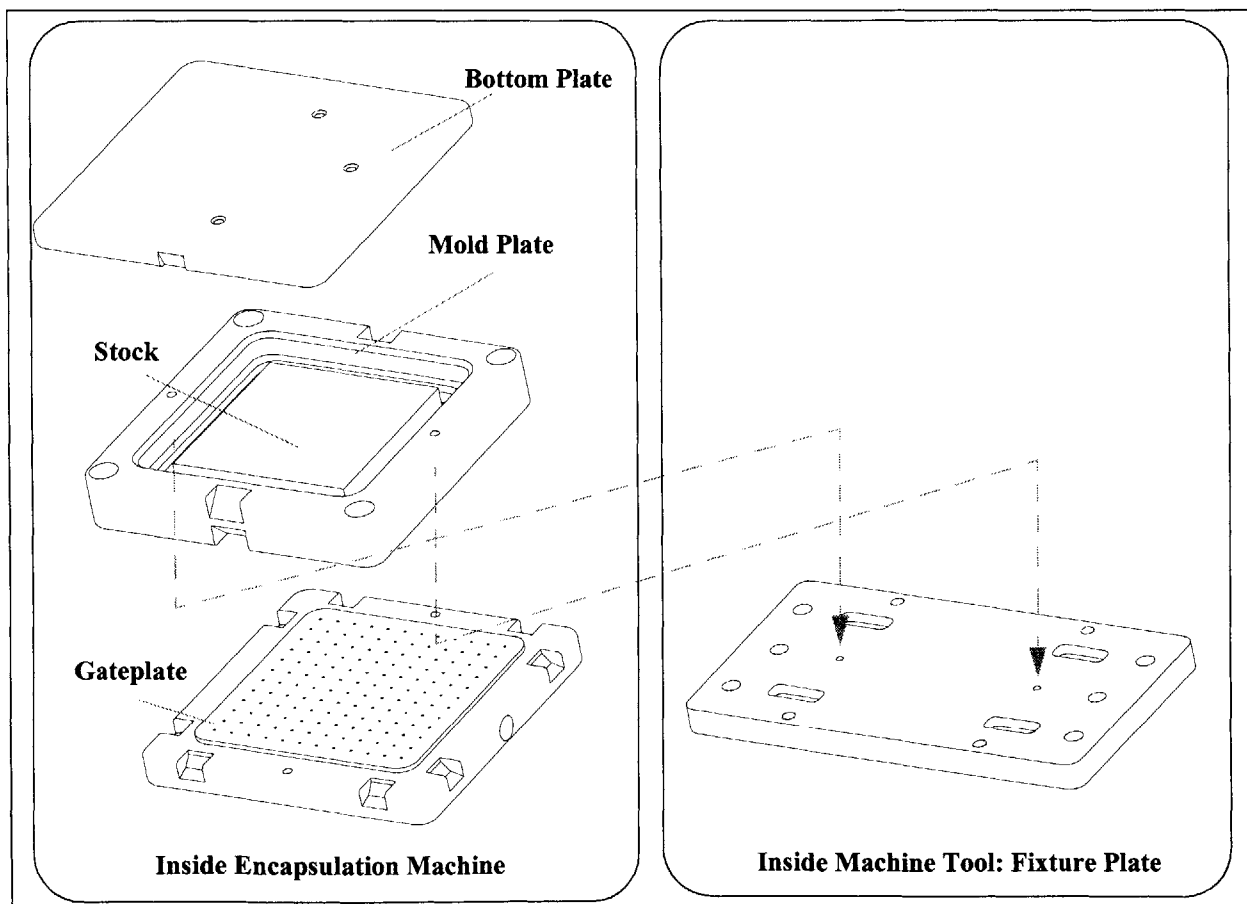
A Pictorial Demonstration of the 2-D Universal, Automatable Encapsulation Fixturing System

The part being prototyped is an actual part given to us by the FORD motor company. The part is called a body mount and is located between a car's chassis and frame. In production, the body mount would be stamped and pressed to its final shape, costing tens of cents per piece to manufacture. The part is encapsulated within an elastomer before installation. The function of this part is to isolate vibrations, that the car frame experiences, from the chassis in order to reduce rattling and to make the ride experience more comfortable to the driver and passengers.

In a prototype setting, where small quantities are needed, manufacturing this part through a stamping and pressing process would not be economically feasible. Thus, these parts are usually machined and the price would increase to hundreds of dollars per part, depending on the quantity. Much of this cost is attributed to developing and manufacturing custom tools and fixtures to hold this part while being machined. However, by using the encapsulation fixturing system, the cost can be reduced to approximately \$195 per part. Because of the simplicity of the part, the cost saving, while still substantial, is not demonstrative of the full potential of the fixturing system. As part complexity increases, requiring more sophisticated tooling, the encapsulation fixturing system will provide cost and time saving orders of magnitude greater than what is shown here.

The figure below shows the setup for a 2-D encapsulation fixturing system. 2-D parts are ones in which all features on the part exist and are accessible from 2 opposite sides. Parts manufactured through mass production processes such as injection molding, die casting, stamping, punching, and pressing are good examples of 2-D parts. We have shown in our research that by using the encapsulation fixturing system, we now have, for the first time, an inexpensive, rapid method to prototype these classes of parts.

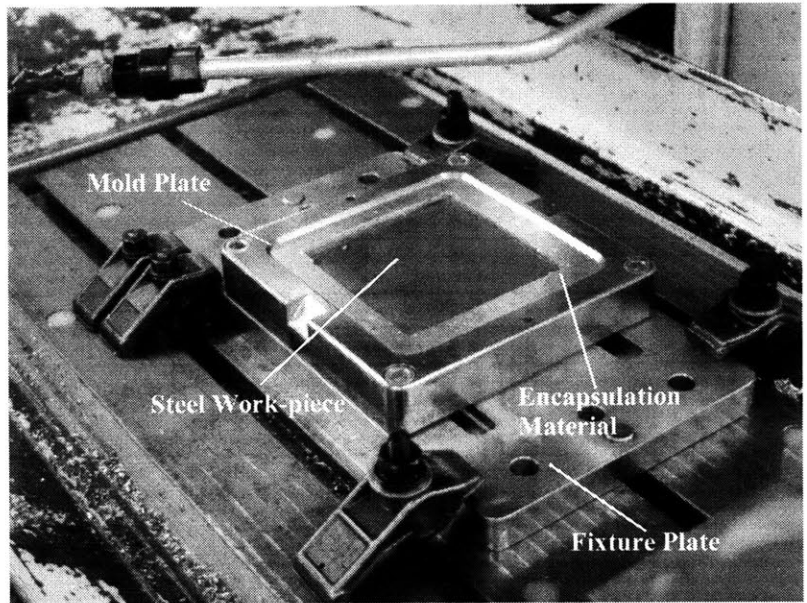
Below is a pictorial demonstration of the fixturing and machining process using RFPE fixturing. It shows the various setups in sequential order.



STEP 1: Installation

A new encapsulation assembly, composed of a 2-D mold plate, a 6" x 6" x 1.25" piece of steel, and the encapsulation alloy which surrounds our work-piece, is installed into a machining center. This assembly is large enough to have 2 of our prototype parts machine from it.

TIME: 15 minutes

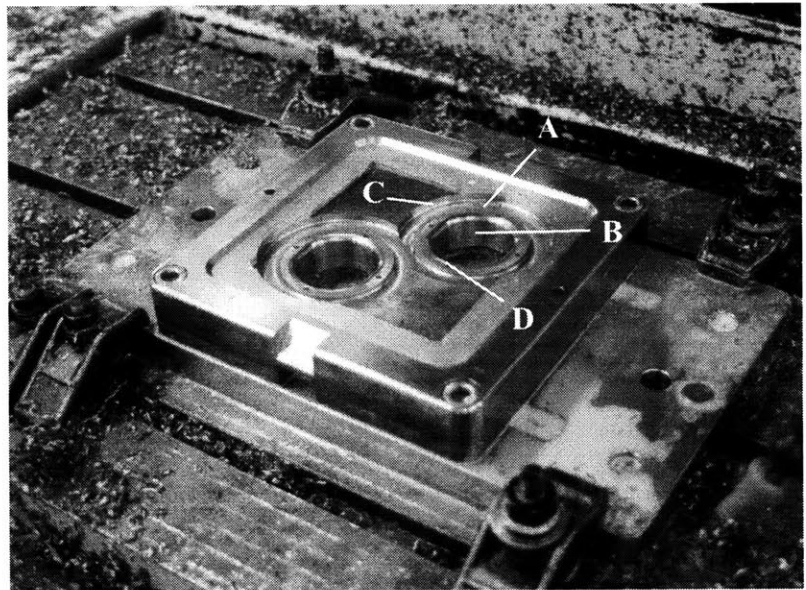


STEP 2: First Side-Machining

Four machining procedures are placed onto the first side.

- A) A 1" diameter, flat endmill mills the top of each part
- B) A 1" diameter, flat endmill pockets out the center core of each part
- C) A 1/2" diameter, flat endmill, mills the outer circumference of the flange of each part
- D) A 1/4" drill drills 4 holes into each part

TIME: 35 minutes

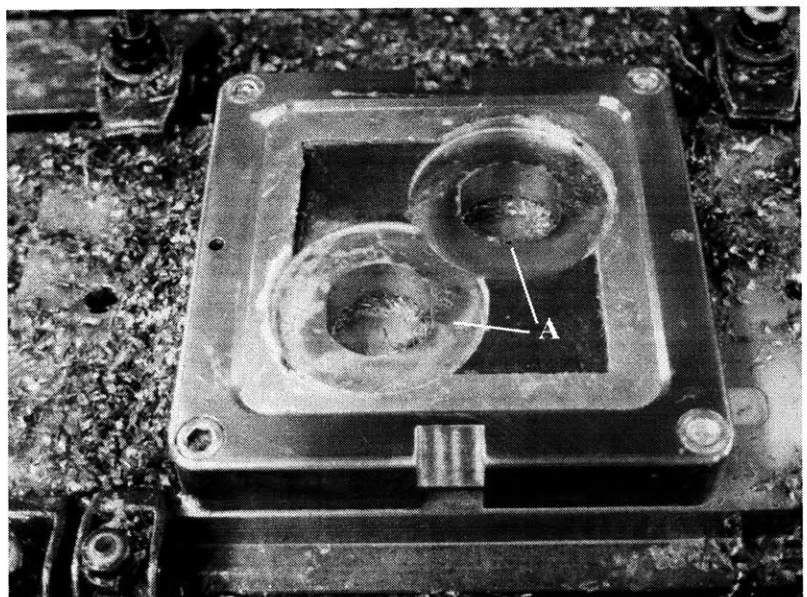


STEP 3: Second Side-Machining

One machining procedure is placed onto the second side before the encapsulation assembly is removed from the machining center, to be re-encapsulated

- A) A 1" diameter, flat endmill mills the part to the correct height for each part

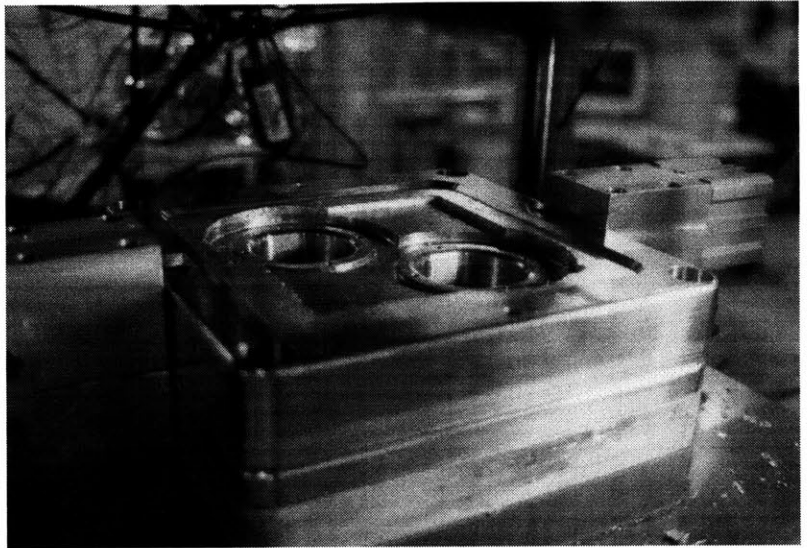
TIME: 10 minutes



STEP 4: Re-Encapsulation

The encapsulation assembly is removed from the machining environment and placed back into the encapsulation machine to fill the cavities created by the previous machining procedures. This assembly will need to be preheated to 390K, filled with the encapsulation alloy under pressure, and allowed to cool.

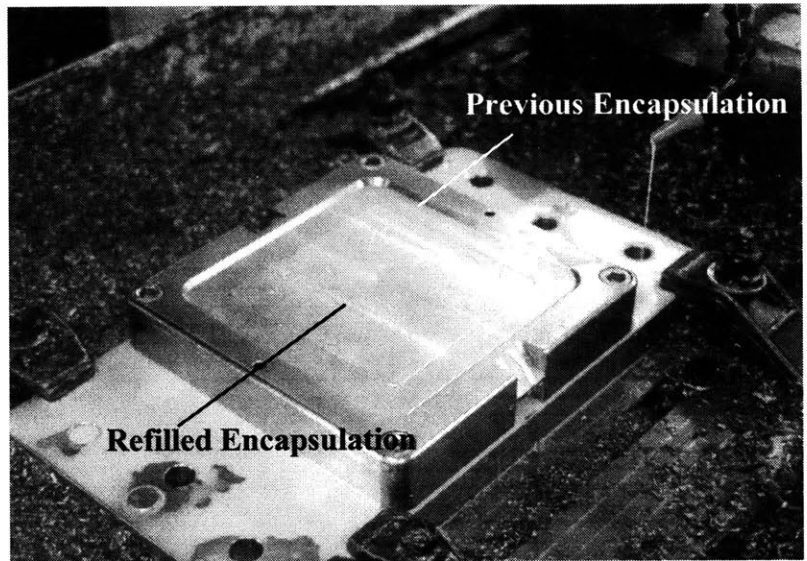
TIME: 20 minutes



STEP 5: Re-Installation

Once re-encapsulation is completed, the assembly is reinstalled into the machining center so that the last machining procedure may be placed into it.

TIME: 5 minute

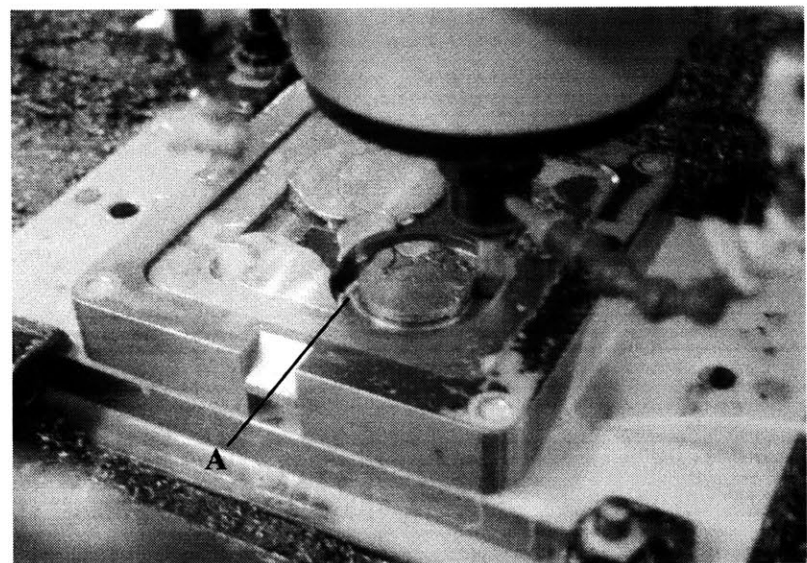


STEP 6: Second Side-Machining

The last machining procedure is placed into the second side

A) A 1/2" diameter endmill mills the outer circumference of the tube body for each part

TIME: 30 minutes



TOTAL TIME TO MACHINE 2 PARTS:

1 hour 55 minute

BIBLIOGRAPHY

- [Alcoa 72]
Aluminum Company of America, *Soldering Alcoa Aluminum*, Pittsburgh, 1972.
- [Allsop 83]
Allsop, D.F., and Kennedy, D., *Pressure Diecasting, Part 2*, Pergamon Press, New York, 1983.
- [Arpaci 91]
Arpaci, V. S. *Conduction Heat Transfer, Abridged Edition*. Ginn Press, Nedham Heights, MA, 1991.
- [Barkman 82]
Barkman, W.E., "Workpiece Fixturing for Precision Machining," *Precision Engineering*, Vol 4, No. 2, P101-105, April 1982.
- [Bar-Meir 96]
Bar-Meir, G., Eckert, E.R.G., Goldstein, R.J., "Pressure Die Casting: A Model of Vacuum Pumping," *Journal of Manufacturing Science and Engineering*, Vol. 118, May, 1996.
- [Beckwith 93]
Beckwith, T.G., Marangoni, R.D., and Lienhard V, J.H., *Mechanical Measurements*, Addison-Wesley Publishing Company, Reading, MA, 1993.
- [Boyes 85]
Boyes, W.E., *Low Cost Jigs and Fixtures for Limited Production*, SME, Dearborn, Michigan, 1985.
- [Carslaw & Jaeger 65]
Carslaw, H.S., Jaeger, J.C., *Conduction of Heat in Solids*, Clarendon Press, Oxford, 1965.
- [Chadwick & Yue 89]
Chadwick, G.A., Yue, T.M., "Principles and Applications of Squeeze Casting," *Hi-Tec Metals Research and Development*, January 1989, P6-12.
- [Coes 72]
Cotes, L., "Workholder for Irregular Shaped Workpieces," US Patent, 3,660,949, May 9th 1972.
- [Fan 00]
Fan, W. *The Effect of Surface Roughness on the Precision of the Encapsulated Fixturing System*, S.M. Thesis, Massachusetts Institute of Technology, 2000

- [Franklin & Das 84]
Franklin, J.R., Das, A.A., "Squeeze Casting- A Review of the Status," *Foundaryman*, April 1984, P150-158.
- [Gandhi & Thompson 84]
Gandhi, M.V., Thompson, B.S., "Status Report on Fixturing Induced by Material Phase-Change," Report ITI-84-3I, Industrial Technology Institute, March 1984.
- [Gandhi & Thompson 85]
Gandhi, M.V., Thompson, B.S., "Phase Change Fixturing for Flexible Manufacturing Systems," *Journal of Manufacturing Systems*, Vol 4, No. 1, P29-40, 1985.
- [Griffith, Grossman, Will, & Garrison 75]
"Quasi-Liquid Vise for a Computer Controller Manipulator," IBM Research Report Number 5451, IBM T.J. Watson Research Center, Yorktown Heights, New York, June 1975.
- [Grigull 84]
Grigull, Ulrich, *Heat Conduction*, Hemisphere Publications Corp, 1984.
- [Guevara 00]
Guevara, Ceani, *Development of the Process Parameter Map for Reference Free Part Encapsulation*, S.M. Thesis, Massachusetts Institute of Technology, 2000.
- [Hoffman 84]
Hoffman, Edward G., *Fundamentals of Tool Design*, Society of Manufacturing Engineers, 1984.
- [Hoffman 85]
Hoffman, Edward G., "Flexible Fixturing," *Modern Machine Shop*, Vol 58, P88, September 1985.
- [Hoffman 96]
Hoffman, Edward G., *Setup Reduction Through Effective Workholding*, Industrial Press, 1996.
- [Hu 98]
Hu, H., "Squeeze Casting of Magnesium Alloys and Their Composites," *Journal of Materials Science*, Vol 33, 1998, P1572-1588.
- [Incropera 90]
Incropera, F.P., and De Witt, D.P., *Fundamentals of Heat and Mass Transfer, Third Edition*, John Wiley and Sons, New York, 1990.

- [Jezowski 01]
Jezowski, Randy, Interview and Professional Quotation from RAMCO, Inc., Rowley, MA, 2001.
- [Kalpakjian 95]
Kalpakjian, S., *Manufacturing Engineering and Technology*, Addison-Wesley Publishing Company, Reading, MA, 1995.
- [Kulkarni 74]
Kulkarni, K.M., "Squeeze Casting Comes of Age," *Foundary Management and Technology*, August 1974, P76-79.
- [M. Argueso and Company, Inc 01]
M. Argueso and Company, Inc, Material datasheets and test data on Rigidax WI green, May 2001.
- [Mills 95]
Mills, A.F., *Basic Heat and Mass Transfer*, Irwin Publishing, Chicago, 1995.
- [Morrison 88]
Morrison, Les, "Flexible Fixturing," *Production Engineer*, October 1988, P44-45.
- [Lee 99]
Lee, Elmer C., *Development of an Encapsulation Process for use in a Universal Automated Fixturing System*. Master of Science Thesis, Massachusetts Institute of Technology, Cambridge, MA, 1999.
- [Perchiney 89]
Pechiney Inc., "Squeeze Casting Machines," *Foundry Trade Journal*, July 1989.
- [Rajagopal 81]
Rajagopal, S., "Squeeze Casting: a Review and Update," *Journal of Applied Metal Working*, January 1981, P3-14.
- [Salmon 01]
Salmon, Norman, Interview and Professional Services from Onyx High Speed Machining, Nashua, NH 2001.
- [Sarma 95]
Sarma, S.E., *A Methodology for Integrating CAD and CAM in Milling*, Ph.D. Thesis, University of California, Berkeley, 1995
- [Slocum 92]
Slocum, A.H., *Precision Machine Design*, Prentice Hall, Englewood Cliffs, NJ, 1992.

[Sprenkle 96]

Sprenkle, J.B., personal interview and plant tour of Pratt and Whitney's New Haven plant, 1996

[Stephany 92]

Stephany, D.M., "The Value of Creative Workholding," *Modern Machine Shop*, Vol 64, No. 12, P94-101, May 1992.

[Suh 90]

Suh, N.P., *The Principles of Design*, Oxford University Press, New York, 1990.

[Thompson 86]

Thompson, B.S., "Flexible Fixturing-A Current Frontier in the Evolution of Flexible Manufacturing Cells," ASME Paper No. 84-WA/Prod-16

[Upton 82]

Upton, B., *Pressure Diecasting, Part 1*, Pergamon Press, New York, 1982.

[Valdivia 00]

Valdivia, P. *Investigation of the Remolding Step in Reference Free Part Encapsulation*, S.M. Thesis, Massachusetts Institute of Technology, 2000.